STUDIES ON INCLUSION COMPLEXES OF CYCLODEXTRIN AND DYES; I. SYNTHESIS AND PROPERTIES OF DYE ROTAXANES, II. FORMATION OF ANISOTROPIC SUPRAMOLECULES

A Thesis

Presented to

The Academic Faculty

By

Jong Seung Park

In Partial Fulfillment

Of the Requirements for the Degree

Doctor of Philosophy in School of Polymer, Textile and Fiber Engineering

Georgia Institute of Technology

December 2005

STUDIES ON INCLUSION COMPLEXES OF CYCLODEXTRIN AND DYES; I. SYNTHESIS AND PROPERTIES OF DYE ROTAXANES, II. FORMATION OF ANISOTROPIC SUPRAMOLECULES

Approved by:

Dr. Mohan Srinivasarao, Advisor
School of Polymer, Textile and Fiber Engineering
Georgia Institute of Technology

Dr. Uwe H. F. Bunz, Co-advisor
School of Chemistry and Biochemistry
Georgia Institute of Technology

Dr. Anselm Griffin
School of Polymer, Textile and Fiber Engineering
Georgia Institute of Technology

Dr. Laren M. Tolbert
School of Chemistry and Biochemistry
Georgia Institute of Technology

Dr. Haskell Beckham
School of Polymer, Textile and Fiber Engineering
Georgia Institute of Technology

Dr. Jung O. Park
School of Polymer, Textile and Fiber Engineering
Georgia Institute of Technology

Date Approved : August 26, 2005

ACKNOWLEDGEMENTS

The number of persons who have had an impact on my thesis work here at Georgia Tech is very large. I can think of lots of grateful people who helped and supported me during my pursuit of a Ph.D. First of all, I would like to thank my thesis advisor, Prof. Mohan Srinivasarao, for all his help with my research and thesis works. His understanding and stimulus have been a main driving force in keeping me through all this process. It's been quite tough to meet all his requirements, but with his guidance, I've always been encouraged to do better science. I thank my co-advisor, Prof. Uwe H. F. Bunz, for his support in providing numerous advices and wonderful chemical lab space and facility on my synthesis. Without his generous help, I could have done the most difficult projects in my thesis (Chapter 4 and Chapter 5). I feel deeply grateful to Dr. Jung Ok Park for a number of suggestions with spiritual encouragements. I especially thank her for making such a helpful comment in every manuscript I've made.

Many thanks go to former and present group members in Srinivasarao group (KyeoungWeon Park, Vivek Sharma, Matija Crne, Raymond René, David Jenkins, Haixia Wu, Jian Zhou and Lulu Song) and Bunz group (Ik Bum Kim, Yiqing Wang, Brian Englert, Sandra Shotwell, Selma Bakbak). I especially thank James Wilson for being my lab partner and helping me out with acetylene based synthesis.

I would like to thank all my committee members, Prof. Laren Tolbert, Prof. Anselm Griffin, and Prof. Haskell Beckham for pointing out many valuable suggestions for my thesis. I'm indebted to Dr. Allen Tonelli (in NCSU). He allowed me to stay in his lab a couple of times, and during those stays I came to learn a lot about cyclodextins and

their inclusion complex formation. I want to thank Dr. Saif A. Haque (in Imperial College). I enjoyed all academic collaboration with him, and personal discussion as well. Collaboration with him enabled what I had in Chapter 2 and Chapter 3.

Finally, I would like to thank the people who have supported me all this year, my parents and parents-in-law for their constant supports and confidence in me. I'm much indebted to my beloved wife, Jeong-Eun, who has supported the family in my place. Her effort and sacrifice have enabled me to complete this work, and will not be forgotten. I want to express a deep affection to her and our precious daughter, Jeong-Bin.

TABLE OF CONTENTS

LIST OF TABLES

LIST OF FIGURES

LIST OF ABBREVIATIONS

8-HQ	8-Hydroxyquinoline
AzoFD	Azo dye (non-rotaxanated)
AzoRD	Azo dye rotaxane
AzoxFD	Azoxine dye (non-rotaxanated)
AzoxRD	Azoxine dye rotaxane
CD	Cyclodextrin
COSY	Correlated spectroscopy
DAAB	Diaminoazobenzene
DSC	Differential scanning calorimeter
ESI	Electrospray ionization
FD	Free dye (non-rotaxnated acetylene dye)
FT-IR	Fourier transform infra-red
HOMO	Highest occupied molecular orbital
IR	Infra-red
LUMO	Lowest unoccupied molecular orbital
MALDI-TOF	Matrix assisted laser desorption ionization – time of flight
MO	Methyl orange
NOE	Nuclear overhauser effect
OLED	Organic light-emitting device
PLED	polymer light-emitting device
PP	Polypropylene
PPE	Poly(phenyleneethynylene)s
PPO	2,5-Diphenyloxazole
Py	Pyrene
RD	Rotaxanated dye (acetylene dye rotaxane)
ROESY	Rotating overhauser effect spectroscopy
TEM	Transmission electron microscopy
WAXD	Wide angle X-ray diffraction

Zn-AzoxFD	Complex formed by Zn and AzoxFD
Zn-AzoxRD	Complex formed by Zn and AzoxRD

LIST OF SCHEMES

SUMMARY

Supramolecular chemistry covers intermolecular interactions where non-covalent interactions are involved, and many of them are based on host-guest interactions. Cyclodextrins (CDs) are cyclic oligosaccharides consisting of 6-, 7- or 8-glucose units, which are called α-, β- or γ-CDs, respectively. They have hydrophobic interior and hydrophilic exterior, and are widely being used as hosts for various organic molecules. The formation of CD inclusion complexes with a variety of dyes has continuously drawn our interests, largely due to the ability of the CDs to alter the physical properties of the dyes.

The present thesis covers the study of inclusion complexes of CDs and chromophore dyes, largely in two ways; rotaxane and pseudorotaxane. The stable rotaxane structure is achieved with the synthesis of dye rotaxane. The introduction of CD ring around azo chromophore provides a simple way to improve the solubility and stability of azo dye. We have shown that by incorporating proper compounds as a coupler, azo dye rotaxanes can be used as pH indicators and metal ion sensors. We have described the synthesis of novel acetylene dye rotaxane using the Pd-catalyzed reaction of Heck-Cassar-Sonogashira-Hagihara type. Its fluorescence properties in the solid state as well as in solutions are examined and compared with those of free dye. Free dye, which has tetra-carboxylic groups, is found to be highly sensitive to various metal ions, exhibiting high Stern-Volmer constants, K_{SV}. On the contrary, acetylene dye rotaxane exhibits much less quenching against various quenchers.

The appearance of an anisotropic phase that is fluorescent has been observed when an acetylene dye and γ-CD are mixed in aqueous solution. Its structural nature is studied by various techniques, including light microscopy, fluorescence, fluorescence anisotropy, wide angle X-ray scattering (WAXD) and differential scanning calorimetry (DSC) measurements. Methyl orange, an acid azo dye, also forms a dimeric inclusion complex with γ-CD, resulting in the formation of stable anisotropic phase, a liquid crystal. Several other azo dyes are also found to form anisotropic phases in the presence of γ-CD, and their structural characteristic has been discussed in terms of the number and position of solubilizing groups.

CHAPTER 1

INTRODUCTION

Cyclodextrins (CDs) are cyclic oligosaccharides, and have been studied extensively as a host molecule in supramolecular chemistry.[1] Three most commonly used CDs are: α-CD (having six glucose units), β-CD (seven glucose units), and γ-CD (eight glucose units). The chemical structures of these CDs are shown in Figure 1.1, in which the glucose units are connected through glycoside α-1,4 bonds.[2]

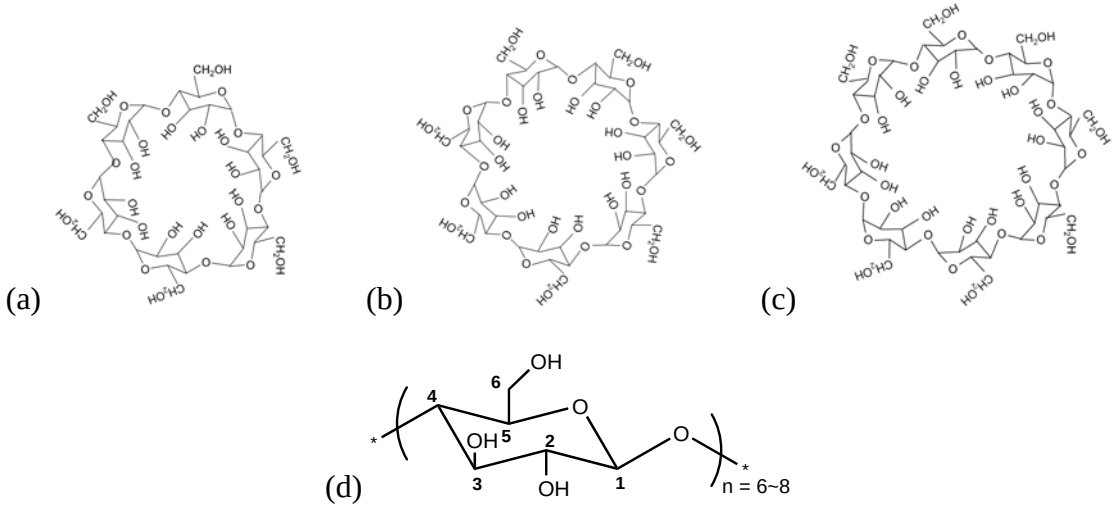

Figure 1.1. Chemical structures of (a) α-CD, (b) β-CD and (c) γ-CD. Glycoside α-1,4 bond is shown in (d) (from ref 2).

Supramolecular chemistry covers all intermolecular interactions where covalent bonds are not involved in interacting components. Many of these interactions are based on host-guest interactions. Since CDs have a large intramolecular cavity, they are one of the most important hosts. CDs have ability to include guest molecules altering their physical, chemical, and biological properties through the formation of inclusion complexes.[1-4] Aside from this, CDs have numerous advantages as a host material; (1) it

is biocompatible and is produced naturally in the degradation of starch, (2) they are relatively cheap, and (3) CDs are non-toxic, leading to applications for drugs, foods, and cosmetics.[1]

1.1. The physical properties of cyclodextrins

The three major CDs are crystalline, non-hygroscopic, and torus-like macrocycles. The approximate cavity dimensions are given in Table 1.1.[2,3] Due to the conical shapes of CDs and deviations from ideal symmetry, their dimensions are accurate to within 0.5 Å.[2] The cavity size increases with the number of glucose units, while the height remains constant at 7.9-8.0 Å. Physical models of CDs are constructed using Corey-Pauling-Kultun (CPK) molecular model, in which the atoms are represented as spheres whose radii are proportional to the atom's van der Waals radius. Such models reveal the actual dimensions of three CD's (Figure 1.2).[5,6]

Table 1.1. Some physical properties of the CDs. Height of the CD: 7.9-8.0 Å (from ref 2 and ref 7).

Property		α-CD	β-CD	γ-CD
Number of glucose units		6	7	8
Molecular weight		972	1135	1297
Water solubility (g/100ml, 25°C)		14.5	1.85	23.0
$[\alpha]_D^{25}$		150.5±0.5	162.5±0.5	177.4±0.5
Diameter (Å)	Cavity	4.7-5.2	6.0-6.4	7.5-8.3
	External	14.6±0.4	15.4±0.4	17.5±0.4
Approx. volume of cavity, (Å^3)		174	262	427
Approx. cavity volume in 1 mol CD (ml)		104	157	256
ΔH^o (solution), (kcal mol^{-1})		7.67	8.31	7.73
ΔS^o (solution), (kcal mol^{-1})		13.8	11.7	14.7

where $[\alpha]_D^{25}$ is specific rotation of sodium D line at 25 °C.

In spite of the apparent trends in size in the series of α-CD, β-CD and γ-CD, the solubility does not follow this trend. β-CD is considerably less soluble in water, compared with other two CDs. The interruption by aggregated β-CD, which has odd (7-fold) symmetry, of the hydrogen-bond structure of water was claimed to be responsible for its unusually low solubility.[3] It was also proposed that the intramolecular hydrogen bonds of the β-CD rim are responsible for its low solubility.[7] However, there are still a lot of controversial discussions ongoing about this aspect.

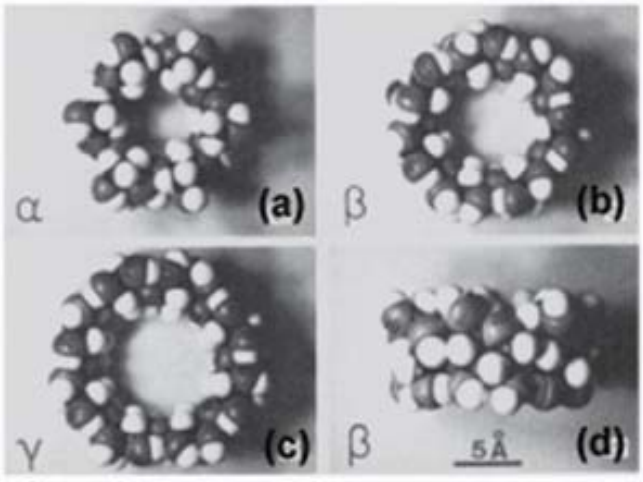

Figure 1.2. Views of CPK models from O(6) side of (a) α-CD, (b) β-CD and (c) γ-CD with a closed ring of O(3)…O(2) hydrogen bonds between adjacent glucose units; (d) side view of β-CD (from ref 5).

There are numerous publications with X-ray structures of CD hydrates and other complexes.[3-14] Crystalline CDs bind 6-13% water, depending on cavity size. α-CD usually forms hexahydrate, α-CD·6H_2O.[7] Four of the six hydration water molecules are located outside the cavity and are part of an extensive hydrogen bonding network. The two remaining water molecules are hydrogen bonded to one another and the water

molecule nearer to the O(6) side is hydrogen bonded to two O(6) hydroxyl groups. Another form, α-CD·7.57H_2O was reported to form when crystallized from aqueous $BaCl_2$.[8] β-CD normally exists as the undecahydrate, β-CD·11H_2O and as the dodecahydrate, β-CD·12H_2O.[9,10] Later it was reported that actual water content depends on ambient humidity, ranging from 12.3H_2O at 100% to about 9.4H_2O at 15% humidity.[11] γ-CD is known to crystallize in its hydrated form, with 7-18 molecules of water.[2,12] Unlike the fixed location of cavity-bound water in α-CD·6H_2O, other CD hydrates have their included water statistically distributed among several possible sites. As a whole, there are two types of water in CD crystals, and included water and interstitial water, and it has been suggested that the cavity-bound water is lost first upon dehydration.[11,13,14]

1.2. The driving force in the inclusion complex with cyclodextrins

The identification of the driving forces involved in the CD inclusion complex is fundamental in understanding CD complexing behaviors, and several reviews have been written dealing with CD complexation.[2,15,16] However, despite numerous efforts to understand the complexation,[14-16] the driving force leading to CD complexation remains unclear and controversial. In this section, we present a summary of the various driving forces thought to be responsible for the formation of host-guest complexes that involves CDs.

The *electrostatic interaction* occurs when two molecules with opposite charge interact each other. Three kinds of electrostatic interactions are frequently mentioned; ion-ion, ion-dipole, dipole-dipole interaction. Since all CDs are basically neutral

molecules, no ion-ion interaction occurs, except for substituted CDs.[17] It is not easy to detect whether ion-dipole interaction is involved in CD complexation. Recently, CD was observed to include some species in the gas phase with mass spectroscopy, in which the ion-dipole interaction is considered to be critical.[18] Unlike these two, dipole-dipole interaction is known to play an important role. Substituted benzoic acids in the para-positions are reported to show increased binding due to this interaction.[19] Also the acidities of 4-substituted phenols are enhanced as a result of CD complexation.[20] Dipole moments of the benzoic acids and phenols are responsible for this behavior, and they are usually directed from the hydroxyl group to the *para* substituent. Thus, the dipole-dipole interaction is considered to be important in the formation of a CD complex.

The involvement of *van der Waals interaction* in CD complexation has been shown by correlation analysis between the strength of binding and the structural features of the substrates.[21-23] A study revealed that bulky guest molecules are in close van der Waals contact with the CD cavities.[24] Sometimes, van der Waals interaction exerts so strongly that the hydrophobic bulky side of the guest molecule can enter the CD cavity. For instance, the sulfonate group in azo dye is observed to be included in the CD complexation.[25] The fact that CDs can form stable complexes with guests in organic solvents such as DMF, DMSO, and even heptanes confirms that van der Waals interaction is quite important.[26]

Hydrophobic interaction is favored after the release of the included water, leading to the aggregation of non-polar solutes in aqueous solution.[27] Thermodynamic measurements for the association of nonpolar molecules in water show that CD complexation accompanies negative values in enthalpy and entropy changes.[28] This may

indicate that hydrophobic interaction is not a major driving force in CD complexation. Interestingly, the binding constants of CD increase when D_2O is used as the solvent instead of H_2O, which can be caused since the hydrophobic interaction is stronger in the case of D_2O than in H_2O.[29] Also, an increase in the hydrophobicity of the substituents of the guest molecule enhances the complexation.[30] Other evidence shows that the strength of CD complexation is usually weakened upon the addition of organic cosolvent.[31] Therefore, the role of the hydrophobic interaction in CD complexation is still a controversial problem.

Hydrogen bonding is typically an interaction involving an electronegative donor, a hydrogen atom, and an acceptor, F, O and N atoms. The crystal structures of CD complexes clearly show the well-defined hydrogen bonds between the substrates and the hydroxyls of CDs.[32] Usually, the host-guest hydrogen bondings come from the primary O(6)-H groups of CDs which are flexible and can rotate about the C(5)-C(6) bond. In contrast, the secondary O(2) and O(3) atoms are rigid. However, sometimes there are also C-H…O, C-H…N, and C-H…π interactions between the cavity wall of CDs and the guest molecules.[33] β-CD shows a strong binding constant at higher pH conditions, when complexed with carboxylic acid derivatives.[34] It is due to hydrogen bonding between the deprotonated secondary OH and the hydroxyl group of the substrate at higher pH range. But, after β-CD is converted into heptakis (2,3,6-tri-O-methyl)-β-CD (TM-β-CD), there are little changes in binding constant, probably because TM-β-CD cannot undergo deprotonation even under the same condition.[34] Therefore, hydrogen bonding plays an important role in the formation of CD complex.

Enthalpy-entropy compensation is the phenomenon in which the change in enthalpy is offset by a corresponding change in entropy resulting in a smaller net free energy change, and it is believed to play an important role in the reactions in solution.[35] In CD chemistry, a systematic study on this behavior has been conducted, and it is suggested that the slope and intercept of the enthalpy – entropy (ΔH - $T\Delta S$) plot can lead to quantitative measures of the conformational change and extent of desolvation upon complexation.[36]

Obviously, the formation of CD inclusion complex is quite complicated. As a whole, it is accepted, however, that van der Waals interaction and hydrophobic interaction are considered to be the major driving forces for CD complexation, while electrostatic interaction and hydrogen bonding can exert the conformation of the inclusion complex in some cases.

1.3 Cyclodextrin inclusion complex

As mentioned earlier, a supramolecular structure results from non-covalent interaction between individual molecules. Generally, host molecules provide cavity so that a guest molecule can be included within their cavity. Due to the hydrophilic nature of CD exterior, a lot of inclusion complexes are reported to form in aqueous solution.[37,38] A variety of CD inclusion compounds have been reported and the topology of the inclusion is schematically shown in Figure 1.3.

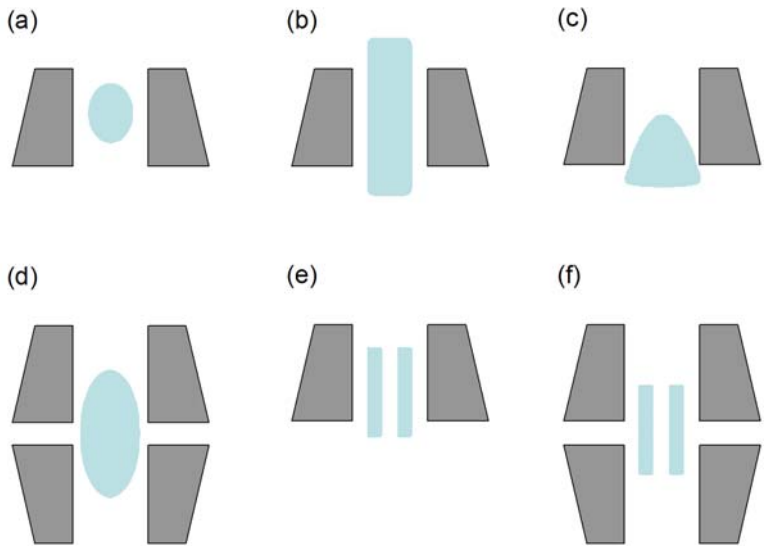

Figure 1.3. Topology of CD inclusion complexes: (a) complete, (b) axial, (c) partial, (d) sandwich-type, (e) 1:2 and (f) 2:2 inclusion complexes (from ref 38).

1.3.1 Dye rotaxane

A rotaxane is a supramolecular assembly of a dumbbell-like shape that has a macrocycle around the molecular axis. It is generally formed when molecules thread the cavities of macrocycles and bulky terminal groups on both sides of the CD cavity prevent the threaded molecule from escaping (Figure 1.4).[39,40]

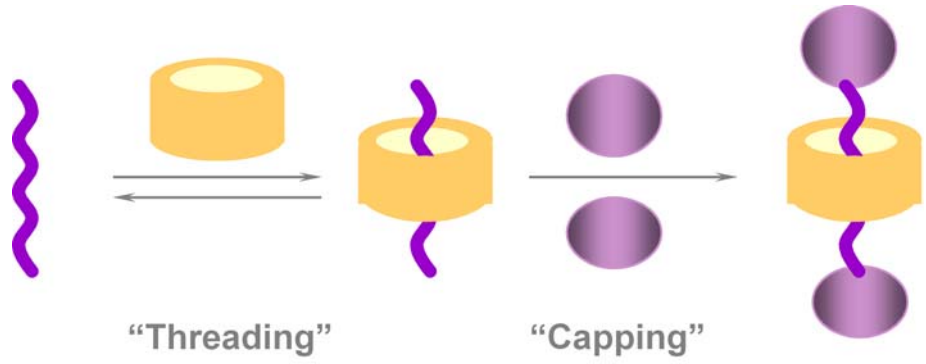

Figure 1.4. Rotaxane formation via threading and capping (from ref 40).

A variety of water soluble azo-dye rotaxanes have been synthesized using the hydrophobic effect to direct rotaxane formation, where cyclophane and α- and β-CD were used as macrocycles.[41] The isolation of rotaxane dyes from free dye and free CDs was quite difficult, and the yield was reported to be low. In their crystal structure, the macrocycle was found to embrace the center of azo dye.[42] CD can act as a protective sheath for azo dye by including its chromophore inside the cavity. Azo dye [3]rotaxane was synthesized by using 2,6-dimethylphenol as couplers.[43] It is surprising, as the authors mentioned, to yield an azo dye [3]rotaxane as a single stereoisomer, with the 2,3-rims of both CDs pointing outwards. It was reported that rotaxane-encapsulation enhances the stability of azo dye without detrimentally preventing the dye from binding to the surface of the fibers.[44] When cellulose was dyed with a chlorotriazine-functionalized azo dye rotaxane, its stability to bleaching treatment was dramatically increased. This was the first report of its synthesis in quantitative yield on a gram scale, which opened promising commercial applications. The improved stability also suggests that azo dye rotaxane has promising applications in areas where chromophore stability is required. Benefits obtained by forming dye rotaxane with CDs are summarized (Figure 1.5).

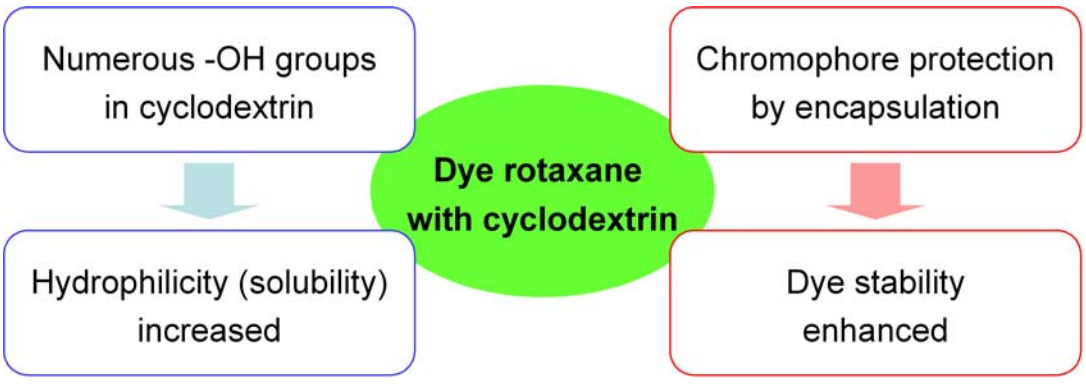

Figure 1.5. Benefits from rotaxane formation with CDs.

When cyanine dyes, which have extended conjugation, were encapsulated within CDs, their fluorescence efficiency and photostability were increased.[45] The fluorescence is enhanced in various non-aqueous solvents, due to the reduction of the quenching effect of an aqueous environment. The fluorescence efficiency was enhanced due to the reduced flexibility of the encapsulated chromophore. Encapsulation also results in a red shift in the absorption and emission spectra of cyanine rotaxane. The inclusion of cyanine dyes in CD improved the photostability both by reducing the rate of singlet oxygen formation and by reducing the rate of reaction between singlet oxygen and the dye.[46] However, the yield of the reaction, which was based on the condensation between 3-(9-julolidinyl)prop-2-en-1-al and N-(1-adamantyl)-4-methylpyridinium chloride in the presence of α-CD, was reported to be very low and it was extremely hard to isolate the final product. Due to the rotaxane formation, however, a cyanine dye can undergo reversible redox processes, and its kinetic stability is increased.[47] This result is significant in that rotaxane encapsulation protects the chromophore both in its excited state and in its oxidized and reduced forms.

The synthesis of fluorescent stilbene and tolan rotaxanes were reported in fairly good yield using the aqueous Suzuki coupling (Figure 1.6).[48] CD reduced the rate of non-radiative decay by restricting the flexibility of the excited state, and by hindering the quenchers. The discovery and application of Suzuki coupling in the synthesis of rotaxane structure are of great importance. The right combination of aryl iodide stopper, diboronic acid core and CDs gives highly fluorescent dye rotaxanes in high yield. The synthesis of a genuine polyrotaxane, which will be discussed later (see chapter 1.3.2), is also based on Suzuki coupling.

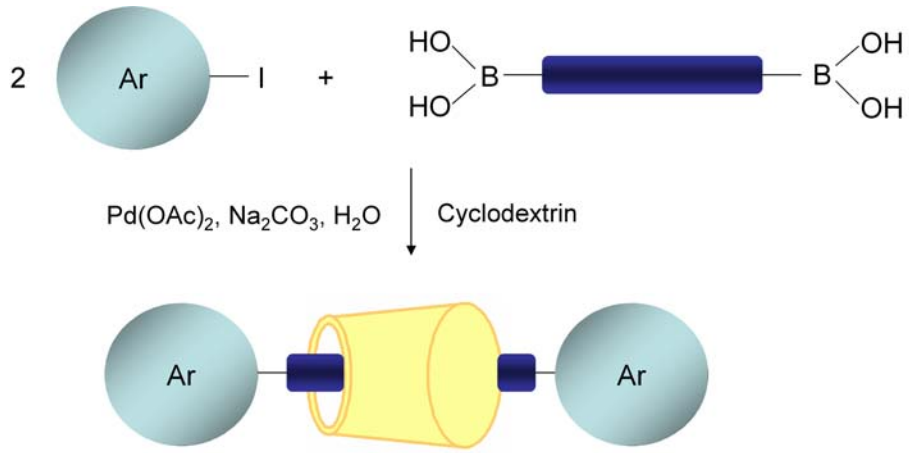

Figure 1.6. Synthetic schemes for the synthesis of fluorescent dye rotaxane using Suzuki coupling (from ref 48).

E/Z photoisomerization within the rotaxane structure was investigated.[49] It was shown that threaded CD macrocycle could shuttle along the dye molecule by the external stimulus of light without forming any by-products. The presence of CD reduces the fluorescence quantum yield $\phi_{E\rightarrow Z}$, without any changes on $\phi_{Z\rightarrow E}$. Based on these results, more probable mechanism for rotaxane photoisomerization was proposed (Route 2 in Figure 1.7).

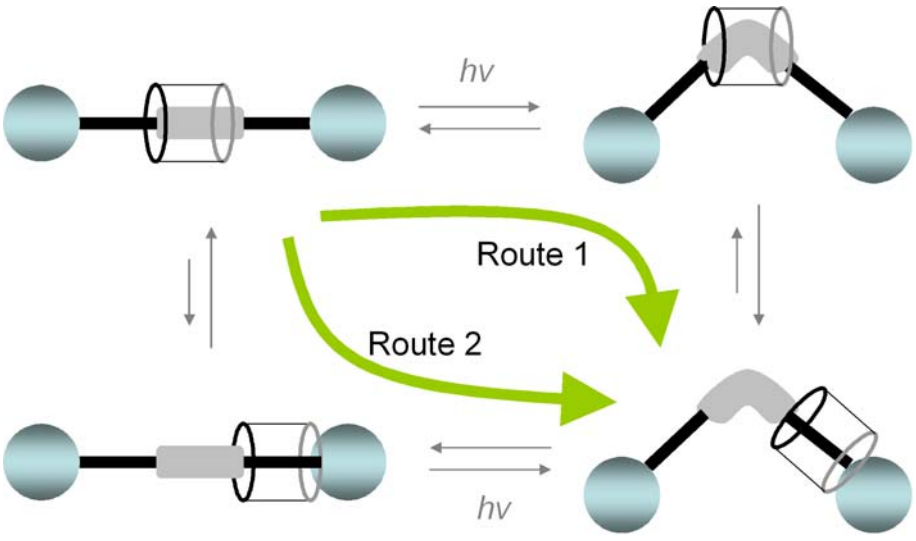

Figure 1.7. Photoisomerization mechanism for rotaxane structure (from ref 49).

1.3.2 Polyrotaxane of conjugate polymers

The conjugated polymers, such as Poly(para-phenylenevinylene)s, are of great interest and are being extensively studied due to their efficient luminescence and charge-transport properties which lead to useful applications in light emitting diodes, sensors and lasers.[50-52] In polymer light-emitting devices (PLEDs), electrons and holes are injected from a cathode and anode respectively into the luminescent semiconducting polymer (Figure 1.8).[53] The electrons and holes are transported through the polymer and combine to create the excited state that emits light. For optimum device performance, the polymeric semiconductor must have good electron and hole mobility as well as high efficiency for the conversion of each excited state into a photon of light. It is required to create polymers with intermolecular electronic interactions, in order to have high electron and hole mobility.[54] However, to maintain high efficiency emission, on the contrary, such interactions need to be avoided, since the planar and rigid nature of the conductive polymers causes face-to-face stacking, resulting in strong intermolecular interactions that usually lead to low luminescence efficiencies.[55,56]

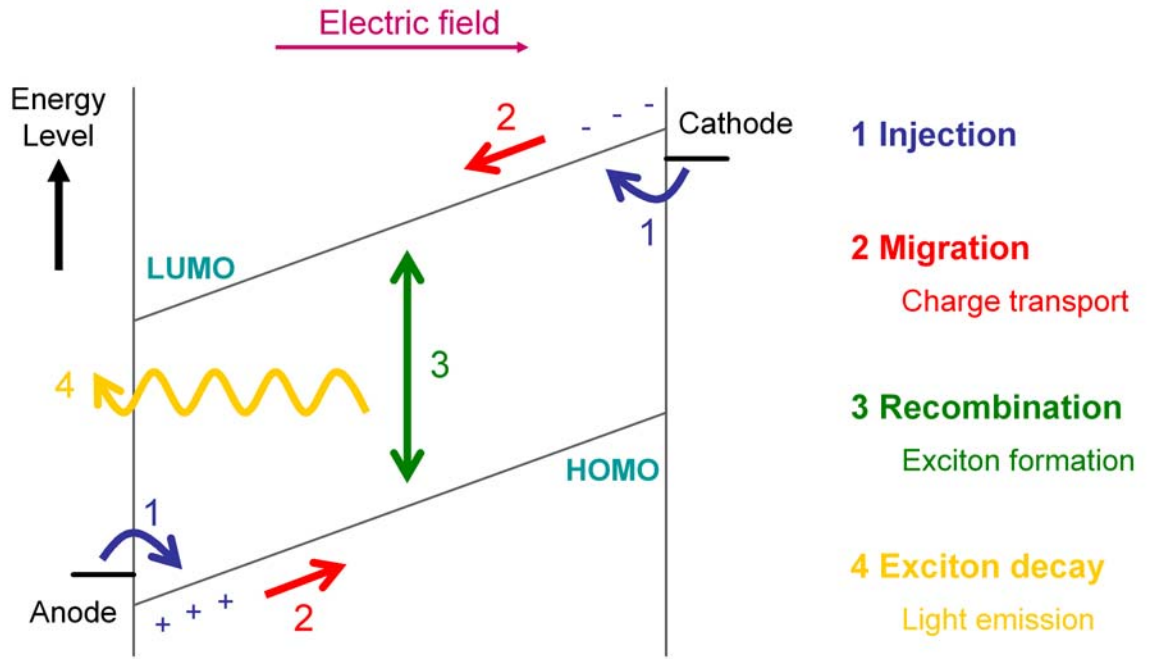

Figure 1.8. Device operation of polymer light-emitting devices (PLEDs) (from ref 53).

In order to produce charge-transporting materials, attempts have been made to thread these conjugated polymers through CDs, to from conjugated polyrotaxanes as a form of "insulated molecular wire" (Figure 1.9).[57] The CD insulation was intended to prevent above-mentioned detrimental intermolecular interactions in PLED applications, while still allowing the polymers to be close enough to have charge transfer.[58] Molecular electronic materials are often highly reactive, which leads to the polymer being unstable. Stability of the polymer could be improved by the use of molecular insulation, since CD acts as protective sheath, and the insulation should reduce cofacial π-interactions.

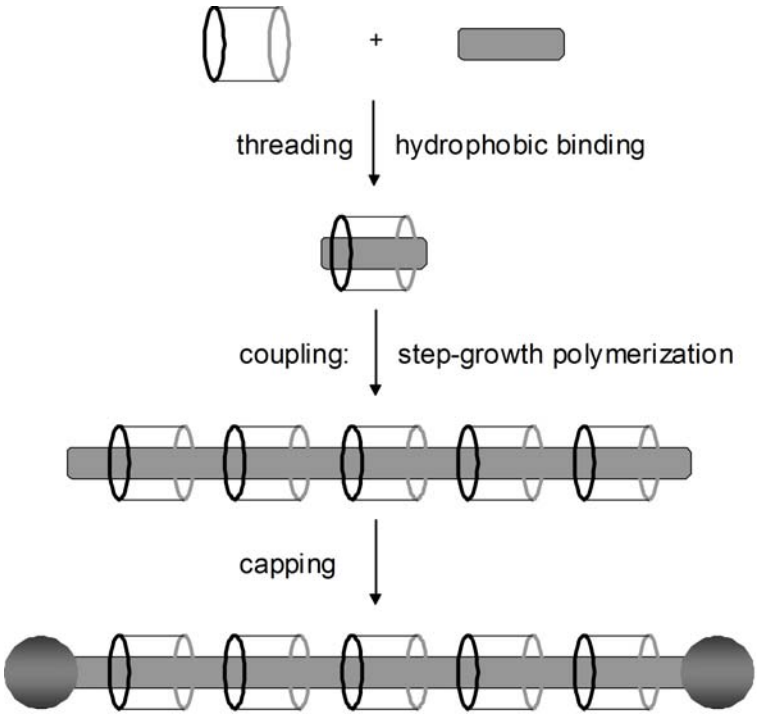

Figure 1.9. The synthesis of an insulated molecular wire (from ref 57).

The first polyrotaxane with conjugated backbone was synthesized using cyclophane as macrocycles, in which its emission intensity was found to be several times stronger than that of free dumbbell.[59] The presence of cyclophane rings increases the fluorescent efficiency by hindering quenching and increasing the kinetic stability of the excited state. However, polyrotaxanes higher than [3]rotaxanes couldn't be made, due to inherent problems of unthreading, aggregation, and precipitation of the growing polymer chains during synthetic processes.[60]

Genuine polyrotaxane in the form of molecular wire was realized, using β-cyclodextrin (β-CD) as the macrocycle and Suzuki coupling as the polymerization reaction.[57-61] Upon rotaxanation, there is a large change in its electronic absorption and fluorescent spectra; encapsulation of the chromophore results in a blue shift of 20 nm in emission along with significant enhancement in its fluorescence quantum yield.

Photochemical properties of these polyrotaxanes were examined for PLED applications.[58] The formation of CD inclusion does not change the frontier energy level according to cyclic voltammetry measurements. However, the inclusion within CD cavity makes some changes in the optical absorption and emission spectra of thin films. First, the linear absorption coefficient α for the polyrotaxanes is found to be smaller than free polymers, since the presence of CD dilutes the conjugation density. Second, the photoluminescence spectra of polyrotaxanes are blue-shifted, up to 30 nm, due to the reduction of intermolecular π-π interactions. Third, higher photoluminescence efficiency is observed in the rotaxanated forms, partly due to the chromophore protection by CD against quenching of the luminescence by outside stimulus.

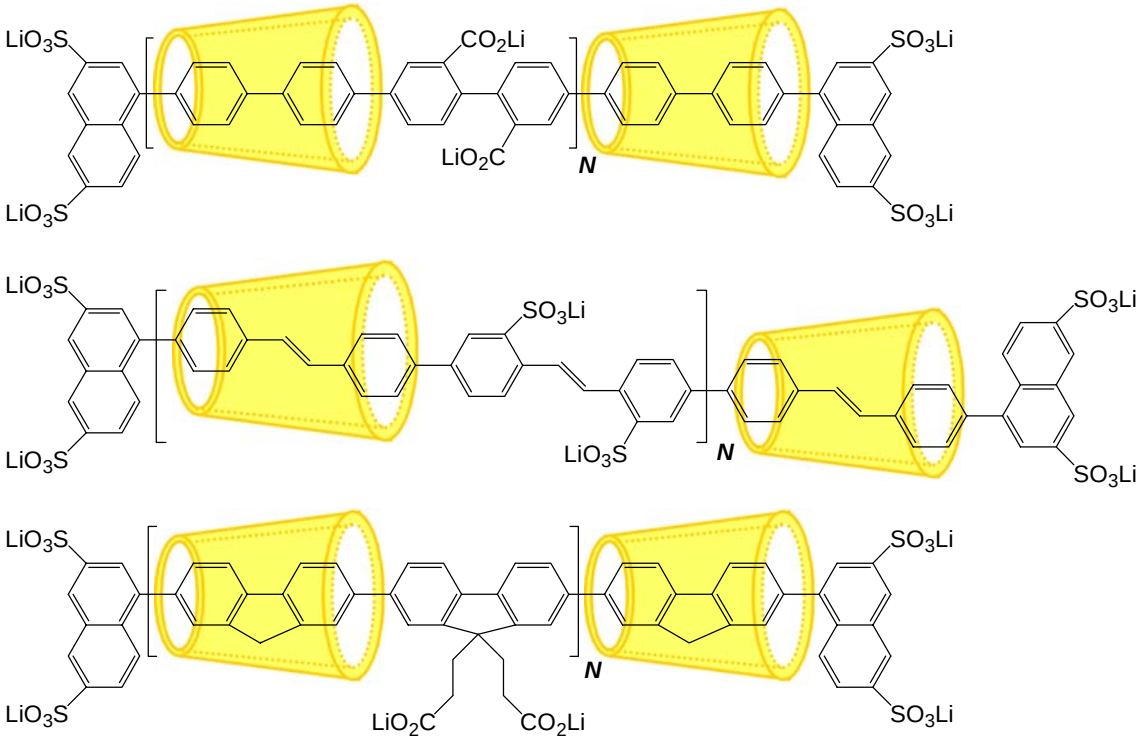

Figure 1.10. Chemical structures of polyrotaxanes; poly-para-phenylene with β-CD (β-CD-PPP, upper), poly(4,4'-diphenylenevinylene) with α-CD (α-CD-PDV, middle) and polyfluorene with β-CD (β-CD-PF, lower) (from ref 58).

Rotaxane structure provides an efficient way to prevent π-π stacking at a fixed separation, determined by the size of CD macrocycle, and this physical separation is large enough to prevent self-quenching.[62] The rotaxane formation clearly shows the beneficial effect of supramolecular architecture in terms of both external quantum efficiency and luminescence. The useful aspects of polyrotaxanes are reported as follows; the aggregation of conjugated backbone is prohibited, luminescence efficiency is improved with blue-shifted emission, protected chromophore becomes more stable, and aqueous solubility is increased.

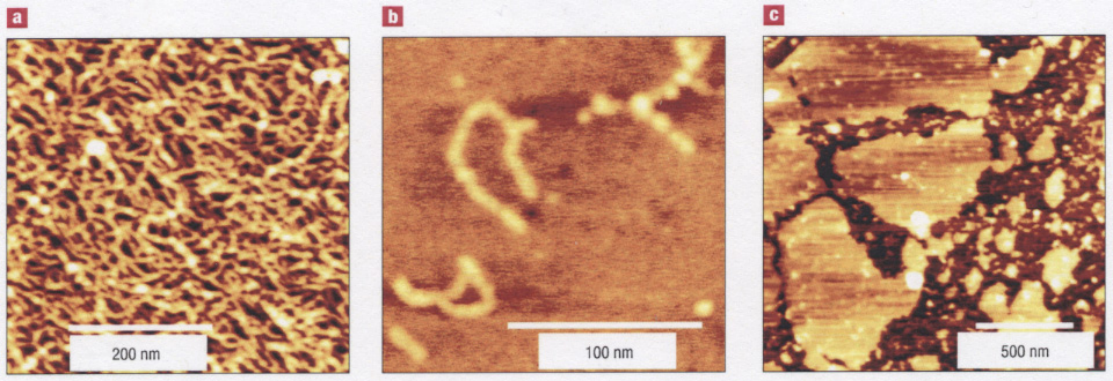

Figure 1.11. Tapping mode scanning force microscopy (TM-SFM) images of polyrotaxane. (a) & (b) β-CD-PPP : The polyrotaxanes are densely packed, still allowing individual molecules to be distinguished from one another, (c) free PPP : unrotaxanated polymer assembles into domains by forming π-π staking of polymer chains (from ref 58).

1.3.3 Dye inclusion complex

Some dye molecules are known to differently behave when trapped inside a small cavity. The most frequently investigated molecules as guests in inclusion complexes are acid azo dyes. The interaction of azo dyes with CDs has been investigated as a measure to control their stability, solubility and aggregation.[63,64] There are systematic studies concerning the interaction of methyl orange and orange II with γ-CD (Figure 1.12).[65-68] In

order to elucidate the direction of inclusion and the stacking mode, various characterization methods were used, including ^{1}H / ^{13}C-NMR, UV-vis spectra, and circular dichroism. It was also reported the Orange II with CD can form liquid crystalline phase.[69] Orange II and γ-cyclodextrin were found to form 2:1 and 2:2 complexes, leading to the formation of a fibroid aggregate when observed in optical microscope.[70] The azo dyes that have a tight fit in the CD cavity exhibit exciton interaction between two molecules of the chromophoric dye included in the complexes.[71] The decrease in conductance was observed, since resultant inclusion complex is less conductive due to its large molecular weight.[72] The method of Benesi and Hildebrand (B-H) has been the most popular method for estimating the equilibrium constant (K) and the extinction coefficient (ε) of the 1:1 complex.[73] A modified method was suggested, by which 2:1 complex of γ-CD with azo dyes could be successfully explained.[74]

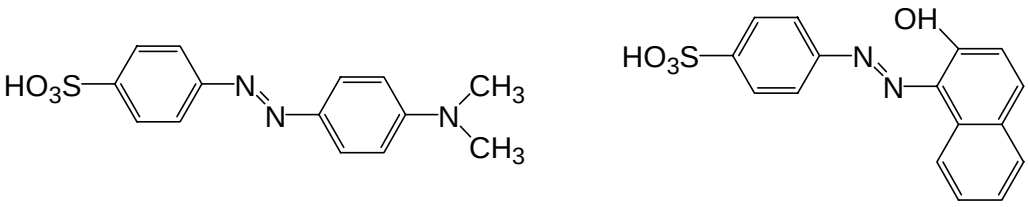

Figure 1.12. Chemical structure of Methyl Orange (left) and Orange II (right).

The cis-trans thermal isomerization of *p*-aminoazobenzenes proceeds in two possible routes as shown in Figure 1.13; inversion or rotation mechanism.[75] It was found out that in the presence of β-CD, the isomerization rate was measured to be very slow, and that inversion route was preferred than rotation.[75] It was attributed to the formation of an inclusion complex between dyes and β-CD which hinders the rotation of the N=N bond. Recently, femtosecond transient absorption measurement was carried out in order

to address the kinetics of photoisomerization of azobenzene.[76] The experimental results reveal that excitation of the S_1 (n-π*) band of azobenzene leads to photoisomerization via inversion at one of the nitrogen atoms. The photoisomerization of methyl orange in the presence of CDs was measured using the femtosecond time-resolved spectroscopy.[77] The transient absorption measurement showed that 1:1 dye:α-CD complex was almost the same as that of free dye, while 1:2 dye:α-CD showed slower relaxation and lower yield of cis isomer. This behavior was due to the steric effect in CD-dye interactions. In the case of γ-CD, 2:2 complex was observed to have significantly slower relaxation, and form no cis isomer. Upon photo-excitation, the intermolecular interaction of two dye molecules was enhanced, resulting in the formation of an aggregate in the large cavity of γ-CD.

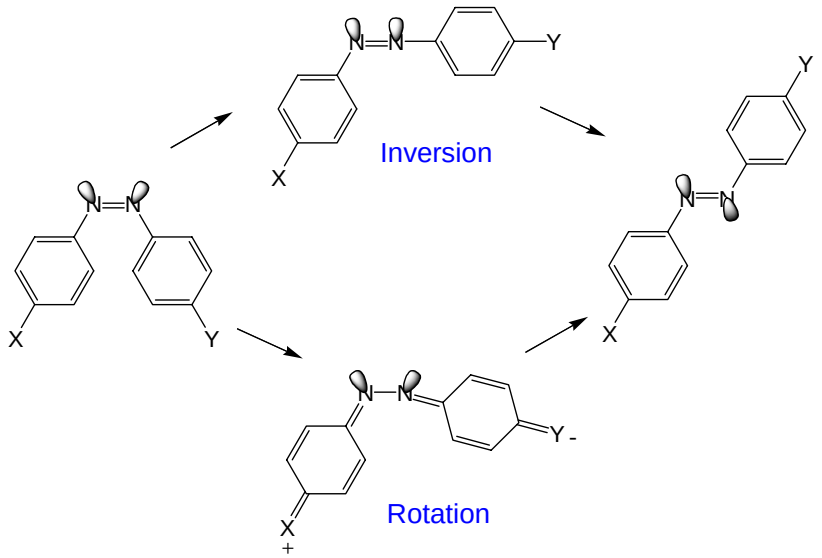

Figure 1.13. The thermal *Z-E* isomerization of *p*-substituted azobenzene (from ref 75).

There have been several reports about fluorescent property changes for one host-two guests complexation in the presence of γ-CD.[78-81] Unlike the other CDs, larger cavity

of γ-CD enable dimeric inclusion.[80,81] It was proposed that two pyrene (Py) molecules enter the γ-CD cavity to form 2:1 Py:γ-CD inclusion complex that emits the excimer fluorescence.[82] 2:2 Py:γ-CD inclusion complexes are also reported, and depending on complexing ratios, different fluorescent behaviors are reported.[83] 2,5-Diphenyloxazole (DPO) drew a great deal of interest, since it showed a very long fluorescence lifetime due to excimer formation. DPO was found to self-assemble within the cavity of CDs forming extended molecular aggregates, held together by inclusion complexation.[84] Oxadiazole derivatives showed similar behavior as DPO, forming higher order aggregation at high concentration, and the emission of these rod-like aggregates was found to be highly polarized.[85]

1.4. The thesis outline

The formation of CD inclusion complexes with dyes has continuously drawn our interest due to their various beneficial effects mentioned earlier. This thesis covers the study of inclusion complexes of CDs and chromophore dyes, largely in two ways; rotaxane and pseudorotaxane. The stable rotaxane structure is achieved with the synthesis of dye rotaxane. A couple of azo dye rotaxanes and a acetylene dye rotaxane have been synthesized and their physical properties have studied in this thesis. The study about inclusion behaviors of CDs, in terms of pseudorotaxane, is done with fluorescent acetylene dye-γ-CD complex and methyl orange-γ-CD complex.

Chapter 2 describes the synthesis of azo dye rotaxane and its property changes in terms of its solubility and stability. Its pH sensitivity is examined and compared with that of free dye. Chapter 3 describes the synthesis of azoxine dye rotaxane and its polymeric

metal complex. Its characteristic properties as pH indicators and metal ion sensors are discussed. Dyeing property of azoxine dye rotaxane for polypropylene fiber is examined. Chapter 4 covers the synthesis of a fluorescent acetylene dye rotaxane. Its fluorescence properties in the solid state as well as in solutions are examined. Fluorescence quenching behavior is investigated in the presence of various metal ions. Chapter 5 exploits the appearance of fluorescent anisotropic structure by the formation of inclusion complex between acetylene dye and γ-CD. Its structural nature is studied by fluorescence, WAXD, and DSC measurements. In Chapter 6, we demonstrate the formation of anisotropic supramolecules with methyl orange and γ-CD. The complex formation is estimated by UV measurements. The pH dependency on the appearance of anisotropy is also described. In Chapter 7, the important results of the study are summarized and recommendations for future work are suggested.

From the present studies, we expect to get some fundamental understanding of CD-dye complexes, and see their beneficial characteristics. This will lead to facile and effective modification in dyes' properties for the promising applications.

REFERENCES

[1] Szejtli, J. “Introduction and general overview of cyclodextrin chemistry”, *Chem. Rev.* **1998**, *98*, 1743.

[2] Connors, K. A. “The stability of cyclodextrin complexes in solution”, *Chem. Rev.* **1997**, *97*, 1325.

[3] Szejtli, J. *Cyclodextrin Technology*, Kluwer: Dordrecht, 1988.

[4] Uekama, K.; Hirayama, F.; Irie, T. “Cyclodextrin drug carrier systems”, *Chem. Rev.* **1998**, *98*, 2045.

[5] Saenger, W. “Cyclodextrin inclusion compounds in research and industry”, *Angew. Chem. Int. Ed. Engl.* **1980**, *19*, 344.

[6] Lichtenthaler, F.W.; Immel, S. “Molecular modeling of saccharides. 9. On the hydrophobic characteristics of cyclodextrins: Computer-aided visualization of molecular lipophilicity patterns”, *Liebig’s Ann.* **1996**, (1), 27.

[7] Manor, P. C.; Saenger, W. “Topography of cyclodextrin inclusion complexes. III. Crystall and molecular structure of cyclohexaamylose hexadrate, the (H2O)2 inclusion complex”, *J. Am. Chem. Soc.* **1974**, *96*, 3630.

[8] Chacko, K. K.; Saenger, W. “Topography of cyclodextrin inclusion complexes. 15. Crystal and molecular structure of the cyclohexaamylose-7.57 water complex, Form III. Four and six-membered circular hydrogen bonds”, *J. Am. Chem. Soc.* **1981**, *103*, 1708.

[9] Lindner, K.; Saenger, W. “β-cyclodextrin dodecahydrat-crowding of water-molecules within a hydrophobic cavity”, *Angew. Chem. Int. Ed.* **1978**, *17*, 694.

[10] Fujiwara, T.; Yamazaki, M.; Tomizu, Y.; Tokuoka, R.; Tomita, K.; Matsuo, T.; Suga, H.; Saenger, W. “The crystal-structure of a new form of β-cyclodextrin water inclusion compound and thermal properties of β-cyclodextrin inclusion complexes”, *Nippon Kagaku Kaishi* **1983**, *(2)*, 181.

[11] Steiner, T.; Koellner, G. “Crystalline β-cyclodextrin hydrate at various humidities: fast, continuous, and reversible dehydration studied by X-ray diffraction”, *J. Am. Chem. Soc.* **1994**, *116*, 5122.

[12] Usha, M. G.; Wittebort, R. J. "Structural and dynamical studies of the hydrate, exchangeable hydrogens, and included molecules in β- and γ-cyclodextrins by powder and single-crystal deuterium magnetic resonance", *J. Am. Chem. Soc.* **1992**, *114*, 1541.

[13] Danil de Namor, A. F.; Traboulssi, R.; Lewis, D. F. V. "Host properties of cyclodextrins toward anion constituents of antigenic determinants. A thermodynamic study in water and in N,N-dimethylformamide", *J. Am. Chem. Soc.* **1990**, *12*, 8442.

[14] Koschmidder, M.; Uruska, I. "Influence of inorganic ions on the enthalpies of solution of β-cyclodextrin in aqueous solutions", *Thermochim. Acta* **1995**, *249*, 63.

[15] Griffiths, D. W.; Bender, M. L. "Orientational catalysis by cyclohexaamylose", *J. Am. Chem. Soc.* **1973**, *95*, 1679.

[16] Tabushi, I.; kuroda, Y.; Mizutani, T. "Functionalized cyclodextrins as artificial receptors – guest binding to bisimidazolyl-beta-cyclodextrin.zinc", *Tetrahedron* **1984**, *40*, 545.

[17] Yatsimirskii, A. K.; Eliseev, A. V. "Hydroxylaion selectivity of phenol and o-protected phenols in the Fe (II)-catechol-H_2O_2 system", *J Chem. Soc. Perkin Trans. 2* **1991**, 1769.

[18] Ramirez, J.; Ahn, S.; Grigorean, G.; Lebrilla, C. B. "Chiral recognition in gas-phase cyclodextrin: amino acid complexes – Is the three point interaction still valid in the gas phase", *J. Am. Soc.Mass Spec.* **2001**, *12*, 278.

[19] Connors, K. A.; Lin, S. F.; Wong, A. B. "Potentiometric study of molecular-complexes of weak acids and based applied to complexes of alpha-cyclodextrin with para-substituted benzoic acids", *J Pharm. Sci.* **1982**, *71*, 217.

[20] Wong, A. B.; Lin, S. F.; Connors, K. A. "Stability-constants for complex-formation between alpha-cyclodextrin and some amines", *J Pharm. Sci.* **1983**, *72*, 388.

[21] Harata, K. "Temperature effects on CD spectra of beta-cyclodextrin complexes with 2-substituted naphthalenes", *Bull. Chem. Soc. Jpn.* **1979**, *52*, 1807.

[22] Bertrand G. L.; Faulkner, J. R.; Han, S. M.; Armstrong, D. W. "Substituted effects on the binding of phenols to cyclodextrins in aqueous-solution", *J. Phys. Chem.* **1989**, *93*, 6863.

[23] Eftink, M. R.; Andy, M. L.; Bystrom, K.; Perlmutter, H. D.; Kristol, D. S. "Cyclodextrin inclusion complexes-studies of the variation in the size of alicyclic guests", *J. Am. Chem. Soc.* **1989**, *111*, 6765.

[24] Mcmullan, R. K.; Saenger, W.; Fayos, J.; Mootz, D. "Topography of cyclodextrin inclusion complexes. 2. Iodine-cyclohexaamylose tetrahydrate complex – its molecular geometry and cage-type crystal structure", *Carbohydr. Res.* **1973**, *31*, 211.

[25] Suzuki, M.; Kajrar, M.; Szejtli, J.; Vikmon, M.; Fenyvesi, E. "Inclusion compounds of cyclodextrins and azo dyes. 10. Induced circular-dichroism spectra of complexes of cyclomaltooligosaccharides an azo dyes containing naphthalene nuclei", *Carbohyd. Res.* **1992**, *223*, 71.

[26] Manka, J. S.; Lawrence, D. S. "Self-assembly of a hydrophobic groove", *Tetrahedron Lett.* **1989**, *30*, 7341.

[27] Nemethy, G.; Scheraga, H. A. "Structure of water and hydrophobic bonding in proteins. 1. Model for thermodynamic properties of liquid water", *J. Chem. Phys.* **1962**, *36*, 3382.

[28] Rekharsky, M. V.; Inoue, Y. "Complexation thermodynamics of cyclodextrins", *Chem. Rev.* **1998**, *98*, 1875.

[29] Kresheck, G. C.; Schneider, H.; Scheraga, H. A. "Thermodynamic parameters of hydrophobic bond formation in a model system", *J. Phys. Chem.* **1965**, *69*, 3132.

[30] Matsuura, N.; Takenaka, S.; Tokura, N. "Formation of inclusion complexes of benzophenone derivatives – Beta-cyclodextrin studied by induced circular dichroism", *J Chem. Soc. Perkin Trans. 2* **1977**, 1419.

[31] Tee, O. S.; Mazza, C.; Lazano-Hemmer, R. "Ester cleavage by cyclodextrins in aqueous dimethylsulfoxide mixtures – substrate binding versus transition-state binding", *J Org. Chem.* **1994**, *59*, 7602.

[32] Hamilton, J. A.; Chen, L. Y. "Crystal structure of an inclusion complex of beta-cyclodextrin with racemic fenoprofen – direct evidence for chiral recognition", *J Am. Chem. Soc.* **1988**, *110*, 5833.

[33] Steiner, T.; Saenger, W. "Geometry of C-H…O hydrogen bonds in carbohydrate crystal structures – Analysis of neutron diffraction data", *J Am. Chem. Soc.* **1992**, *114*, 10146.

[34] Yi, Z. P.; Chen, H. L.; Huang, Z. Z.; Huang, Q.; Yu, J. S. "Contribution of weak interactions to the inclusion complextion of 3-hydroxynaphthalene-2-carboxylic acid and its analogues with cyclodextrins", *J Chem. Soc. Perkin Trans. 2* **2000**, 121.

[35] Inoue, Y.; Hakushi, T.; Liu, Y.; Tong, L. H.; Shen, B. J.; Jin, D. S. "Thermodynamics of molecular recognition by cyclodextrins. 1. Calorimetric titration of inclusion complexation of naphthalenesulfonates with alpha-cyclodextrin, beta-cyclodextrin, and gamma-cyclodextrin – Enthalph entropy compensation", *J. Am. Chem. Soc.* **1993**, *115*, 475.

[36] Inoue, Y.; Liu, Y.; Tong, L. H.; Shen, B. J.; jin, D. S. "Thermodynamics of molecular recognition by cyclodextrins. 2. Calorimetric titration of inclusion complexation with modified beta-cyclodextrins – Enthalpy – entropy compensation in host-guest complexation – From ionophore to cyclodextrin and cyclophane", *J. Am. Chem. Soc.* **1993**, *115*, 10637.

[37] Schneider, H.-J. "Mechanism of molecular recognition: Investigations of organic host-guest complexes", *Angew, Chem. Int. Ed.* **1991**, *30*, 1417.

[38] Wenz, G. "Cyclodextrins as building blocks for supramolecular structures and functional units", *Angew. Chem. Int. Ed. Engl.* **1994**, *33*, 803.

[39] Nepogodiev, S. A.; Stoddart, J. F. "Cyclodextrin-based catenanes and rotaxanes", *Chem. Rev*. **1998,** *98*, 1959.

[40] Harada, A. "Cyclodextrin-based molecular machines", *Acc. Chem. Re*s. **2001,** *34*, 456.

[41] Anderson, S.; Claridge, T. D. W.; Anderson, H. L. "Azo-dye rotaxanes", *Angew. Chem. Int. Ed.* **1997**, *36*, 1310.

[42] Anderson, S.; Clegg, W.; Anderson H. L. "Crystal structure of an azo dye rotaxane", *Chem. Comm.* **1998**, (21), 2379.

[43] Craig, M. R.; Claridge, T. D. W.; Hutchings, M. G.; Anderson, H. L. "Synthesis of a cyclodextrin azo dye [3]rotaxane as a single isomer", *Chem. Comm.* **1999**, (16), 1539.

[44] Craig, M. R.; Hutchings, M. G.; Claridge, T. D. W.; Anderson H. L. "Rotaxane-encapsulation enhances the stability of an azo dye, in solution and when bonded to cellulose", *Angew. Chem. Int. Ed.* **2001**, *40*, 1071.

[45] Buston J. E. H.; Young, J. R.; Anderson, H. L. "Rotaxane-encapsulated cyanine dyes: enhanced fluorescence efficiency and photostability", *Chem. Comm.* **2000**, (11), 905.

[46] Matsuzawa, Y.; Tamura, S.; Matsuzawa, N.; Ata, M. "Light-stability of a β-cyclodextrin (cyclomaltoheptaose) inclusion complex of a cyanine dye", *J. Chem. Soc., Faraday Trans.* **1990**, *90*, 3517.

[47] Buston J. E. H.; Marken, F.; Anderson, H. L. “Enhanced chemical reversibility of redox processes in cyanine dye rotaxanes”, *Chem. Comm.* **2001**, (11), 1046.

[48] Stanier, C. A.; O’Connell, M. J.; Clegg, W.; Anderson, H. L. “Synthesis of fluorescent stilbene and tolan rotaxanes by Suzuki coupling”, *Chem. Comm.* **2001**, (8), 493.

[49] Stanier, C. A.; Alderman, S. J.; Claridge, T. D. W.; Anderson, H. L. “Unidirectional photoinduced shuttling in a rotaxane with a symmetric stilbene dumbbell”, *Angew. Chem. Int. Ed.* **2002**, *41*, 1769.

[50] Kraft, A.; Grimsdale, A. C.; Holmes, A. B. “Electroluminescent conjugated polymers – Seeing polymers in a new light”, *Angew. Chem. Int. Ed.* **1998**, 37, 403.

[51] Hide, F.; Diaz-Garcia, M. A.; Shcwartz, B. J.; Heeger, A. J. “New Developments in the photonic applications of conjugated polymers”, *Acc. Chem. Res.* **1997**, 30, 430.

[52] Davis, W. B.; Svec, W. A.; Ratner, M. A.; Wasielewski, M. R. “Molecular-wire behavior in p-phenylenevinylene oligomers”, *Nature*, **1998**, 396, 60.

[53] Friend, R. H.; Gymer, R. H.; Holmes, A. B.; Burroughes, J. H.; Marks, R. N.; Raliani, C.; Bradley, D. D. C.; Dos Santos, D. A.; Bredas, J. L.; Logdlund, M.; Salaneck, W. R. “Electroluminescence in conjugated polymers”, *Nature* **1999**, 397, 121.

[54] Sirringhaus, h.; Brown, P. J.; Friend, R. H.; Nielsen, M. M.; Bechgaard, K.; Langeveld-Voss, B. M. W.; Spiering, A. J. H.; Janssen, R. A. J.; Meijer, E. W.; Herwig, P.; de Leeuw, D. M. “Two-dimensional charge transport in self-organized, high-mobility conjugated polymers”, *Nature* **1999**, 401, 685.

[55] Cornil, J.; Dos Santos, D. A.; Crispin, X.; Silbey, R; Bredas, J. L. “Influence of interchain interactions on the absorption and luminescence of conjugated oligomers and polymers: A quantum-chemical characterization”, *J. Am. Chem. Soc.* **1998**, 120 , 1289.

[56] Cornil, J.; Heeger, A. J.; Bredas, J. L. “Effects of intermolecular interactions on the lowest excited state in luminescent conjugated polymers and oligomers” *Chem. Phys. Lett.* **1997**, 272, 463.

[57] Taylor, P. N.; O’Connell, M. J.; McNeill, L. A.; Hall, M. J.; Aplin, R. T.; Anderson H. L. “Insulated molecular wires: synthesis of conjugate polyrotaxanes by Suzuki coupling in water”, *Angew. Chem. Int. Ed.* **2000**, 39, 3456.

[58] Cacialli, F.; Wilson J. S.; Michels, J. J.; Daniel, C.; Silva, C.; Friend, R. H.; Severin, N.; Samori, P.; Rabe, J. P.; O’Connell, M. J.; Taylor, P. N.; Anderson, H. L.

"Cyclodextrin-threaded conjugated polyrotaxanes as insulated molecular wires with reduced interstrand interactions", *Nature Materials* **2002**, 1, 160.

[59] Anderson, S.; Anderson, H. L. "Synthesis of a water-soluble conjugated [3]rotaxane", *Angew. Chem. Int. Ed.* **1996**, 35, 1956.

[60] Anderson, S.; Aplin, R. T.; Claridge, T. D. W.; Goodson III, T.; Maciel, A. C.; Rumbles, G.; Ryan, J. F.; Anderson H. L. "An approach to insulated molecular wires: synthesis of water-soluble conjugated rotaxanes", *J. Chem. Soc. Perkin Trans. 1* **1998**, 2383.

[61] Suzuki, A. "Recent advances in the cross-coupling reactions of organoboron derivatives with organic electrophiles, 1995-1998", *J. Organomet. Chem.* **1999**, 576, 147.

[62] McQuade, D. T.; Kim, J.; Swager, T. M. "Two-dimensional conjugated polymer assemblies: interchain spacing for control of photophysics", *J. Am. Chem. Soc.* **2000**, 122, 5885.

[63] Bortolus, P.; Monti, S. "Cis-trans photoisomerization of azobenzene-cyclodextrin inclusion complexes", *J. Phys. Chem.* **1987**, *91*, 5046.

[64] Tawarah, K. M. "A thermodynamic study of the association of the acid form of methyl orange with cyclodextrins", *Dyes Pigments* **1992**, *19*, 59.

[65] Suzuki, M.; Sasaki, Y. "Inclusion compounds of cyclodextrin and azo dye. 1. Methyl-Orange", *Chem. Pharm. Bull.* **1979**, *27*, 609.

[66] Suzuki, M.; Sasaki, Y. "Inclusion compounds of cyclodextrin and azo dyes. 2. ^{1}H nuclear magnetic resonance and circular dichroism spectra of cyclodextrin and azo dyes with a naphthalene nucleus", *Chem. Pharm. Bull.* **1979**, *27*, 1343.

[67] Suzuki, M.; Sasaki, Y.; Sugiura, M. "Inclusion compounds of cyclodextrin and azo dyes. 3. ^{13}C nuclear magnetic resonance spectra of cyclodextrin and azo dyes with a naphthalene nucleus", *Chem. Pharm. Bull.* **1979**, *27*, 1797.

[68] Suzuki, M.; Sasaki, Y. "Nuclear magnetic resonance and circular dichroism spectra of γ-cyclodextrin and orange-II in the solution state", *Chem. Pharm. Bull.* **1984**, *32*, 832.

[69] Suzuki, M.; Sasaki, Y. "Inclusion compounds of cyclodextrin and azo dyes – formation of a liquid crystal", *Chem. Pharm. Bull.* **1981**, *29*, 585.

[70] Suzuki, M.; Ohmori, H.; Kajtar, M.; Szejtli, J.; Vikmon, M. "The association of inclusion complexes of cyclodextrins with azo dyes", *J. Inclus. Phenom. Mol.* **1994**, *18*, 255.

[71] Suzuki, M.; Kajrar, M.; Szejtli, J.; Vikmon, M.; Fenyvesi, E. "Inclusion compounds of cyclodextrins and azo dyes. 10. Induced circular-dichroism spectra of complexes of cyclomaltooligosaccharides an azo dyes containing naphthalene nuclei", *Carbohyd. Res.* **1992**, *223*, 71.

[72] Tawarah, K. M.; Wazwaz, A. A. "Conductance study of the binding of methyl orange, o-methyl red and p-methyl red anions by α-cyclodextrin in water", *J. Chem. Soc. Faraday Trans.* **1993**, *89*, 1729.

[73] Benesi, H. A.; Hildebrand, J. H. "A spectrophotometric investigation of the interaction of iodine with aromatic hydrocarbons", *J. Am. Chem. Soc.* **1949**, *71*, 2703.

[74] Hirai, H. Toshima, N. Uenoyama, S. "Inclusion complex formation of γ-cyclodextrin. One host-two guest complexation with water-soluble dyes in ground state", *Bull. Chem. Soc. Jpn.* **1985**, *58*, 1156.

[75] Sanchez, A. M.; de Rossi, R. H. "Effect of β-cyclodextrin on the thermal cis-trans isomerization of azobenzenes", *J. Org. Chem.* **1996**, *61*, 3446.

[76] Nagele, T.; Hoche, R.; Zinth, W.; Wachtveitl, J. "Femtosecond photoisomerization of cis-azobenzene", *Chem. Phys. Lett.* **1997**, *272*, 489.

[77] Takei, M.; Yui, H.; Hirose, Y.; Sawada, T. "Femtosecond time-resolved spectroscopy of photoisomerization of methyl orange in cyclodextrins", *J. Phys. Chem. A* **2001**, *105*, 11395.

[78] Edwards, H. E.; Thomas, J. K. "A flurorescence-probe study of the interaction of cycloheptaamylose with arenes an amphiphilic molecules", *Carbohydr. Res.* **1978**, *65*, 173.

[79] Yorozu, T.; Hoshino, M.; Imamura, M. "Fluorescence studies of pyrene inclusion complexes wih α-, β- and γ-cyclodextrins in aqueous solutions. Evidence of formation of pyrene dimer in γ-cyclodextrin cavity", *J. Phys. Chem.* **1982**, *86*, 4426.

[80] Arad-Yellln, R.; Eaton, D. F. "Excited-state reactivity changes induced by complexation with cyclodextrins: Inclusion of 2,2-bis(α-naphthylmethyl)-1,3-dithiane into β- and γ-cyclodextrins", *J. Phys. Chem.* **1983**, *87*, 5051.

[81] Herkstroeter, W. G.; Martic, P. A.; Evans, T. R.; Farid, S. “Cyclodextrin inclusion complexes of 1-pyrenebutyrate: The role of coinclusion of amphiphiles”, *J. Am. Chem. Soc.* **1986**, *108*, 3275.

[82] Kano, K.; Takenoshita, I.; Ogawa, T. “γ-Cyclodextrin-enhanced excimer fluorescence of pyrene and effect of n-butyl alcohol”, *Chem. Lett.* **1982**, 321.

[83] Kobayashi, N.; Saito, R.; Hino, H.; Hino, Y.; Ueno, A.; Osa, T. “Fluorescence and induced circular-dichroism studies on host-guest complexaton between γ-cyclodextrin and pyrene”, *J. Chem. Soc. Perkin Trans. 2* **1983**, 1031.

[84] Agbaria, R. A.; Gill, D. “Extended 2,5-diphenyloxazole-γ-cyclodextrin aggregates emitting 2,5-diphenyloxazole excimer fluorescence”, *J. Phys. Chem.* **1988**, *92*, 1052.

[85] Agbaria, R. A.; Gill, D. “Non-covalent polymers of oxadiazole derivatives induced by γ-cyclodextrin in aqueous solutions-fluorescence study”, *J. Photochem. Photobio. A: Chem.* **1994**, *78*, 161.

CHAPTER 2

SYNTHESIS AND PROPERTIES OF AZO DYE ROTAXANE

2.1. Introduction

A rotaxane is a supramolecular assembly of a dumbbell-like shape that has a macrocycle around the molecular axis. It is generally formed when a molecule threads the cavity of macrocycles and bulky terminal groups on both sides prevent the threaded molecule from escaping.[1,2] The formation of rotaxane protects chromophores from the external stimulus, and thus enhances the fluorescent property and the stability of dyes.[3,4] Cyclodextrins (CDs) are cyclic oligosaccharides, most commonly consisting of 6-, 7- or 8- glucose units, which are called α-, β- or γ-CDs respectively. CDs have a conical shape with the primary hydroxyl groups on the narrow side of torus glucose residues and the secondary hydroxyl groups on the wider side. They have hydrophobic interior and hydrophilic exterior, and are widely being used as hosts for various organic molecules including polymers.[1,5] Many dyes have been found to form inclusion complexes with CDs in aqueous solution, they are mostly based on a pseudorotaxane structure that can easily associate and dissociate in aqueous medium.[6-8]

The synthesis of genuine azo dye rotaxanes was first reported by Anderson and his coworkers.[9] The rotaxane structure was induced by the hydrophobic effect and various macrocycles including cyclophane, α- and β-CD were used. In the solid state, it was found that the macrocycle is located over the center of azo linkage, deduced from its crystal structure.[10] Surprisingly, it was possible to yield an azo dye [3]rotaxane as a single stereoisomer, with the 2,3-rims of both CDs pointing outwards.[11] It was also reported that

rotaxane encapsulation enhances the stability of azo dye without preventing the dye from binding to the the cellulosic fibers.[12]

In this chapter, we report the synthesis of a novel azo dye rotaxane with α-CD. The inclusion of the chromophore by α-CD renders the possibility of changing the physical and chemical properties of the azo dye without synthesizing new dyes. The structure of azo dye rotaxane is characterized using ^{1}H NMR and 2D COSY NMR techniques, and the property changes with the rotaxane formation are examined in terms of UV-visible spectra, dye solubility and dye stability. The absorption spectra of aminoazobenzene dye are examined under different pH conditions, and compared with the corresponding rotaxane formation. The sol-gel coating film doped with a dye rotaxane is prepared, and its pH sensitivity is measured. Not so many reports have been made yet on the effect of CD macrocycle on the color of threaded azo dye. From these experiments, we attempt to understand the spectral changes of azo dye with pH in the presence of CD macrocycle.

2.2. Experimental

2.2.1. Preparation of azo dye rotaxane. The synthetic scheme is shown (Scheme 2.1).

4-Amino-4'-sodium(anilinomethane)sulfonate azo benzene (1): *p*-nitroaniline (2.76 g, 0.02 mol) was suspended in water (10 mL) at 0-5 ^{o}C. HCl (35 %, 4.4 mL, 0.05 mol) and $NaNO_2$ (1.38 g, 0.02 mol) were added slowly, and then the mixture was stirred for 1 hr to complete diazotization. Sodium(anilinomethane)sulfonate was formed first and used as a coupling component. To prevent the triazine structure, coupling component was prepared following a literature procedure.[13] $NaHSO_3$ (2.08 g, 0.02 mol) was added to the solution

of water (40 mL) and ethanol (50 mL), and then heated to 60 ^{o}C. After cooling the reaction mixture to room temperature, aniline (1.86 g, 1.82 mL, 0.02 mol) and HCHO (1.6 mL, 0.02 mol) were added to the solution, followed by stirring for 1 hr. Then, the coupling solution was slowly added to the diazotization solution, and stirred at room temperature overnight. After reaction, the pH of the solution was adjusted to 5.0 by adding CH_3COONa, and the crude product was collected by filtration. The intermediate **1** was purified by recrystallization in ethanol (3.6 g, yield 50%). ^{1}H NMR (300 MHz, $CDCl_3$): δ_H = 8.4 (d, 2H), 8.2 (d, 2H), 7.8 (d, 2H), 6.6 (d, 2H), 5.2 (s, 2H). ^{13}C NMR (75 MHz, $CDCl_3$): δ_C = 158.5, 150.6, 145.8, 141.0, 75.0.

4,4'-Diaminoazobenzene (2): The intermediate **1** was dissolved in 1% NaOH aqueous solution, which was then heated at reflux under condenser for 4 hrs. The solution was cooled to room temperature, and 4-nitro-4'-aminoazobenzene was collected by filtration. The terminal nitro group was reduced using equivalent sodiumsulfidenonahydrate to have amino end groups at both ends following earlier literature.[14] 4-Nitro-4'-aminoazobenzene (0.23 g, 1 mmol) was dissolved in ethanol (20 mL). $Na_2S.9H_2O$ (0.48 g, 2 mmol) in water (20 mL) was added dropwise, and then the combined solution was refluxed for 3 hrs. On completion of the reaction, the mixture was poured into cold water (100 mL). Precipitate **2**, diaminoazobenzene (DAAB), was filtered off, washed with water, and dried *in vacuo* (0.15 g, yield 65%). ^{1}H NMR (300 MHz, $CDCl_3$): δ_H = 7.7 (d, 2H), 6.7 (d, 2H). ^{13}C NMR (75 MHz, $CDCl_3$): δ_C = 148.0, 140.5, 124.9, 116.2.

Azo dye rotaxane (3): DAAB (60 mg, 0.28 mmol) was suspended in a mixture of water (5 mL) and ethanol (1 mL) at 0-5 ^{o}C. Dilute HCl (3.7%, 1.2 mL, 1.1 mmol) and $NaNO_2$ (41 mg, 0.59 mmol) solutions were added successively, and then the solution was stirred

for 1 hr to complete diazotization. α-CD (780 mg, 0.80 mmol) in water was added to above reaction mixture and stirred for 1 hr at 0-5 ^{o}C. N,N-dimethyl-1-naphthylamine (96 mg, 0.56 mmol) was added dropwise and the mixture was stirred for 4 hr at room temperature. Dilute sodium acetate was added to increase pH up to 6.5, and dye precipitate was collected by filtering the solution. Rotaxanated dye **3** (referred to as AzoRD hereafter) was purified by soxhlet extraction using a series of organic solvents, such as toluene, hexane and chloroform, and purified by column chromatography on silica using methylethylketone / ammonium hydroxide / 1-propanol (1 / 1 / 1 vol) as an eluent. The total yield was 30%. The ^{1}H NMR and 2D COSY NMR spectra were obtained using Mercury Vx 300 (Varian, 300MHz). δ_H (300 MHz, DMSO-d_6) 9.1 (d, 1H), 9.0 (d, 1H), 8.5 (d, 2H), 8.2-8.1 (m, 6H), 8.0-7.9 (m, 4H), 7.6-7.7 (m, 4H), 7.2-7.1 (q, 2H), 5.3 (s, 6H), 5.2 (s, 6H), 4.7 (d, 6H), 4.3 (s, 6H), 3.7-3.1 (m, 36H). ^{13}C NMR (75 MHz, $CDCl_3$): δ_C = 191.9, 155.8, 152.7, 145.3, 142.3, 128.3, 126.5, 124.6, 124.0, 113.8, 102.8, 82.6, 73.8, 72.7, 72.1, 60.3, 45.1.

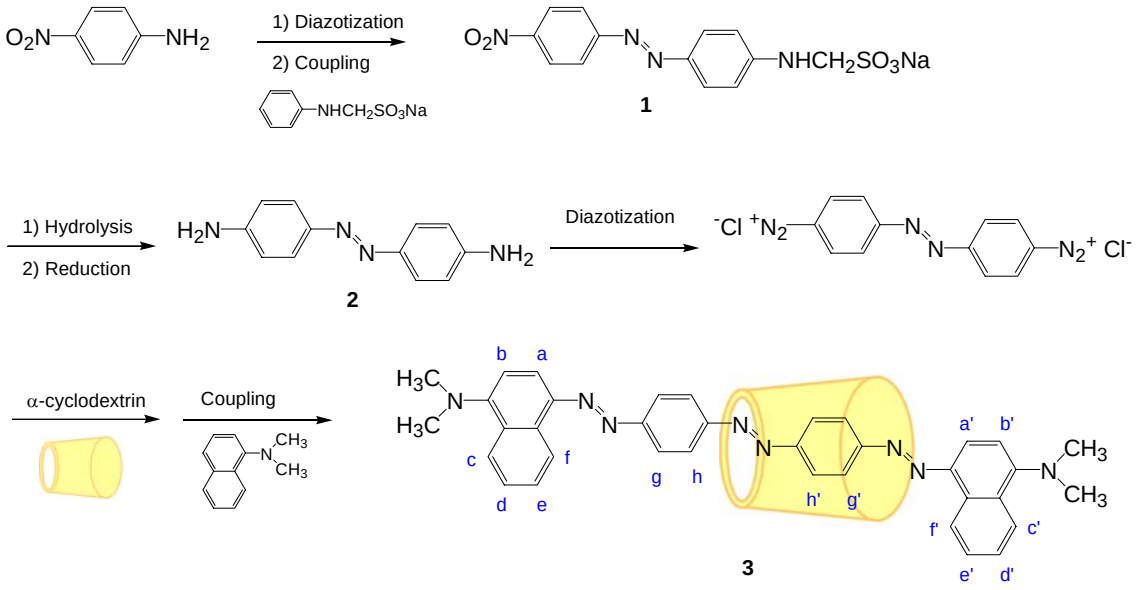

Scheme 2.1. Synthesis of azo dye rotaxane (AzoRD).

Free dye (AzoFD hereafter) was synthesized following the same routes, but without the addition of α-CD. It was purified by column chromatography with an eluent of ethylacetate-toluene (1:6 v/v). Yield 70%. δ_H (300 MHz, $CDCl_3$) 9.07 (d, 2H), 8.2 (d, 2H), 8.1 (q, 8H), 7.9 (d, 2H), 7.6-7.5 (m, 4H), 7.1 (d, 2H). ^{13}C NMR (75 MHz, $CDCl_3$): δ_C = 154.2, 147.5, 125.6, 123.5, 120.3, 115.3, 44.0.

2.2.2. Property investigation. In order to check the solubility changes, DMSO was used as solvent with the addition of different amount of water. The absorption spectra of each dye in DMSO / water mixed solvents were obtained at room temperature on a Lambda 7 (Perkin Elmer) UV-Vis spectrophotometer in 1 cm cuvette. The stability to reductive bleaching was measured under varying concentration of sodium sulfide. Absorbance at various pH values was measured in ethyl alcohol / water mixed solvents.

2.2.3. Sol-gel film preparation. In a typical preparation of sol-gel coating film,[15,16] 20 mg AzoRD in 2.75 mL tetraethylorthosilicate, 4.5 mL ethyl alcohol and 3 mL water was sonicated for 30 min. To the above solution, 0.15 mL of 0.5 M HCl was added as acidic catalyst. The mixture was allowed to sit for two days. About 0.5 mL sol was put on a pre-cleaned glass slide for 1 min and then spin-coated at 1500 rpm for 50 sec to cast transparent and uniform silicate film. The film was dried at ambient conditions for a day and then baked at 100^{o}C for 2 hours.[15,16] In comparison, as for AzoFD, it had limited solubility in given sol mixtures, and thus the cast film showed very uneven and irregular surface. The absorption spectra were measured after the sol-gel glass was dipped in given pH solutions for about 10 min. pH solutions were adjusted by adding dilute HCl.

2.3. Results

The formation of dye rotaxane is characterized by ^{1}H NMR spectroscopy (Figure 2.1). The twenty aromatic protons appear as complex and split peaks in the proton NMR spectra at δ = 7.0 – 9.2 ppm, but can be readily assigned by comparison of all peaks in AzoFD and AzoRD. Aromatic protons from the uncovered part of AzoRD show their peaks at the same positions as those of free dyes. COSY (COrrelated SpectroscopY) experiment confirms the assigned peaks to their corresponding protons (Figure 2.2). In the plot of the COSY cross-peaks, AzoRD clearly shows nonequivalent environment of aromatic protons at both ends making proton peaks of aromatic more split, which results from the threading of azo chromophore within the conical structure of α-CD.

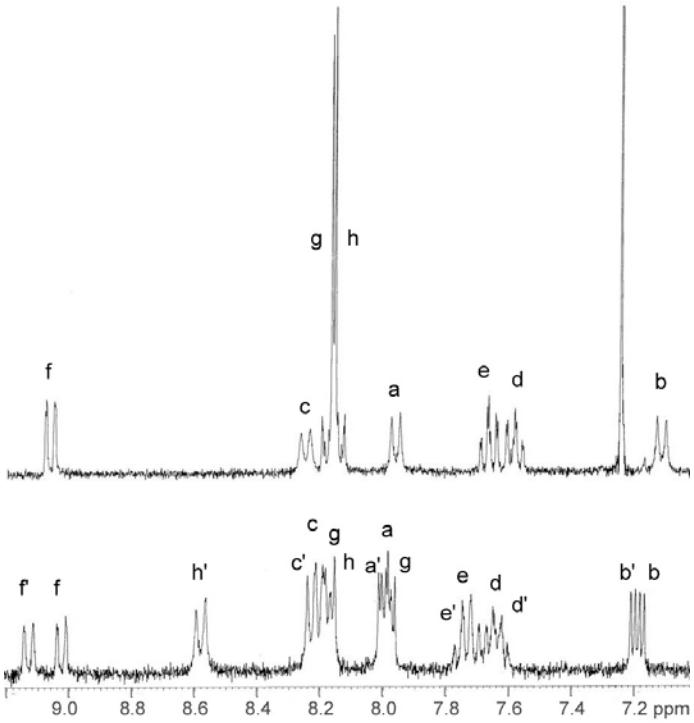

Figure 2.1. ^{1}H NMR of AzoFD (upper, $CDCl_3$) and AzoRD (lower, DMSO).

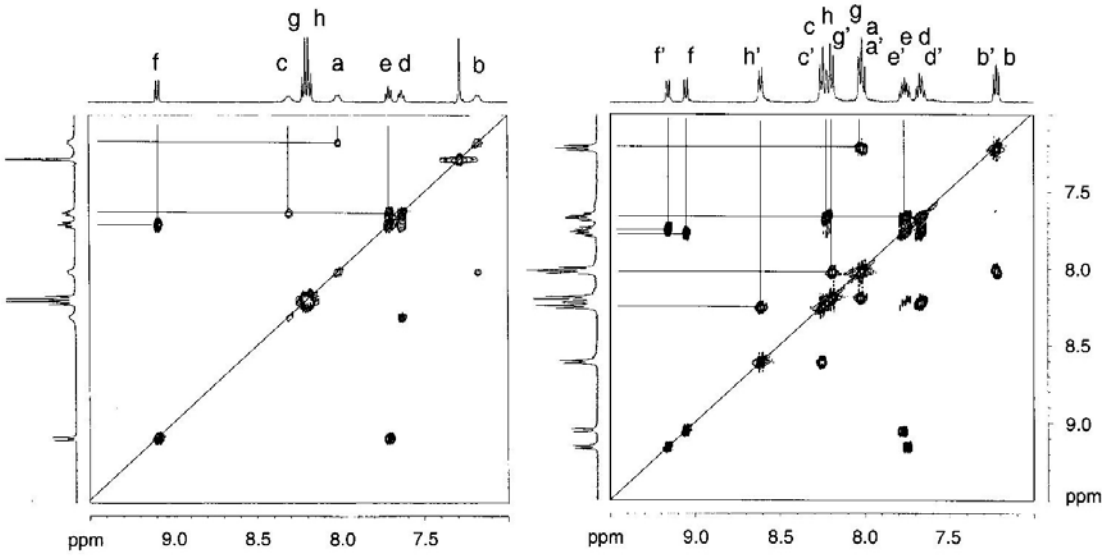

Figure 2.2. 2D COSY ^{1}H NMR of AzoFD (left, $CDCl_3$) and AzoRD (right, DMSO).

Compared with free dye (AzoFD), the rotaxanated one (AzoRD) exhibits its maximum absorption at longer wavelength, along with higher color intensity (Table 2.1). This result is more obvious in ethyl alcohol. Azo dyes with hydrophobic substituents on terminal phenyl rings are highly subject to intermolecular interactions, especially a face-to-face arrangement of dye molecules (H-aggregates),[17] which is thought to be responsible for blue shift of AzoFD in absorption spectra. As for AzoRD, CD macrocycle around the chromophore can hinder dyes' aggregation, and it promotes the existence of monomeric state of dye molecule. This leads to an increase in color strength, with a higher ε_{max} value.

Table 2.1. Absorption properties of AzoFD and AzoRD in DMSO and ethyl alcohol.

Dye	Solvent	λ_{max}	ε_{max}
AzoFD	dimethylsulfoxide	545 nm	40,980
AzoRD	(DMSO)	550 nm	44,384
AzoFD	Ethyl alcohol	510 nm	20,910
AzoRD		524 nm	42,800

The chemical structure of AzoFD resembles that of disperse dye, since it does not contain any solubilizing group**.** Due to its limited solubility, therefore, with increasing water content, it begins to precipitate out of the solution. However, once rotaxanated, AzoRD shows increased hydrophilicity due to hydroxyl groups on the CDs. The UV-visible spectra of two dyes in DMSO / water mixed solvents are shown (Figure 2.3). As is evident, the two dyes show different behaviors with increasing amounts of water. As for AzoFD, its absorbance quickly decreases, which is mainly due to the formation of precipitate and settling out of the solution. Meanwhile, AzoRD remains soluble even in water-rich condition, showing a slight increase and then decrease in absorbance. AzoRD also shows a red shift in its maximum absorbance (λ_{max}).

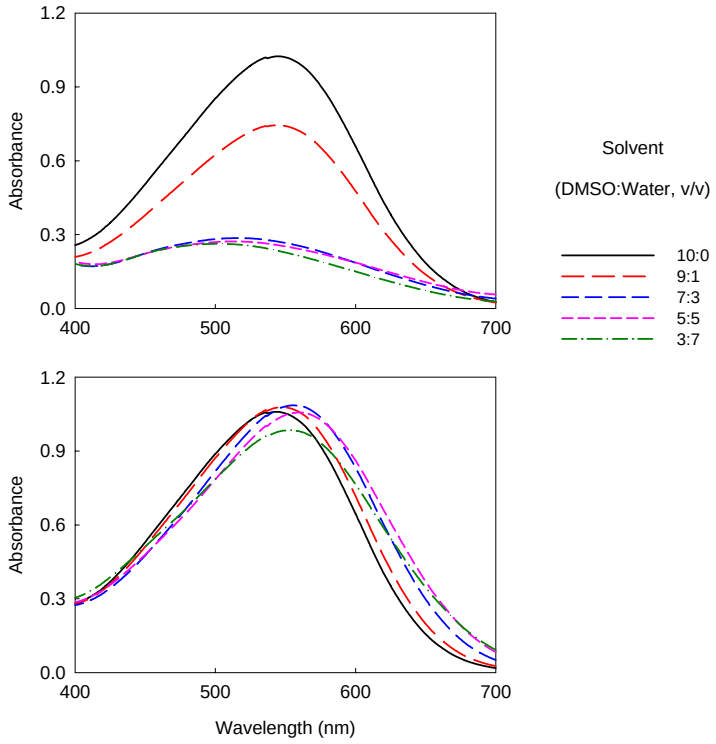

Figure 2.3. UV-visible spectra of both dyes in DMSO / water mixed solvents; AzoFD (upper) / AzoRD (lower), 2.5 x 10^{-4} M, 25^{o}C. Legends indicate volume ratios of the solvent between DMSO and water (distilled, no pH adjustment).

The stability to reductive bleaching was measured by adding sodium sulfide to the dye solutions (Figure 2.4). The addition of sodium sulfide bleaches both dyes, leading to a decrease in their absorbances. However, AzoFD is found to fade much more severely, compared with AzoRD. Under given experimental conditions, the absorbance values of AzoRD maintain above 90 % of the original one.

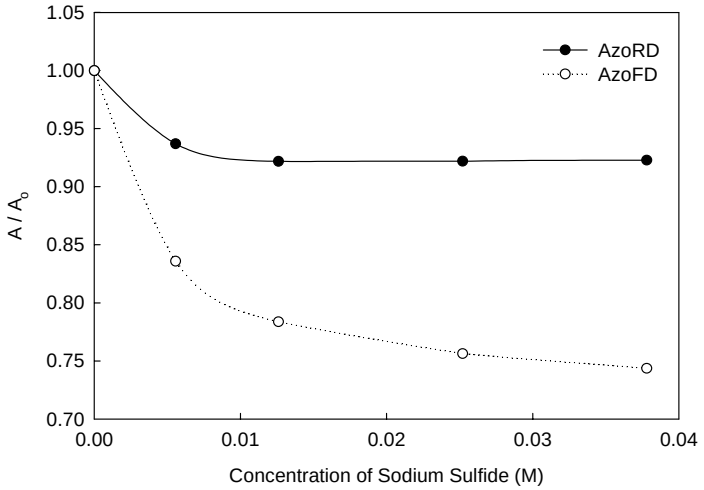

Figure 2.4. Reductive bleaching of AzoFD and AzoRD with sodium sulfide (2.5×10^{-4} M, 298 K, measured in 30 min after mixing).

Absorption spectra were examined under different pH conditions (Figure 2.5). In ethyl alcohol / water mixed solvents, AzoFD shows a red shift, and its absorbance intensity is observed to increase at lower pH. This is attributed to the tautomeric equilibrium of amionazo dye.[18] AzoRD shows a similar behavior as AzoFD. It implies that the presence of CD around azo chromophore does not prevent the protonation of threaded aminoazobenzene dye. There is no isosbestic point observed in both free and rotaxanated dyes. It is understandable because there are two protonation sites, N,N'-dimethyl groups, in its chemical structure. Spectral data under different pH conditions are listed (Table 2.2).

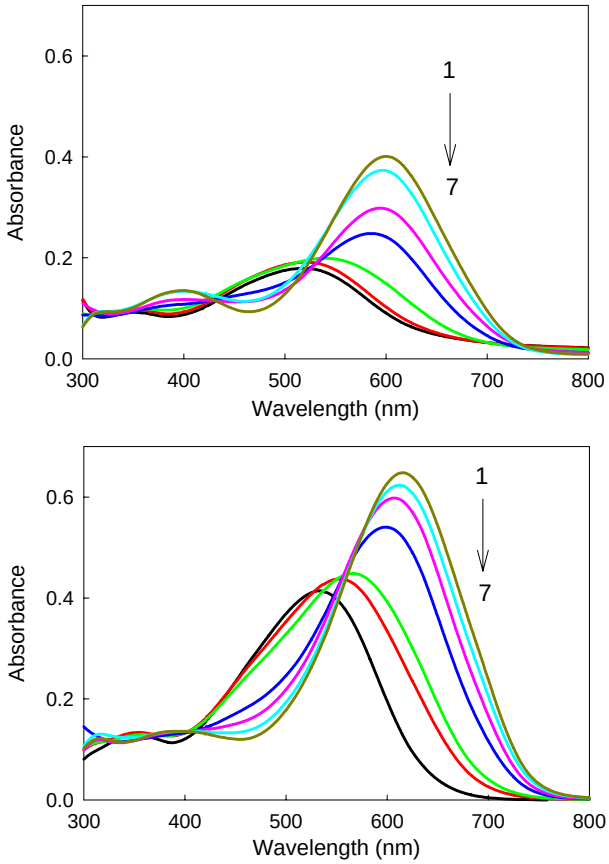

Figure 2.5. Variation of absorption spectra with pH for AzoFD (upper) and AzoRD (lower). The concentrations of both dyes are 1.0 x 10^{-5} M. Ethanol / water (5:1 vol) mixed solvents were used. Legends indicate pHs of the solutions (1→7): 0.82, 1.44, 1.77, 2.08, 2.51, 2.79, 3.94.

Table 2.2. Absorption bands in different pHs. Ethanol / water (5:1 vol) mixed solvents were used.

pH	AzoFD		AzoRD	
	λ_{max}	ε_{max}	λ_{max}	ε_{max}
3.94	521 nm	17,910	534 nm	41,430
2.79	521 nm	19,140	553 nm	43,790
2.51	536 nm	19,920	566 nm	44,870
2.08	584 nm	24,820	599 nm	54,050
1.77	594 nm	29,850	607 nm	59,790
1.44	597 nm	37,330	612 nm	62,340
0.82	599 nm	40,090	617 nm	64,820

In order to investigate the use of rotaxane structure as a pH indicator, AzoRD was entrapped in sol-gel film on a glass slide. The absorption spectra of the sol-gel film under different pH are shown (Figure 2.6). Even in solid matrix, AzoRD is observed to be pH sensitive, exhibiting a red shift in pH ranging from neutral to acidic conditions. This behavior is similar to that in aqueous solution. However, its sensitivity, in terms of changes in intensity and λ_{max}, is not as big as in aqueous solution. Catalytic amount of acid is already added in the preparation of sol-gel film, and this may have an effect on tautomeric equilibrium of the entrapped dye.

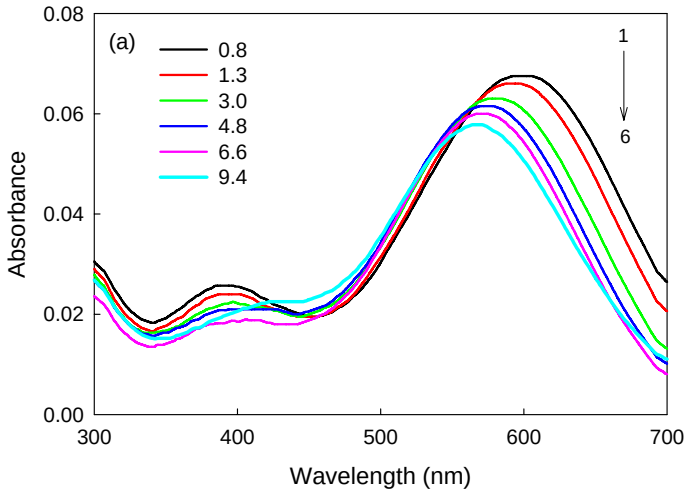

Figure 2.6. (a) The absorption spectra of AzoRD sol-gel film with pH. Legends indicate pHs of the solutions. pH was adjusted by addition of dilute HCl solution, by phosphate buffer (pH 6.6), and by ethanolamine buffer (pH 9.4). Legends indicate pHs of the solutions (1→6): 0.8, 1.3, 3.0, 4.8, 6.6, 9.4.

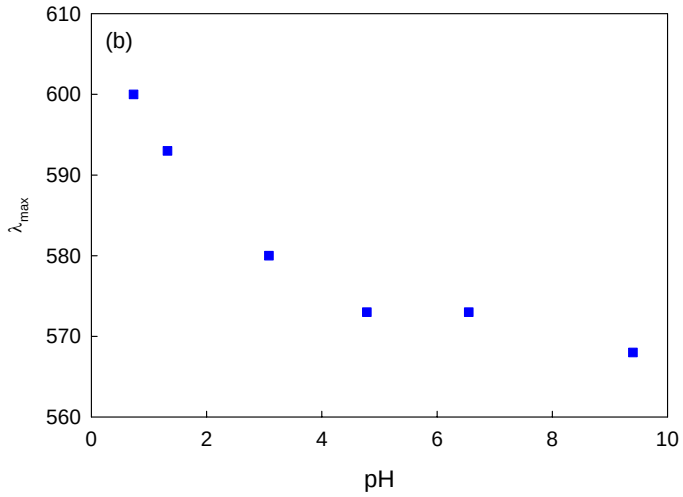

Figure 2.6. (continued) (b) The plot of a change in λ_{max} with pH.

2.4 Discussion

The aromatic part of dye in the NMR spectra shows that CD makes both ends of azo dye nonequivalent, while its axi-symmetry is maintained since it rapidly rotates around its guest on the NMR timescale. When ^{1}H NMR spectra are recorded in DMSO-d_6, all the signals for hydroxyl groups in CD are sharp and easily-identified, showing two primary hydroxyls at δ = 5.5 - 5.7 ppm and one secondary hydroxyl at δ = 4.5 ppm. From the relative integrals, the ratio between chromophore and CD in AzoRD is found to be 1:1, forming azo dye [2]rotaxane.

The effect of rotaxane formation upon color changes is easily understood. Both free and rotaxanated dyes are deep purple, with λ_{max} in dimethylsulfoxide (DMSO) at 545 nm (free dye) and 550 nm (rotaxane dye), and rotaxanated dye shows slightly higher color strength (ε_{max} = 44,384) than that of free dye (ε_{max} = 40,980). But the change in other properties is remarkable. The formation of rotaxane structure increases the polarity

of the dye. This makes it soluble only in polar solvents such as DMF, DMSO or other polar solvent and not soluble in non-polar organic solvents such as hexane, benzene and chloroform that are generally good solvents for free dye. The rotaxane structure makes the threaded chromophore more hydrophilic and thus more stable in aqueous condition. This comes from the presence of hydroxyl groups around the threaded dye molecule. From this, we see that rotaxane formation can be an efficient way to increase aqueous solubility of azo dyes.

Azo dyes are easily bleached by sodium sulfide (Na_2S). This reduction reagent attacks the azo chromophore, leading it first to a hydrazine, and then to two amine units.[19] These aromatic amines are potentially carcinogenic, and sometimes cause serious environmental problems.[19] Free dye (AzoFD), which has these free azo groups, shows a severe color fading in the presence of Na_2S. Upon rotaxanation, however, dye stability to reductive bleaching is remarkably enhanced, showing a much less color fading. This behavior comes from the encapsulation with CD, which protects the threaded azo chromophore. The rotaxane formation, therefore, can also be an efficient way to improve the longevity of organic dyes.

Now we turn to the effect of CD macrocycle on the absorption spectra of aminoazobenzene dye. *N*,*N*-Dialkylaminoazo dyes are well-known to undergo a sharp color change in acid.[20,21] This phenomenon, so-called halochromism, is based on tautomeric equilibrium between the ammonium (AM) and azonium (AZ) tautomers (Scheme 2.2).[22,23] The ammonium tautomer, in which its amino end groups no longer possess a lone pair of electrons, resembles azo benzene substituted in *para* position with an electron-withdrawing group.[24] Thus, it generally exhibits blue shift, along with weaker

color strength.[24] In contrast, the azonium tautomer contains a delocalized positive charge (AZ1↔AZ2), and its chemical structure resembles that of cyanine dyes.[25] It is more red shifted and tinctorially stronger. It is known that increasing the acidity increase the proportion of azonium tautomer, which is attributed to the red shift of aminoazobenzene dye in acidic medium.[26]

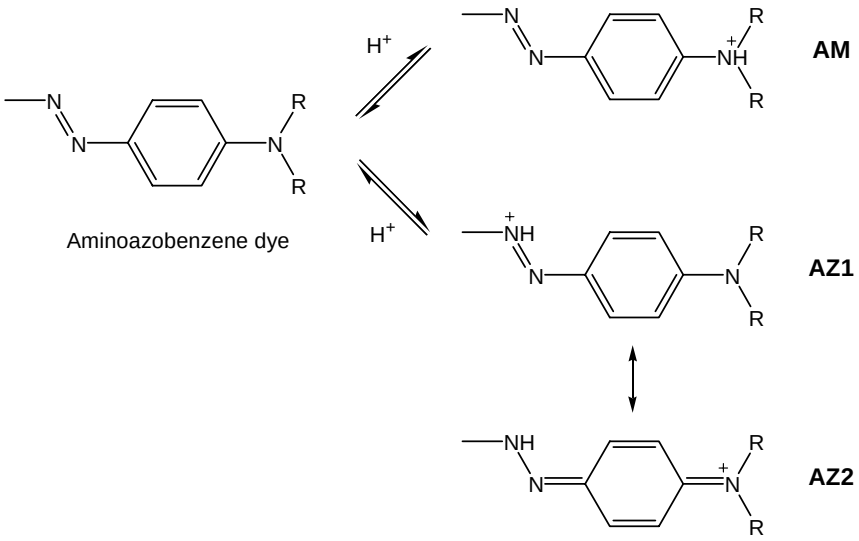

Scheme 2.2. Tautomeric equilibrium between ammonium (AM) and azonium (AZ) tautomers.

According to the measurements in ethyl alcohol / water mixed solvents, AzoFD undergoes protonation in acidic conditions. However, since current AzoFD contains two protonation sites (N,N-dimethylnaphthyl) at both ends, its tautomerism turns out to be more complex (Scheme 2.3). Various azonium equilibria ($AZ_{1A}\leftrightarrow AZ_{1B}$, $AZ_{2A}\leftrightarrow AZ_{2B}$, $AZ_{3A}\leftrightarrow AZ_{3B}$) are expected, and thus it leads to nonexistence of single isosbestic point. AzoRD shows a similar red shift. However, the ratio $\varepsilon_{(pH\ 0.82)} / \varepsilon_{(pH\ 3.94)}$ of AzoRD is found to be smaller than that of AzoFD (2.24 for AzoFD, 1.56 for AzoRD). It is assumed

that the formation of azonium tautomer is dominant at lower pH (pH 0.82). From this result, we see that within CD cavity, the formation of azonium tautomer is hindered.

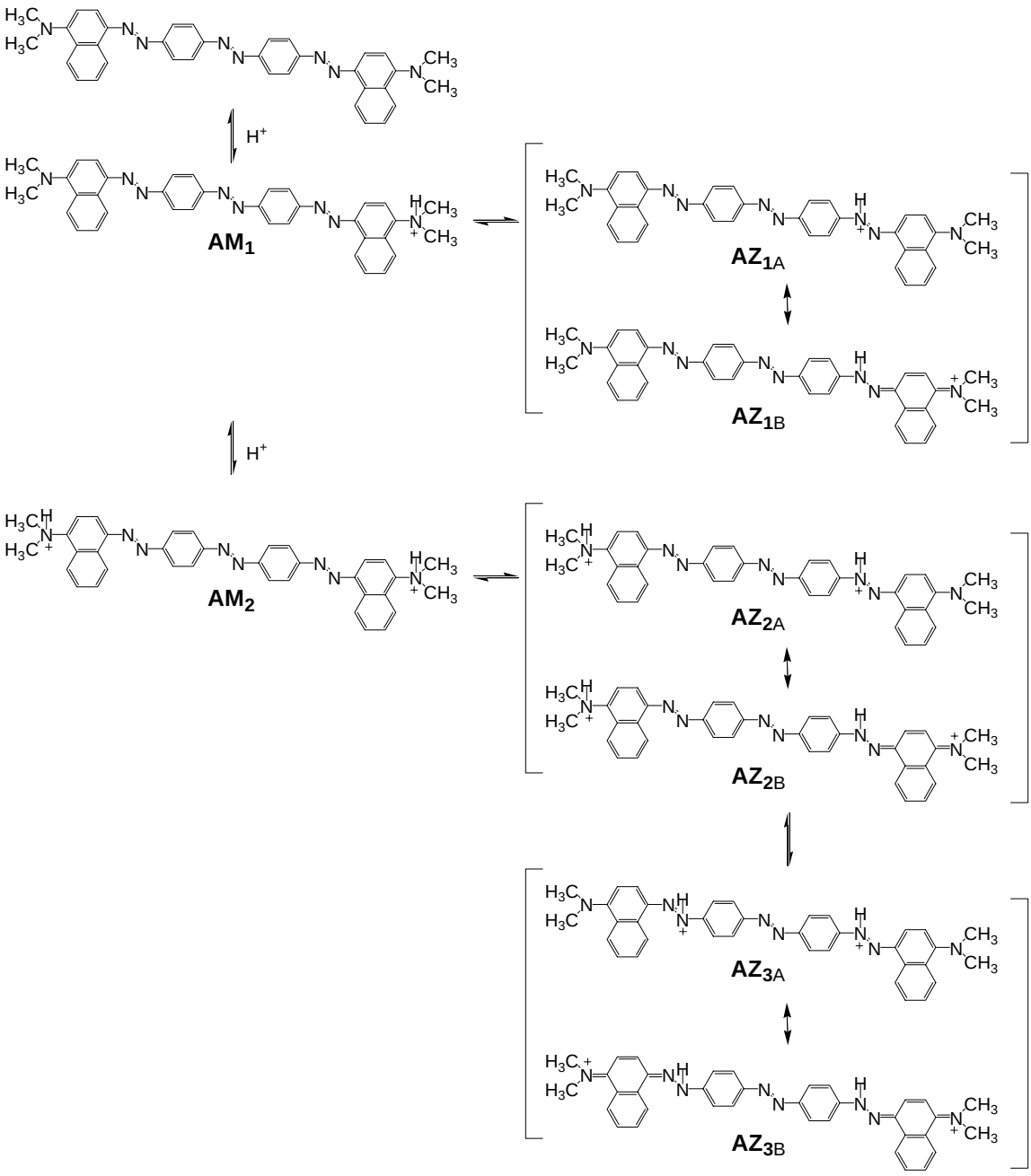

Scheme 2.3. Tautomeric equilibrium of AzoFD between ammonium (AM) and azonium (AZ) tautomers.

Since Avnir and his coworkers first reported on sol-gel glasses doped with various dyes, the sol-gel process has been a very useful method to prepare a solid matrix with entrapment of organic molecules for chemical sensor applications. [27-30] The typical entrapment process of organic molecules in a sol-gel matrix is presented in Figure 2.7.[28] Generally, host materials, tetramethoxysilane or tetraethoxysilane depending on the solvent system, can be polymerized in the presence of water with catalytic amounts of acid or alkali. When the polymerization is complete, the dopants, dye molecules are entrapped in the inorganic polymeric network.

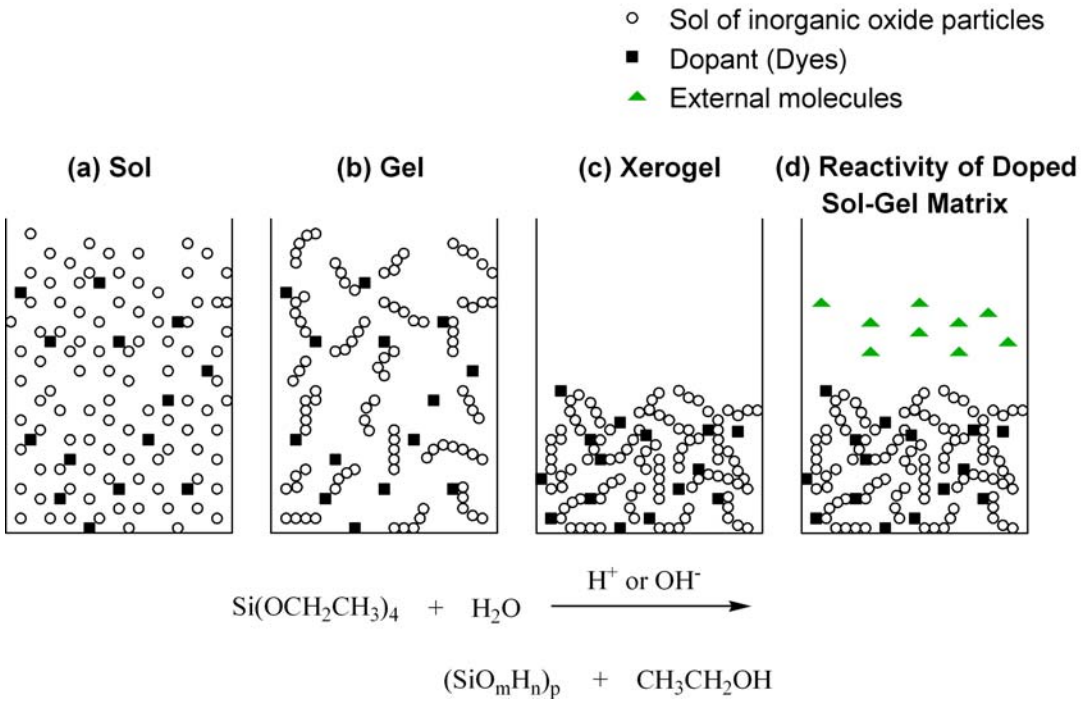

Figure 2.7. The entrapment process; A sol (a) of inorganic oxide particle is prepared by polymerization. The sol becomes a gel (b), then dries and shrink, forming a porous xerogel (c). External molecules diffuse into the pore matrix (d) (from ref 28).

As seen in Figure 2.6., the AzoRD sol-gel film is still pH sensitive, exhibiting similar red shift in the pH range from neutral to acidic conditions. This pH sensitivity was found to be reversible and reproducible, and no damage of the sol-gel film was observed

during repeated measurements. From this, we see that the current sol-gel film with AzoRD is suitable as a pH indicator in the range of acid and neutral conditions. However, in alkaline solutions, slow leaching was observed. This is due to the ionization of hydroxyl groups in α-CDs, leading to an increase in dye solubility. In comparison, as for AzoFD, it has limited solubility in a given sol mixture, and thus the cast film showed uneven and irregular surface. This clearly shows the limitation of water insoluble free dye for this application.[29-31]

2.5. Conclusion

We have successfully synthesized and characterized azo dye rotaxane with α-CD. Rotaxane dye (AzoRD) shows a slight red shift, higher color strength, and improved stability to reductive bleaching. The CD ring around the dye makes it more soluble in water, thus providing a simple way to improve the solubility and stability of azo dye. It was found that the formation of rotaxane structure did not interfere with tautomeric equilibrium of threaded aminoazobenzene dye. In sol-gel film, AzoRD still exhibits pH sensitivity in the ranges from neutral to acidic conditions in a reversible and reproducible way.

The introduction of CD around chromophore to form dye rotaxane would be a simple way to achieve the properties of azo dye as desired; improved aqueous solubility, enhance dye stability, and high pH sensitivity in sol-gel film. All these changes in physical properties could be accomplished without synthesizing a different set of dyes.

REFERENCES

[1] Nepogodiev, S. A.; Stoddart, J. F. "Cyclodextrin-based catenanes and rotaxanes", *Chem. Rev*. **1998,** *98*, 1959.

[2] Harada, A. "Cyclodextrin-based molecular machines", *Acc. Chem. Re*s. **2001,** *34*, 456.

[3] Buston, J. E. H;Young, J. R.; Anderson, H. L. "Rotaxane-encapsulated cyanine dyes: enhanced fluorescence efficiency and photostabiltiy", *Chem. Commun.* **2000**, *34*, 905.

[4] Buston J. E. H.; Marken, F.; Anderson, H. L. "Enhanced chemical reversibility of redox processes in cyanine dye rotaxanes", *Chem. Comm.* **2001**, (11), 1046.

[5] Balzani, V.; Credi, A.; Raymo, F. M.; Stoddart, J. F. "Artificial molecular machines", *Angew. Chem. Int. Ed.* **2000**, *39*, 3349.

[6] Abou-Hamdan, A.; Bugnon, P.; Saudan, C.; Lye, P. G.; Merbach, A. E. "High-pressure studies as a novel approach in determining inclusion mechanisms: thermodynamics and kinetics of the host-guest interactions for α-cyclodextrin complexes", *J. Am. Chem. Soc.* **2000**, *122*, 592.

[7] Flamigni, L. "Inclusion of fluorescein and halogenated derivatives in α-cyclodextrin, β-cyclodextrin, and γ-cyclodextrins – A steady-state and picosecond time-resolved study", *J. Phys. Chem*. **1993**, 97, 9566.

[8] Sanchez, A. M.; de Rossi, R. H. "Effect of β-cyclodextrin on the thermal cis-trans isomerization of azobenzene", *J. Org. Chem.* **1996**, *61*, 3446.

[9] Anderson, S.; Claridge, T. D. W.; Anderson, H. L. "Azo-dye rotaxanes", *Angew. Chem. Int. Ed.* **1997**, *36*, 1310.

[10] Anderson, S.; Clegg, W.; Anderson H. L. "Crystal structure of an azo dye rotaxane", *Chem. Comm.* **1998**, (21), 2379.

[11] Craig, M. R.; Claridge, T. D. W.; Hutchings, M. G.; Anderson, H. L. "Synthesis of a cyclodextrin azo dye [3]rotaxane as a single isomer", *Chem. Comm.* **1999**, (16), 1539.

[12] Craig, M. R.; Hutchings, M. G.; Claridge, T. D. W.; Anderson H. L. "Rotaxane-encapsulation enhances the stability of an azo dye, in solution and when bonded to cellulose", *Angew. Chem. Int. Ed.* **2001**, *40*, 1071.

[13] Venkataraman, K. *The Chemistry of Synthetic Dyes*, Academic Press: New York, 1971.

[14] Matsui, M.; Tanka, N.; Nakay, K.; Funabiki, K.; Shibata, K.; Muramatsu, H.; Abe, Y.; Kaneko, M. "Synthesis of fluorine-containing disazo dyes extended with ester linkages and their application to guest-host liquid crystal displays", *Liq. Cryst.* **1997**, *23*, 217.

[15] Rottman, C.; Grader, G.; Hazan, Y. D.; Melchior, S.; Avnir, D. "Surfactant-induced modification of dopants reactivity in sol-gel matrixes", *J. Am. Chem. Soc.* **1999**, *121*, 8533.

[16] Rottman, C.; Avnir, D. "Getting a library of activities from a single compound: Tunability and very large shifts in acidity constants induced by sol-gel entrapped micelles", *J. Am. Chem. Soc.* **2001**, *123*, 5730.

[17] Fieser, L. F. *Organic synthesis Vol II*, Wiley, New York, **1943**.

[18] Yeh, S. J.; Jaffe, H. H. "Tautomeric equilibria. VI. The structure of the conjugate acid of p-dimethylaminoazobenzene", *J. Am. Chem. Soc.* **1959**, *81*, 3283.

[19] Ganesh, R.; Boardman, G. D.; Michelsen, D. "Fate of azo dyes in sludges" *Water Res.* **1994**, *28*, 1367.

[20] Sawicki, E. "The physical properties of the aminoazobenzene dyes. III. Tautomerism of 4-aminoazobenzene salt cations in acid solution", *J. Org. Chem.* **1956**, *21*, 605.

[21] Sawicki, E. "The physical properties of the aminoazobenzene dyes. IV. The position of proton addition", *J. Org. Chem.* **1957**, *22*, 365.

[22] Stoyanova, T.; Stoyanov, S.; Antonov, L.; Petrova, V. "Ammonium-azonium tautomerism in some N,N-dialkylaminoazo dyes. Part 1. general considerations", *Dyes Pigments* **1996**, *31*, 1.

[23] Stoyanova, T.; Stoyanov, S.; Antonov, L.; Petrova, V. "Ammonium-azonium tautomerism in some N,N-dialkylaminoazo dyes. Part 2. compounds containing more than two protonation sites", *Dyes Pigments* **1996**, *32*, 171.

[24] Cox, R. A.; Buncel, E. *Azo-hydrazone tautomerism of aromatic azo compounds*, London, John Wiley and Sons, **1975**.

[25] Stummer, D. M. *Cyanin dyes. In: Encyclopedia of chemical technology*, New York, Wiley-Interscience, **1979**.

[26] Gordon, P. F.; Gregory, P. *Organic Chemistry in Colour*, Spinger-Verlag Berlin Herdleberg, Germany, **1987**.

[27] Zusman, R.; Rottman, C.; Ottolengi, M.; Avnir, D., "Doped sol-gel glasses as chemical sensors", *J. Non-Cryst. Solids* **1990**, *122*, 107.

[28] Avnir, D. "Organic chemistry within ceramic matrices: Doped sol-gel materials", *Acc. Chem. Res.* **1995**, *28*, 328.

[29] Lin, J.; Brown, C. W. "Sol-gel glass as a matrix for chemical and biochemical sensing", *Trend. Anal. Chem.* **1997**, *16*, 200.

[30] Guo, Y.; Guadalupe, A. R.; Resto, O. Fonseca, L. F.; Weisz, S. Z. "Chemically doped Prussian Blue sol-gel composite thin films", *Chem. Mater.* **1999**, *11*, 135.

[31] Liang, C.; Weaver, M. J.; Dai, S. "Change of pH indicator's pka value via molecular imprinting", *Chem. Comm.* **2002**, 1620.

CHAPTER 3

AZOXINE DYE ROTAXANE AND ITS METAL COMPLEX

3.1. Introduction

8-Hydroxyquinoline (8-HQ) has been widely used in inorganic analysis for the identification and separation of various metal ions.[1] 8-HQ is well-known as a ligand with high reactivity toward metal (II) ions,[2] and its products with two coplanar N, O metal-chelate form an N, N, (O, O) trans geometry.[3] Its complexes with aluminum, Alq_3, and zinc, Znq_2, have been important as the emissive and electron transporting material in organic light-emitting devices (OLEDs).[4,5] However, these metal complexed light emitters are poorly soluble in all the common solvents, and to overcome this limitation, substituted 8-HQs have been studied.[6-9]

In this chapter, we describe the synthesis of azoxine dye rotaxane by coupling 8-HQs with diazo components in the presence of α-cyclodextrin (α-CD). 8-HQ has been used as a coupling component in a series of azo dyes named "azoxines".[10] The ability of 8-HQ to behave as a bidentate ligand is used to form metal chelates. Through the reaction with Zn^{2+} ions, polymeric metal complexed dye rotaxane is achieved. By this approach, it is expected that there will be a dye molecule inside of a CD cavity along the entire length of the metal complexed chain. The structure of azoxine dye rotaxane and its metal coordinate are characterized by NMR, IR and MALDI-TOF spectra. Their spectral characteristics are studied using UV-Vis spectrophotometer. The formation of the products is confirmed by elemental analysis.

Using azoxine dye rotaxane, we develop a novel dyeing method for polypropylene (PP) fiber. PP has become one of very important olefin polymers due to its

low producing cost, superior physical and chemical properties.[11] PP, however, is basically known as a undyeable material due to the lack of dyeing sites, high crystallinity and non-polar aliphatic structure.[11,12] Numerous efforts have been made as a measure to improve its dyeing properties, such as by making blends with other polymers,[12,13] adopting chemical oxidation,[14] and adding some nanoparticles.[15] Most PPs are nowadays dyed by a mass pigmentation method, for high physical properties and low cost. However, pigmented PP fiber makes it hard to achieve uniform color in the case of PP blend fibers, and also flexible color matching is retarded when this kind of fiber is used.[11,14,15] TiO_2 is widely used in the fields of polymer and fiber industry as a white-coloring material, and as for PP fiber, up to 30~40 % of TiO_2 is added for this purpose. TiO_2 forms hydrogen bonding with hydroxyl species existing in any additives in PP and systematic study about their bonds was carried out using IR spectroscopy.[16-18] We utilize the formation of hydrogen bonding between TiO_2 and hydroxyl groups in CD. Through this approach, we intend to provide a novel dyeing method for PP fiber.

3.2. Experimental

3.2.1. Preparation of azo dye rotaxane. The synthetic scheme is shown in Scheme 3.1.

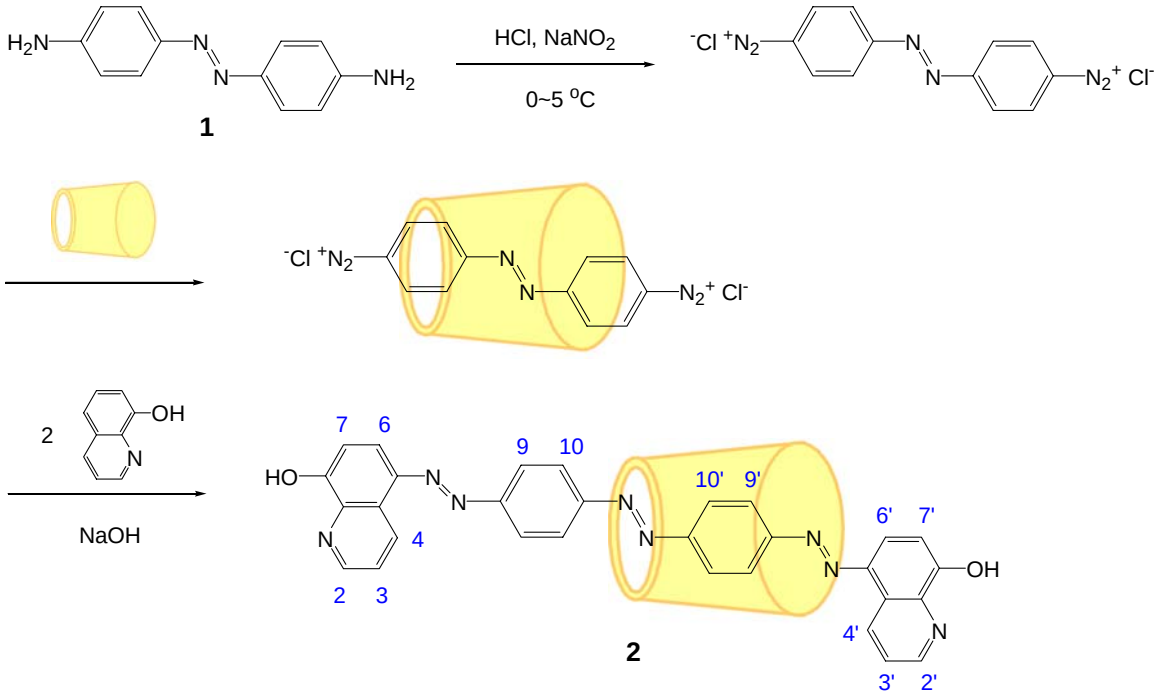

Scheme 3.1. Synthesis of azoxine dye rotaxane (AzoxRD) with 8-hydroxyquinoline as coupling components.

4,4'-Diaminoazobenzene (1): The preparation of 4,4'-diaminoazobenzene (DAAB) was based on known methods [19,20] and explained in detail in Chapter 2.

Azoxine dye rotaxane (2): DAAB (480 mg, 2.24 mmol) was dissolved in water (10mL). 1N HCl (13.6 mL) and 10% $NaNO_2$ aqueous solution (3.1 mL) were added, and the solution was stirred at 0-5 ^oC for 1 hr to complete diazotization. α-CD (9.336 g, 9.6 mmol) in water (15 mL) was added to above mixture and stirred for another 1 hr at 0-5 ^oC. 8-HQ (0.976 mg, 6.72 mmol) in 2 N NaOH (4 mL) was added dropwise for 30 minutes and stirring continued at room temperature overnight. After the reaction, the pH was adjusted to 7.5~8.0, and the dye precipitate was collected by filtration and dried under vacuum. It was dissolved in aqueous alkaline solution (pH ~11 by NaOH), and the free dye was removed by filtration. The pH of the filtrate was then adjusted to neutral,

and the residue was collected. Dissolving and precipitating were repeated twice to ensure the purity of the rotaxane dye (AzoxRD, yield 40% based on DAAB). The ^{1}H and ^{13}C NMR spectra were obtained in DMSO-d_6 using Mercury Vx 300. δ_H (300 MHz, DMSO-d_6) 9.5 (d, 1H), 9.4 (d, 1H), 9.0 (m, 2H), 8.5 (d, 1H), 8.2-8.1 (m, 4H), 7.9 (d, 1H), 7.8 (m, 2H), 7.3 (d, 2H).

Free dye (AzoxFD) was synthesized following the same routes, but without the addition of α-CD. ^{1}H NMR (300 MHz, DMSO-d_6 with NaOH): δ_H = 9.1 (d, 2H), 8.5 (m, 2H), 8.1 (d, 2H), 7.9 (d, 2H), 7.8 (d, 2H), 7.5 (q, 2H), 6.4 (d, 2H). ^{13}C NMR (75 MHz, DMSO-d_6 with NaOH): δ_C = 150.0, 140.9, 132.0, 129.2, 123.9, 120.5.

3.2.2. Preparation of dye-metal complex. Polymeric metal complexed dye rotaxane (Zn-AzoxRD) was prepared by slowly mixing AzoxRD (0.2245 g, 0.15 mmol) in hot ethanol (10 mL) with $Zn(ClO_4)_2 \cdot xH_2O$ (0.0206 g, 0.15 mmol) in absolute ethanol (10 mL), followed by stirring for 6 hrs under reflux (Scheme 3.2). After the reaction, half the solvent was removed and the solution cooled down to room temperature. The dye precipitate was collected by filtration, washed with cold water-ethanol mixture (1 / 1 vol), and dried overnight in vacuum at 40^{o}C. For comparison, metal complex of free dye (Zn-AzoxFD) was synthesized following the same procedure. Due to the limited solubility of the metal complexes in DMSO, NMR spectra show broad peaks in aromatic regions. Elemental analysis was carried out, in order to confirm the formation of dye-Zn complex.

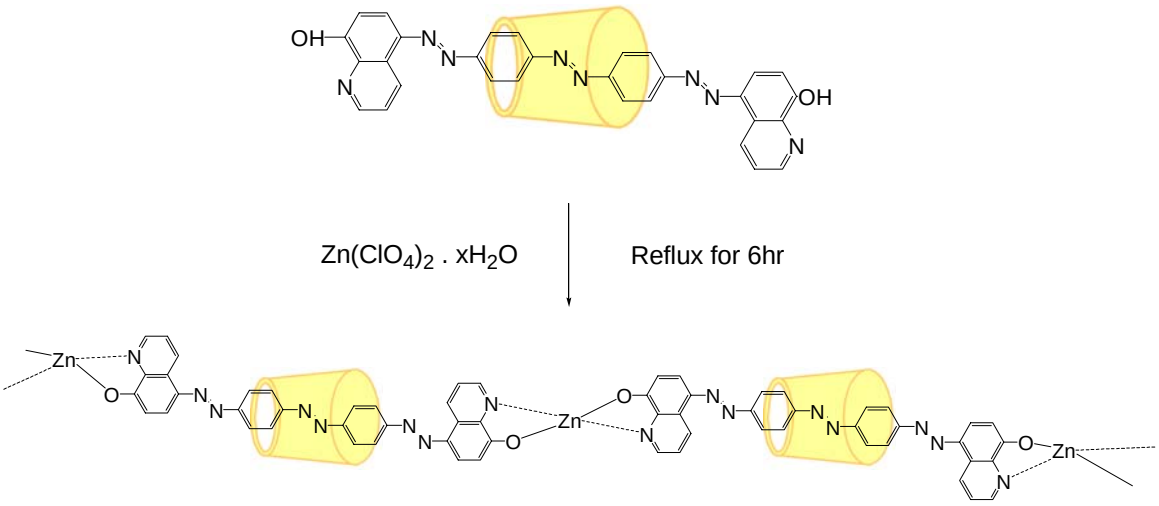

Scheme 3.2. Synthesis of polymeric metal complex of azoxine dye rotaxane (Zn-AzoxRD).

3.2.3. Property investigation. The ^{1}H NMR spectra were measured in DMSO-d_6 using Mercury Vx 300 (Varian, 300MHz) spectrometer. The structure of the dye was characterized using matrix-assisted laser desorption time-of-flight (MALDI-TOF) mass spectroscopy. α-Cyano-4-hydroxycinnamic acid was used as a matrix and an equal volume mixture of acetonitrile and water was used as the solvent. IR spectra were collected using a Perkin Elmer FT-IR microscope. All samples were prepared on KBr pellets for the measurements. Absorption spectra were measured on a Lambda 7 spectrometer (Perkin Elmer) in 1 cm cuvette using DMF / aqueous buffer mixed solvents. Five buffer solutions were prepared, using acetate (pH 4.7), phosphate (pH 6~8), and ethanolamine (pH 9.6) buffer respectively, and all buffer concentrations are maintained at 10 mM. The DSC measurements were carried out at a heating rate of 10 ^{o}C/min from 25 to 250 ^{o}C using a TA Instruments differential scanning calorimeter (DSC Q100).

3.2.4. Polypropylene (PP) dyeing test. All dyeing experiments were carried out at 90 ^{o}C in a closed flask. A PP fiber sample of about 1 g was immersed in a water bath (100 mL) containing 30 mg dye (3% on the weight of fiber) and 0.5 g NaOH. After 3 hours, the dyed sample was washed profusely with water and dried in air overnight. For metal complexing, an aqueous solution (10 mL) of 30 mg $CuSO_4$ was added after 1.5 hours at 90 ^{o}C and maintained for another 1.5 hours. The reflectivities of dyed samples were measured using microspectrometer (SEE 1000 MSP, SEE Inc.), and then their K/S (absorption to scattering coefficient) values were calculated using Kubelka-Munk equation, $K/S = (1-R)^2 / 2R$, where R is reflectivity.[21,22]

3. 3. Results

The dye structures are readily confirmed by ^{1}H NMR spectroscopy (Figure 3.1). Due to the presence of inter- and intra-molecular hydrogen bonding of 8-HQs,[23] it is extremely difficult to dissolve free dye (AzoxFD) in DMSO-d_6. A small amount of alkali, NaOH, is added to make it soluble. The peak assignment in aromatic region is quite straightforward. AzoxFD has symmetrical structure around its central azo group, which shows simple peaks in the aromatic region. From the deprotonation of –OH groups in 8-HQs by NaOH, all peaks appear to shift toward upfield region. As for rotaxanated dye (AzoxRD), due to the existence of hydroxyl groups in α-CD, it easily dissolves in NMR solvent, DMSO-d_6. In the NMR spectrum, it clearly shows the nonequivalent environment at both ends of the dye molecule from more split and complex peaks. This is attributed to the conical shape of α-CD, from which the threading of azo chromophore within the cavity of CD can be confirmed.

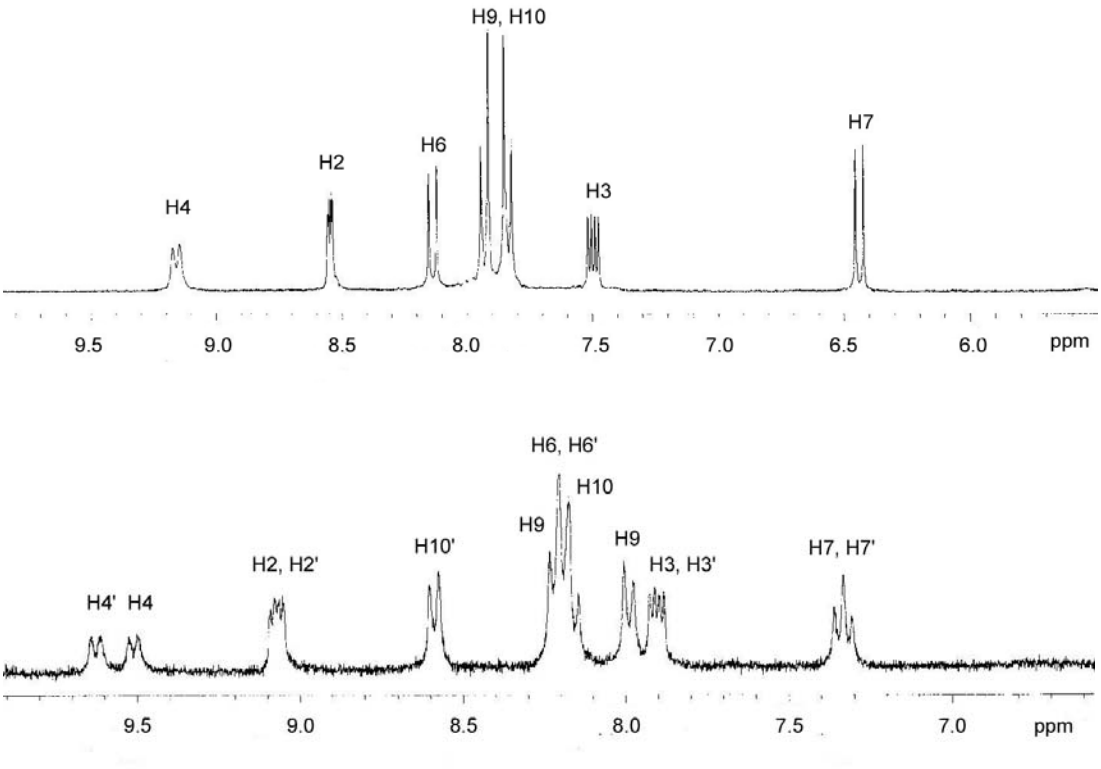

Figure 3.1. ^{1}H NMR of AzoxFD (upper, DMSO, NaOH) and AzoxRD (lower, DMSO).

AzoxRD is found to be highly sensitive to the pH changes according to its absorption spectra (Figure 3.2). At high pH, its absorption maximum shifts to longer wavelength (red shift). This color change is found to be reversible. The same tendency appears regardless of solvent systems used. It is attributed to azo-hydrazone tautomerism. However, at the same pH value, there exists a slight discrepancy depending on the mixing ratio of dimethylsulfonamide (DMF) and aqueous buffer solution, exhibiting solvatochroism (Figure 3.3). Even in water-rich conditions, AzoxRD remains stable, unlike AzoxFD. It is due to the aid of hydroxyl groups in α-CD, even though there is no solubilizing group in its own molecular structure.

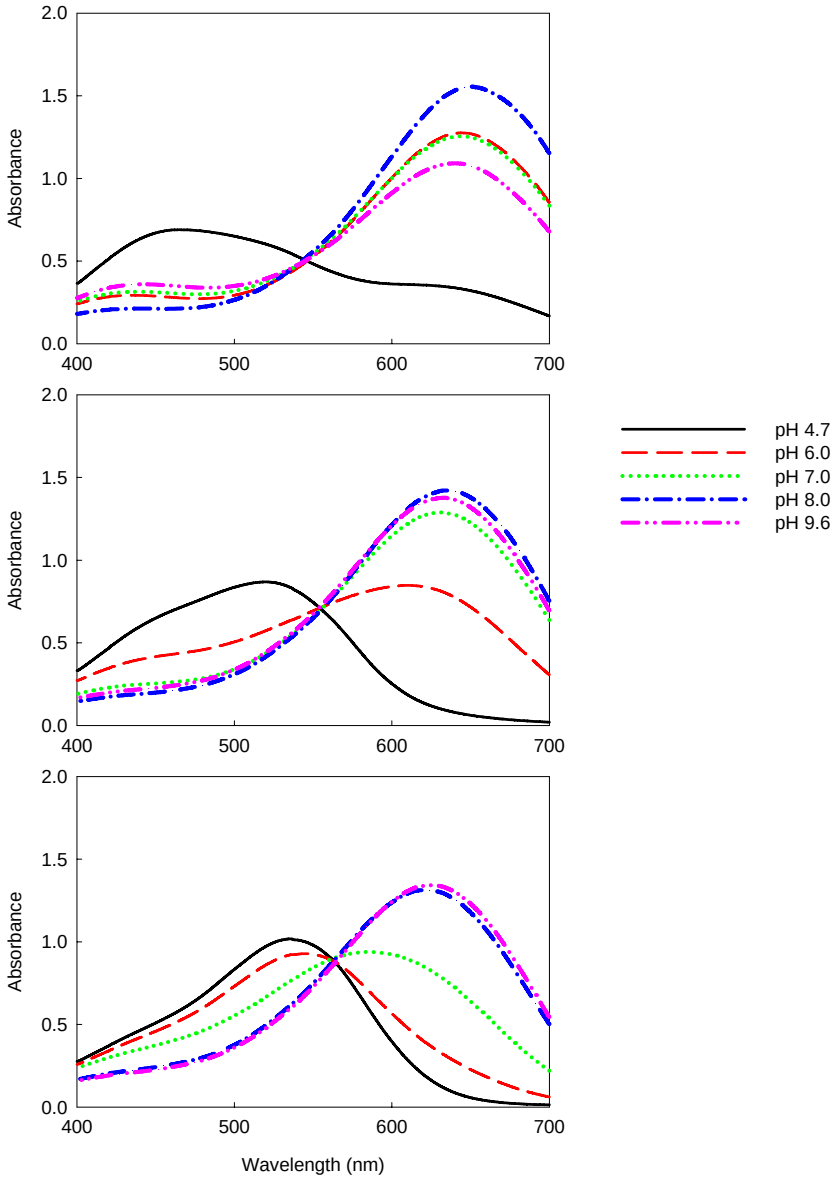

Figure 3.2. Absorption spectra of AzoxRD in different ratio (volume) of solvent mixtures. DMF : aqueous buffer (v:v) = 8 : 2 (upper), 5 : 5 (middle), 2 : 8 (lower). [Dye]=$2x10^{-5}$ M. Legends indicate pHs of the solutions.

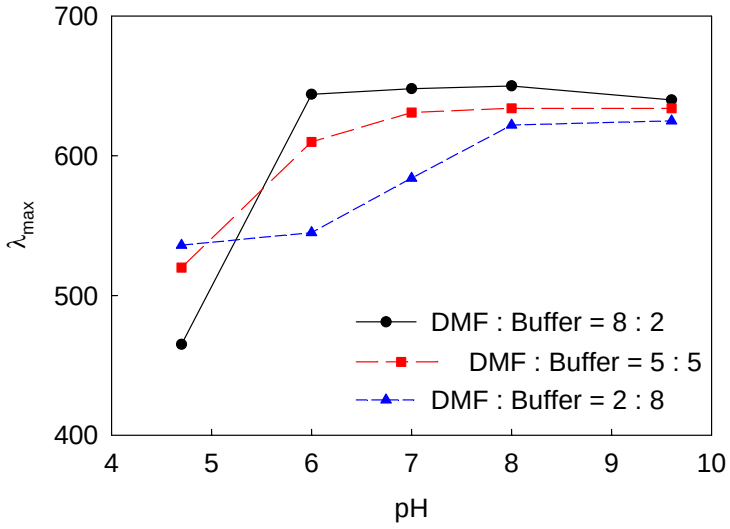

Figure 3.3. The absorption maxima change of AzoxRD with pH and solvent mixing ratio.

The color change of AzoxRD with Zn^{2+} ion was examined, and a large red shift occurs by the addition of Zn^{2+} ion (Figure 3.4). The λ_{max} of the dye (without added Zn) occurs around 530 nm, which corresponds to the characteristic and intense $\pi \rightarrow \pi^*$ transition of –N=N- group.[24,25] The λ_{max} shifts to 615 nm on the addition of Zn. Further increase in zinc amount leads to a decrease in shift to 590 nm, then to 570 nm. This color change, from red to blue-violet, is easily noticeable and can thus be observed even by bare eyes. Obviously, AzoxRD binds to Zn^{2+} ions to form a coordinated complex. This color change is irreversible, since a Zn-dye complex forms a precipitate in a couple of days.

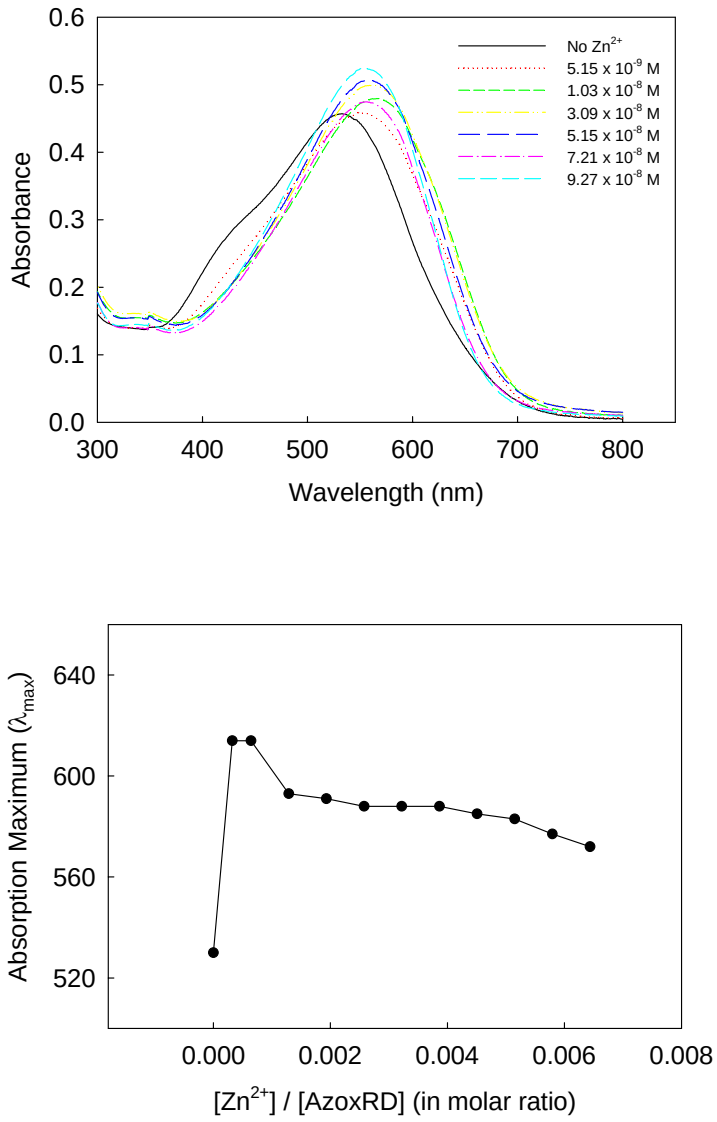

Figure 3.4. (a) The absorption spectra with the addition of Zn^{2+} ion. Mixed solvent (DMF/pH6.0 Buffer, 2:8, v/v) was used. [AzoxRD]=1.6x10^{-5} M. (b) Absorption maxima changes with the addition of Zn^{2+} ion.

^{1}H NMR spectra of CD parts in AzoxRD and Zn-AzoxRD are shown (Figure 3.5). The peaks of CDs become much broader when complexed with Zn^{2+}. It is attributed to the fact that upon metal coordination, the conformational flexibility of CDs is reduced in polymeric structure.[26] From this, the formation of metal-ligand is readily manifested.

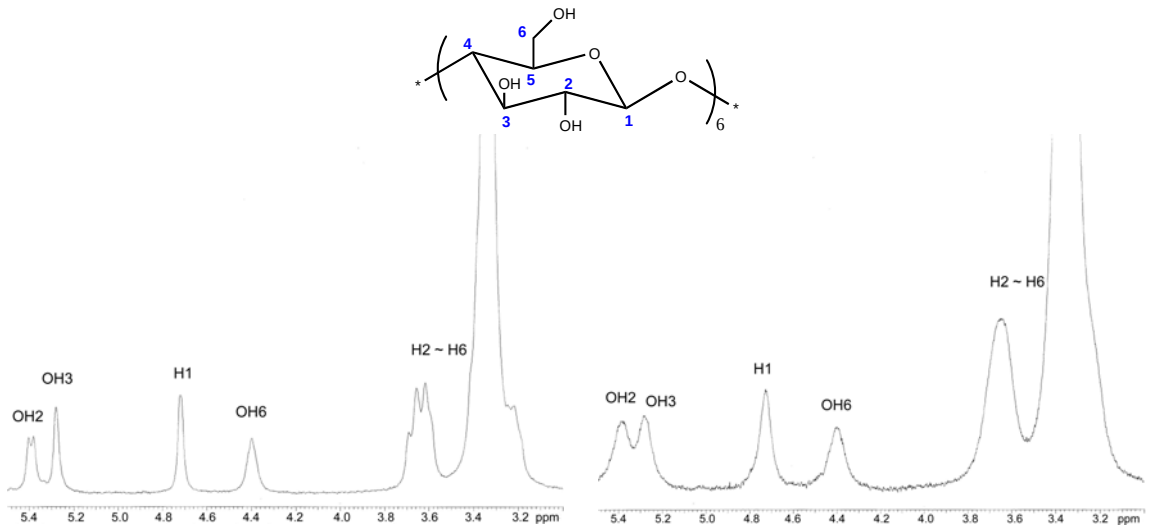

Figure 3.5. ^{1}H NMR of α-CD in AzoxRD (left, DMSO) and Zn-AzoxRD (right, DMSO).

MALDI-TOF spectra of AzoxFD and AzoxRD are shown in Figure 3.6. In their spectra, the positively ionized peaks of AzoxFD and AzoxRD are successfully obtained. The peaks of $[FD+H]^{+}$ and $[FD+Na]^{+}$ appear at 525 and 547 (m/z) respectively. The peak of sodiated AzoxRD, $[RD+Na]^{+}$ appears at 1520 (m/z). However, for metal complexed ones, we couldn't get any data successfully.

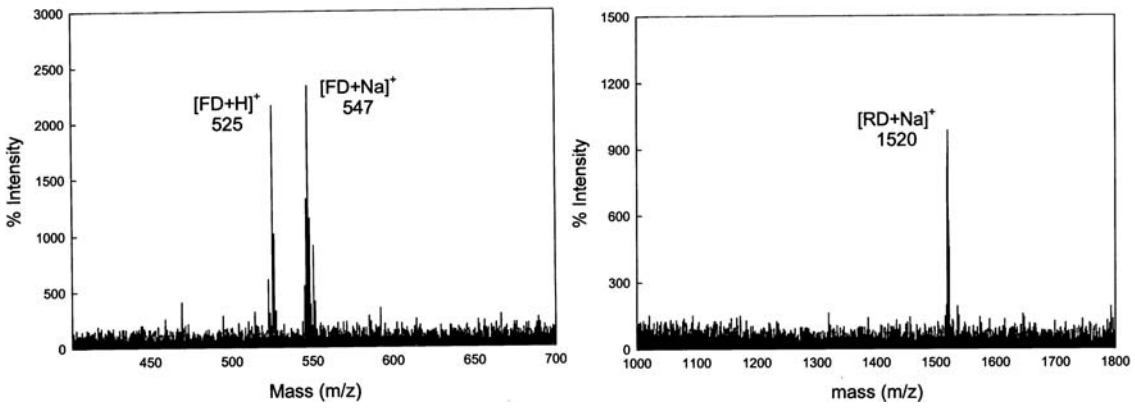

Figure 3.6. MALDI-TOF spectra of AzoxFD (left) and AzoxRD (right).

Elemental analysis of AzoxRD and its zinc complex is given in Table 3.1, from which the proposed formula of the complex is obtained. These data agree well to an empirical formula of [AzoxRD-Zn(II) · $6H_2O$]; one dye molecule coordinates with one metal ion at one end. The stoichiometry of the metal complex is, therefore, found to be 1:1 (dye:Zn). Water molecules, $6H_2O$, are considered to be a hydrated form of α-CD, and still exist both in dye rotaxane and in its Zn complex.

Table 3.1. Elemental Analysis of AzoxRD and Zn-AzoxRD and comparison with possible empirical formulas.

Empirical formula	Measured (Calculated) (%)		
	C	H	N
AzoxRD · $6H_2O$	48.48 (48.29)	5.96 (5.89)	6.82 (6.83)
$[AzoxRD\text{-}Zn(II) \cdot 6H_2O]_n$	46.65 (46.62)	5.62 (5.69)	6.58 (6.58)

In order to understand how the Zn is bound, FT-IR spectra were measured. Several important FT-IR peaks are shown (Figure 3.7). Three major peaks appear for AzoxRD in the regions 1130, 1400 and 1573 cm^{-1}, corresponding to ν(C-O on the phenoxide), ν(N=N in azo group) and ν(C=N between azo group and phenyl ring), respectively.[27] These are shifted to higher wavenumbers, 1151, 1410 and 1597 cm^{-1}, respectively. Two split peaks are observed in 434 and 474 cm^{-1}.

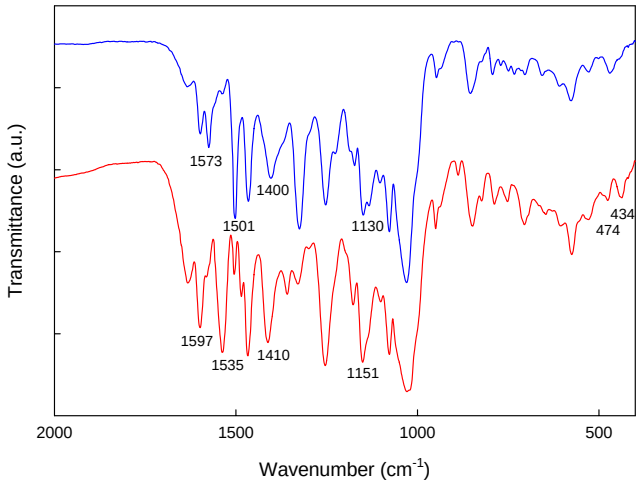

Figure 3.7. FT-IR spectra of AzoxRD (upper) and Zn-AzoxRD (lower).

DSC thermograms of α-CD, AzoxRD, and Zn-AzoxRD are shown in Figure 3.8. The DSC date for α-CD agrees well to a previous report that α-CD hydrate showed three endothermic peaks (in Figure 3.8).[28] They come from the existence of different types of water in the crystal structure of CD hydrate. A report says that there are two kinds of included water in different sites and kind of interstitial water distributed randomly outside the cavity.[29] Meanwhile, a broad endothermic transition is observed for AzoxRD and Zn-AzoxRD, which is considered as the release of included water from CD cavity on heating. Negligible change is observed in the thermograms of AzoxRD and Zn-AzoxRD, except for slight shift to higher transition temperature in the case of Zn-AzoxRD.

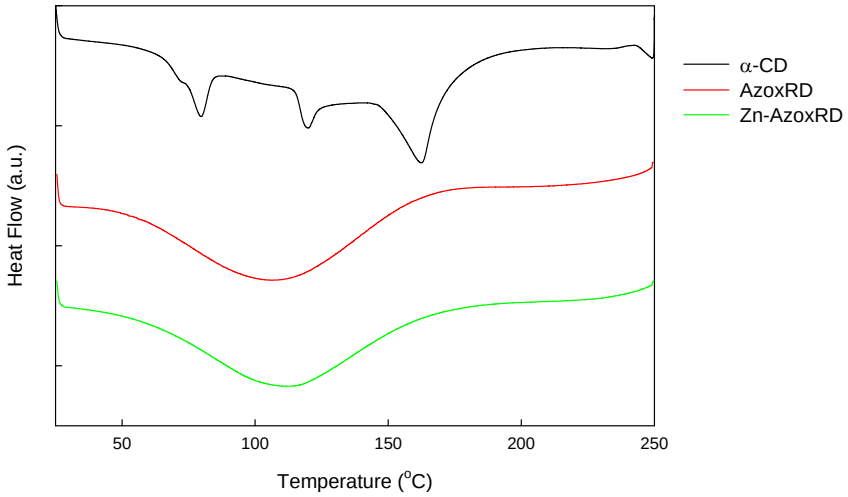

Figure 3.8. DSC diagrams of α-CD, AzoxRD, and Zn-AzoxRD.

We attempted to use the rotaxanated dye for the dyeing PP fiber. Dyed PP samples and their K/S values are shown (Figure 3.9). For comparison, a control PP sample, which was treated under the same condition without the addition of dye, is shown. Obviously, azoxine dye rotaxane enables PP fiber to be dyed, due to the presence of TiO_2 in the fiber. AzoxRD-dyed sample (C) shows a red color with λ_{max} around 520 nm. This maximum absorption is almost identical to that in aqueous solution (see Figure 3.4). Also its shade turns out to be deeper, compared to AzoxFD-dyed sample (B). When copper complexed, in terms of λ_{max}, it exhibits a red shift of about 25 nm (from 520 nm for AzoxRD-dyed to 545 nm for Cu-complexed). The duller shade is also observed for copper complexed fiber, coupled with slight increase in color strength, i.e. K/S values. This agrees well to a previous report about spectral changes with metal coordinated azo dyes.[30]

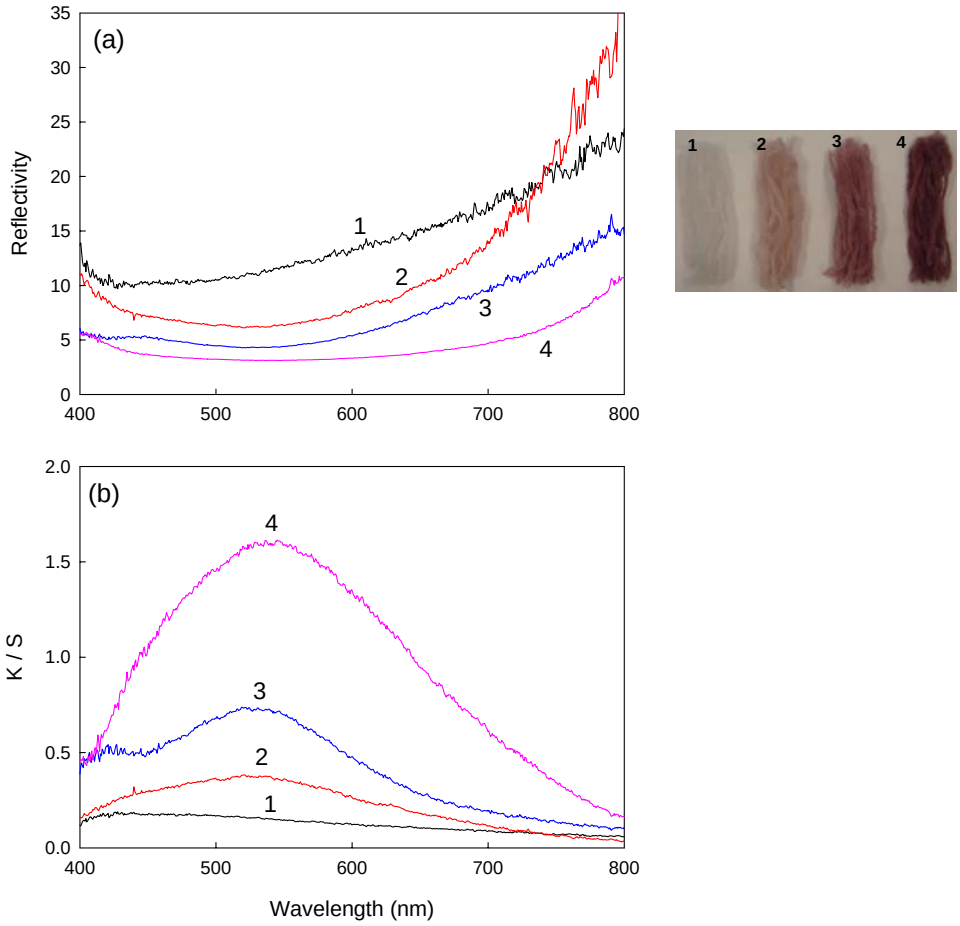

Figure 3.9. (a) Reflectivity and (b) K/S curves of PP fibers; (1) PP before dyeing, (2) after dyed with AzoxFD, (3) after dyed with AzoxRD, (4) after dyed with AzoxRD, and then Cu complexed.

3.4. Discussion

The high pH sensitivity of AzoxRD is explained by azo-hydrazone tautomerism (Scheme 3.3). The polarity of the solvent exerts a profound influence on the tautomeric equilibrium, which is known as solvatochromism. Generally, a more polar solvent favors the hydrazone form (B) whereas less polar solvents favor the azo form (A).[31] The solvent quality has a huge impact on the color of AzoxRD, and so even at the same pH value, it shows different colors depending on the mixing ratio of DMF and water. However,

regardless of the solvents, AzoxRD exhibits a strong red shift with increasing pH. We believe that the red shift is due to the existence of resonance structure (C) at higher pH.[31] The presence of a delocalized electron in (C) stabilizes the energy level of the dye molecule, typically by lowering its LUMO level. This leads to a red shift. AzoxFD shows similar pH sensitivity. In water-rich conditions, however, it readily forms precipitates. This is due to its limited solubility, and especially in neutral pHs, it shows poor solubility.

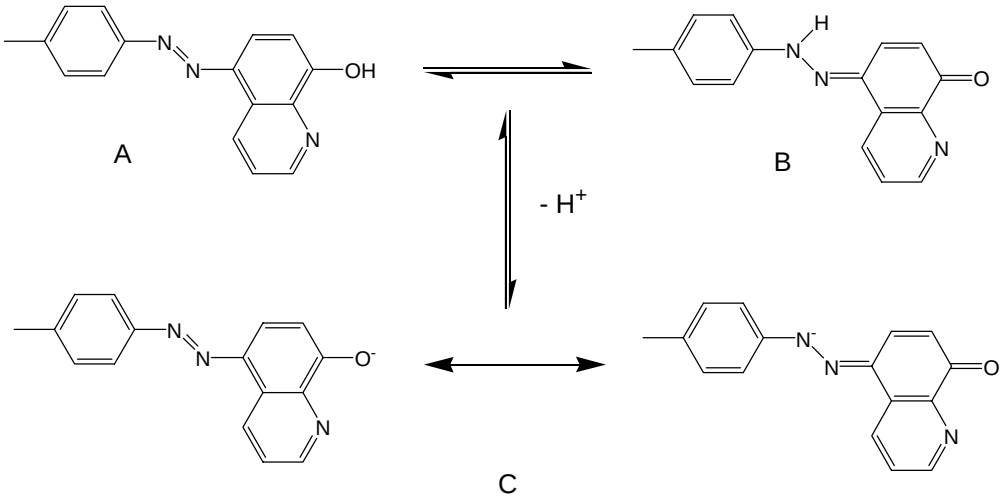

Scheme 3.3. Tautomeric equilibrium of azoxine dye; Azo tautomer (A), hydrazone tautomer (B), and resonance structures (C) at higher pH (taken and modified from ref 31).

AzoxRD exhibits a sensitive red shift in the presence of Zn^{2+} ion. Small amounts of Zn^{2+} ion change the color of a dye solution, which can be detected even by naked eye. The shift is attributed to the complex formation between HQs and Zn^{2+} ion, which increases the conjugation length. This result is suggestive of the fact that the LUMO for the azo dye is lowered upon complexation with zinc, thus leading to a red shift.[32] Such behavior has previously been reported for azo dyes upon complexation.[32]

Metallized azo dyes are one of the most commercially important dye classes and many studies have been reported about them.[33] Generally, in its chemical structure, the

azo group is a coordinating ligand to the metal (as shown in Scheme 3.4).[33] In this case, red shift is caused by chelation of the metal to the major donor and acceptor groups, hydroxyl and azo respectively, which results in a perturbation of the electron distribution. On the contrary, terminally metallized dyes is known to undergo little shade change on metal complex formation.[31] However, it is noteworthy that current azoxine dye exhibits such a huge red shift, even though it is of a terminally metallized kind. This shift is believed to come from the complex formation between HQs and Zn^{2+} ion, which extends chromophore conjugation to adjacent molecules, forming a polymeric complex. Therefore, this kind of structure, which has ligand sites at both ends of dye molecule, expects to find a very useful application for metal ion sensor.

The formation of a metal-dye complex can be observed by FT-IR spectroscopy. In its spectra, AzoxRD exhibits three characteristic bands, and these peaks are shifted to higher wavenumbers upon coordination. The formation of Zn-nitrogen and Zn-oxygen bonds are confirmed by the appearance of two split peaks in 434 and 474 cm^{-1}, respectively.[34] It is a clear evidence that metal coordination occurs through nitrogen and oxygen of the 8-HQs.

Upon addition of zinc ion (as small as 0.065 mole percent of dye), AzoxRD shows a large red shift from 530 nm to 615 nm. Increasing the amount of zinc ion causes a slight blue shift to 590 nm, and then up to 570 nm. This shift at higher concentration is possibly due to the precipitation of Zn-AzoxRD complex. From the shift of absorption maxima, we see that the detection limit of AzoxRD for Zn^{2+} reaches as low as 0.005 μmol, corresponding to 7.5 ppb, under a given condition. However, as noted previously, AzoxRD is also sensitive to other conditions, such as pH and solvent as well as metal ion.

Therefore, the sensitivity of AzoxRD includes numerous factors to be considered. Sensitivity we have obtained only is valid for a given condition (solvent mixture with DMF/pH6.0 Buffer in volume ration of 2:8). Depending on the solvent systems and pH conditions, therefore, we expect to obtain different results.

Polymeric metal complexes have been reported before.[35,36] However, as far as we know, this is the first attempt at making a polymeric dye rotaxane through the formation of metal-ligand bonds by building at the end of the dye as opposed to the azo linkage. Moreover, our case, each dye molecule is locked within α-CD cavity to form a stable rotaxane structure. By this way, CD rings are expected to exist uniformly throughout the polymeric chains. It is generally known that metallized azo dyes have low aqueous solubility. It is due to the formation of large aggregates, and some of them form sheet-like aggregates (Scheme 3.4).[31] The presence of CDs is believed to be beneficial in overcoming the poor solubility of metal complexes. As expected, compared with Zn^{2+} complex of AzoxFD (Zn-AzoxFD), Zn-AzoxRD shows improved solubility in aqueous solutions. At high pH, it remains stably soluble in aqueous conditions with the aid of hydroxyl groups in CD molecules. However, due to the inherent nature of metal complexes, Zn-AzoxRD shows limited solubility in water-rich solution with neutral pH.

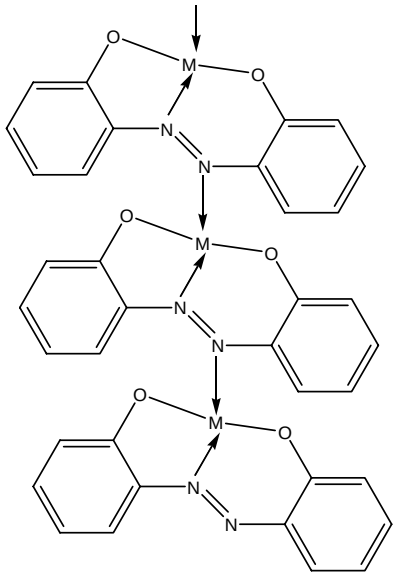

Scheme 3.4. Copper II dyes forming sheet-like aggregates when metal complexed, where M (metal) = Cu (from ref 31).

The formation of metal–ligand bonds was characterized by several spectroscopic methods. In the NMR spectra, broader CD peaks are observed upon metal complexing. However, due to a solubility problem, it is not possible to obtain a proper NMR spectrum in its aromatic region. No corresponding peaks were obtained in measurements of MALDI-TOF spectra. Several reasons are considered to be responsible. First, perhaps the molecular weight of Zn-AzoxRD exceeds the appropriate measurement ranges for the present mass system. Second, metal-ligand bonds concerned here are not strong enough to withstand the intensity of applied laser. Since there are several reports about the use of electrospray ionization (ESI) mass spectroscopy for metal complexes,[37,38] we also tried this method with Zn-AzoxRD, but in this case, the limited solubility of polymeric structure in a given solvent system (acetonitrile/water mixture) inhibited detection of peak.

Elemental analysis (EA) clearly shows that 8-HQs at both ends of the dye act as a dibasic tetradendate ligand, and indicates the formation of metal complexes that have the general formula $[ML]_n$, where M = Zn (II) or other metal (II) ions and L = AzoxRD or other azoxine dyes. This means the formation of linear polymeric metal complexes, as we first expected in Scheme 3.2. It is generally known that α-CD forms hexahydrate, α-CD·$6H_2O$; Four water molecules are located outside the cavity and two remaining water molecules are hydrogen bonded to one another.[39] From EA results, these water molecules are found to still exist in CDs of AzoxRD and its zinc complex.

As shown in Figure 3.9, AzoxRD dyed PP fiber shows higher color strength. We believe that it comes from the formation of hydrogen bondings between the inorganic additive, TiO_2, and hydroxyl group in cyclodextrin (CD) around the chromophore.[40] AzoxFD, which does not have as many –OH groups as AzoxRD, shows small degree of staining on PP fiber. Copper-complexed sample exhibits even higher color strength along with red shift. This shift is attributed to the complex formation between HQs and Cu^{2+} ion. The duller shade is also observed, which is a general spectral characteristic of metal coordinated dyes.[31]

3.5. Conclusion

In summary, we have synthesized an azoxine dye rotaxane (AzoxRD) and its polymeric metal complex with zinc (Zn-AzoxRD). AzoxRD exhibits high pH sensitivity, solvatochromism and zinc (II) ion sensing capability in aqueous solution. These behaviors come from the tautomeric equilibrium between azo-hydrazone tautomers and the formation of extended conjugation. The structure of polymeric zinc complexed dye

rotaxane is confirmed using elemental analysis, NMR and FT-IR measurements. Based on all physical properties and absorption spectra, the formation of linear polymeric metal complex is proposed. AzoxRD is found to be very effective in dyeing of polypropylene containing TiO_2, and it is due to the formation of hydrogen bonding between TiO_2 and hydroxyl groups in CD.

REFERENCES

[1] Hollingshead, R. G. W. *Oxine and its Derivatives* **Vols. I-IV**, Butterworths, London, 1954.

[2] Wang, S. "Luminescence and electroluminescence of Al(III), B(III), Be(II) and Zn(II) complexes with nitrogen donors", *Coord. Chem. Rev.* **2001**, *215*, 79.

3 Hurley, T. J.; Robinson, M. A.; Scruggs, J. A.; Trotz, S. I. "Alkyl- and arylaluminum complexes. I. The reaction of trialkyl- and triarylaluminum with bidendate ligands", *Inorg. Chem.* **1964**, *3*, 692.

[4] Tang, C. W.; VanSlyke, S. A. "Organic electroluminescent diodes", *Appl. Phys. Lett.***1987**, *51*, 913.

[5] Chen, C. H.; Shi, J. "Metal chelates as emitting materials for organic electroluminescence", *Coord. Chem. Rev.* **1998**, *171*, 161.

[6] Ghedini, M.; Deda, M. L.; Aiello, I.; Grisolia, A. "Synthesis and photophysical characterization of soluble photoluminescent metal complexes with substituted 8-hydroxyquinolines", *Synth. Met.* **2003**, *138*, 189.

[7] Meyers A.; Weck, M. "Design and synthesis of Alq(3)-functionalized polymers", *Macromolecules* **2003**, *36*, 1766.

[8] Meyers A.; Weck, M. "Solution and solid-state characterization of Alq(3)-functionalized polymers", *Chem. Mar*. **2004**, *16*, 1183.

[9] Meyers A.; South, C.; Weck, M. "Design, synthesis, characterization and fluorescent studies of the first zinc-quinolate polymer", *Chem.Comm.* **2004**, (10), 1176.

[10] Fritz, J. S.; Lane, W. J.; Bystroff, A. S. "Complexometric titrations using azoxine indicators", *Anal. Chem.* **1957**, *29*, 821.

[11] Ahmed, M. *Polypropylene fibers–science and technology*, Elsevier Scientific Publishing Company, 1982.

[12] Akrman, J.; Prkryl, J. "Dyeing behavior of polypropylene blend fibers. I. Kinetic and thermodynamic parameters of the dyeing system" *J. Appl. Poly. Sci.* **1996**, *62*, 235.

[13] Yu, C.; Zhu, M.; Shong, X.; Chen, Y. “Study on dyeable polypropylene fiber and its properties” *J. Appl. Poly. Sci.* **2001**, *82*, 3172.

[14] Tehrani, A. R.; Shoushtari, A. M.; Malek, R. M. A.; Abdous, M. “Effect of chemical oxidation treatment on dyeability of polypropylene” *Dyes Pigments* **2004**, *63*, 95.

[15] Guo, Z.; Chen, J.; Zeng, X.; Wang, G.; Shao, L. “Assistant effect of nano-CaCO3 particles on the dispersion of TiO2 pigment in polypropylene composites” *J. Mat. Sci.* **2004**, *39*, 2891.

[16] Arellano, M.; Manas-Zloczower, I.; Feke, D. L. “Effect of surfactant treatment on the formation of bound polymer on titanium-dioxide powders”, *Powder Technology* **1995**, *84*, 117.

[17] Allen, N. S.; Katami, H. “Comparison of various thermal and photoageing on the oxidation of titanium dioxide pigmented linear low density polyethylene films”, *Polym. Degrad. Stab.* **1996**, *52*, 311.

[18] Finnie, K. S.; Cassidy, D. J.; Bartlett, J. R.; Woolfrey, J. L. “IR spectroscopy of surface water and hydroxyl species on nanocrystalline TiO2 film”, *Langmuir*, **2001**, *17*, 816.

[19] Venkataraman, K. *The Chemistry of Synthetic Dyes*, New York, Academic Press, p 78, 1971.

[20] Matsui, M.; Tanka, N.; Nakay, K.; Funabiki, K.; Shibata, K.; Muramatsu, H.; Y. Abe, Y.; Kaneko, M. “Synthesis of fluorine-containing disazo dyes extended with ester linkages and their applications to guest-host liquid crystal displays”, *Liq. Cryst.* **1997**, *23*. 217.

[21] Kubelka, P. “New contributions to the optics of intensely light-scattering materials”, *J. Opt. Soc. Am.* **1948**, *38*, 448.

[22] Kubelka, P. “New contributions to the optics of intensely light-scattering materials. 2. Nonhomogeneous layers”, *J. Opt. Soc. Am.* **1954**, *44*, 330.

[23] El-Sonbati, A. Z.; El-Bindary, A. A.; Al-Saway, A. A. “Stereochemistry of new nitrogen containing heterocyclic aldehyde. IX. Spectroscopic studies on novel mixed-ligand complexes of RH(III)”, *Spectrochim. Acta A.* **2002**, *58*, 2771.

[24] Osman, A. H.; Zidan, A. S. A.; El-Said, A. I.; Aly, A. A. M. “Synthesis an photochemistry of binary and mixed-ligand complexes of copper(II) containing 5-arylazo-8-hydroxyquinoline derivatives and alkyl xanthates”, *Transition Met. Chem.* **1993**, *18*, 34.

[25] Rau, H. “Spectroscopic properties of organic azo-compounds”, *Angew. Chem. Int. Ed.* **1973**, *12*, 224.

[26] Zhao, T.; Beckham, H. W. “Direct synthesis of cyclodextrin-rotaxanated poly(ethylene glycol)s and their self-diffusion behavior in dilute solution”, *Macromolecules* **2003**, *36*, 9859.

[27] Zidan, A. S. A.; El-Said, A. I.; El-Meligy, M. S.; Aly, A. A. M.; Mohammed, O. F. “Mixed ligand complexes of 5-arylazo-8-hydroxyqinoline and α-amino acids with Co(II), Ni(II) and Cu(II)”, *J. Therm. Anal. Cal.* **2000**, *62*, 665.

[28] Jozwiakowski, M. J.; Connors, K. A. “Aqueous solubility behavior of 3 cyclodextrins”, *Carbohyd. Res.* **1985**, *143*, 51.

[29] Steiner, T.; Koellner, G. “Crystalline β-cyclodextrin hydrate at various humidities: fast, continuous, and reversible dehydration studied by X-ray diffraction”, *J. Am. Chem. Soc.* **1994**, *116*, 5122.

[30] Sebe, I.; Tarabasanu-Mihaila, C. “Coordinating acid azo dyes and direct dyes derived from 8-hydroxyquinoline”, *Rev. Rouma. Chim.* **1995**, *40*, 275.

[31] Gordon, P. F.; Gregory, P. *Organic Chemistry in Colour*, Spinger-Verlag Berlin Herdleberg, Germany, **1987**.

[32] Ghedini, M.; Deda, M. L.; Aiello, I.; Grisolia, A. “Synthesis and photophysical characterization of luminescent zinc complexes with 5-substituted-8-hydroxyquinolines”, *J. Chem. Soc. Dalton Trans.* **2002**, 3406.

[33] Price, R. *The chemistry of metal complex dyestuffs. In: The chemistry of synthetic dyes, Venkataraman, K. Vol. III.* New York, Academic Press 1970.

[34] Ahmed, S. M.; Shahata, M. M.; Kamal, M. M. “Spectrophotometric studies of the coordination polymers based on poly(8-hydroxyquinoline) matrix”, *J. Inorg. Organomet. Polym.* **2003**, *13*, 171.

[35] El-Sonbati, A.Z.; Belal, A. A. M.; El-Wakeel, S. I.; Hussien, M. A. “Stereochemistry of new nitrogen containing heterocyclic compounds. X. Supramolecular structures and stereochemical versatility of polymeric complexes”, *Spectrochim. Acta, Part A: Mole. Biomole. Spectro.* **2004**, *60*, 965.

[36] Kim, S.; Cui, J.; Park, J.; Ryu, J.; Han, E.; Park, S.; Jin, S.; Koh, K.; Gal, Y. “Synthesis and light emitting properties of polymeric metal complex dyes based on hydroxyquinoline moiety”, *Dyes Pigments* **2002**, *55*, 91.

[37] Ross, A. R. S.; Ikonomou, M. G.; Thompson, J. A. J.; Orians, K. J. “Determination of dissolved metal species by electrospray ionization mass spectrometry”, *Anal. Chem.* **1998**, *70*, 2225.

[38] Ross, A. R. S.; Ikonomou, M. G.; Orians, K. J. “Electrospray ionization of alkali and alkaline earth metal species. Electrochemical oxidation and pH effects”, *J. Mass Spctrom.* **2000**, *35*, 981.

[39] Manor, P. C.; Saenger, W. “Topography of cyclodextrin inclusion complexes. III. Crystall and molecular structure of cyclohexaamylose hexadrate, the (H2O)2 inclusion complex”, *J. Am. Chem. Soc.* **1974**, *96*, 3630.

[40] Haque, S. A.; Park, J. S.; Srinivasarao, M.; Durrant, J. R. “Molecular-level insulation: An approach to controlling interfacial charge transfer”, *Adv. Mar.* **2004**, *16*, 1177.

CHAPTER 4

ACETYLENE DYE ROTAXANE

4.1. Introduction

Fluorescent dyes are known to behave differently when trapped inside the cavity of cyclodextrins (CDs).[1-4] When cyanine dyes, with extended conjugation, were encapsulated within CDs, their fluorescence efficiency and photostability were reported to increase.[1] The fluorescence efficiency was enhanced due to the reduced flexibility of the encapsulated chromophore. In its absorption and emission spectra, CD encapsulation caused red shift. The inclusion of cyanine dyes in CD also improved the photostability both by reducing the rate of singlet oxygen formation and by reducing the rate of reaction between singlet oxygen and the threaded dye.[2] Upon rotaxanation, fluorescent dye exhibited reversible redox process, and its kinetic stability was increased.[3] The synthesis of fluorescent stilbene and tolan rotaxanes was reported, in which Suzuki coupling using Pd catalyst in aqueous condition gave dye rotaxane in fairly good yields.[4] CD reduced the rate of non-radiative decay by restricting the flexibility of the excited state, and by hindering the quenchers available. Rotaxane structure of fluorescence dye, as in above-mentioned examples, has numerous advantages. This would be a promising way of improving the stability and brightness of luminescent and electro-luminescent materials in various applications, such as for polymeric light emitting diodes and biological probes.[5]

In an effort to synthesize fluorescent dye rotaxane, we tried to synthesize acetylene dye rotaxane. In the molecular structure, it corresponds to a monomer unit of poly(phenyleneethynylene)s (PPEs), which are characterized by high fluorescence

quantum yield [6,7] and higher oxidation potential due to an electron-withdrawing effect of the –C≡C- unit.[8] In this chapter, we describe the synthesis of novel acetylene dye rotaxane using the Pd-catalyzed reaction of Heck-Cassar-Sonogashira-Hagihara type.[9] The chemical structures of both free and rotaxanated dyes were confirmed using various spectroscopic methods, such as ^{1}H-NMR, ^{13}C-NMR, electrospray spectrometry (ESI-MS), and ROESY (Rotating Overhauser Effect SpectroscopY) NMR spectroscopy. The fluorescence properties of acetylene dye rotaxane were measured and compared with those of free dye in the solid state as well as in solutions. Fluorescence intensity at various pH conditions was measured. Fluorescence quenching behavior was investigated in the presence of various metal ions.

In its synthesis, the condensation was done by reacting 1,4-diethynylbiphenyl with 5-iodo-isophthalic acid in the presence of α-CD. A water soluble palladium (Pd) catalyst was used as a catalyst and cuprous iodide as a co-catalyst, and triethylamine and K_2CO_3 were added to maintain alkaline pH condition. The water-soluble Pd catalyst was generated *in situ* from palladium acetate and tris(m-sulfophenyl)phosphine trisodium salt, as previously reported.[10,11]

Free dye was synthesized using the same synthetic scheme without the addition of α-CD, and its emission spectra shows high sensitivity to fluorescence quenchers. In the presence of various metal ions, it exhibits significant fluorescence quenching. Its degree of quenching is almost equivalent to that of conjugated polymers, which are generally known to have sensitivity enhancements over single receptor analogue.[12] Amplified quenching of fluophores has received considerable attention due to its promising application for chemo- and bio-sensors.[13~16] This fluorescence quenching is related to

photoinduced electron transfer.[17] To our surprise, however, upon rotaxanation, acetylene dye rotaxane shows a huge difference in its sensitivity towards metal ions, exhibiting far less quenching. We attribute this reduced quenching to the existence of CD, which protects the threaded chromophore against outside quenchers while providing increased solubility in aqueous conditions with numerous hydroxyl (-OH) groups.

4.2. Experimental

4.2.1. Preparation of acetylene dye rotaxane.

4,4'-Diethynylbiphenyl (1): 4,4'-Diiodobiphenyl (10 g, 24.6 mmol) was dissolved in THF (50 mL) with piperidine (5 mL), $(Ph_3P)_2PdCl_2$ (0.35 g, 0.5 mmol), CuI 0.475 g (2.5 mmol), and trimethylsilylacetylene (8.7 mL, 61.6 mmol) was slowly added under nitrogen. The mixture was warmed up to 40^{o}C for 30 minutes, and then stirred overnight at room temperature. Then, excess hexane was added and all salts including Pd catalyst were removed by filtering the mixture through silica gel. The filtrate was collected, then evaporated. The residue was dissolved in methanol (1 L) and purified by recrystallization, to collect the precipitate. To remove the silyl protection groups, the filtrate was dissolved in ethanol (500 mL) in the presence of KOH (10 g), and stirred overnight. Two-thirds of solvent was removed by evaporation, and gradual addition of water gave a pale brownish precipitate. The aqueous layer was extracted with CH_2Cl_2, and then the solvent was evaporated to give the product **1**. (4.48 g, yield 90%). ^{1}H NMR (300 MHz, $CDCl_3$): δ_H = 7.4 (b, 8H), 3.1 (s, 2H), ^{13}C NMR (75 MHz, $CDCl_3$): δ_C = 136.3, 132.6, 127.0, 121.2, 84.0, 79.0. m/z (ESI MS) 201.1 (M^-).

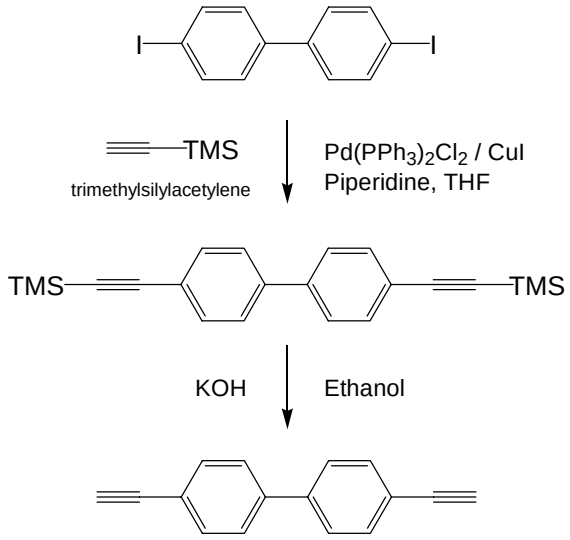

Scheme 4.1. Synthesis of 4,4'-diethynylbiphenyl **1**.

5-Iodo-isophthalic acid (2): A previous report was followed for the synthesis.[12] 5-Aminoisophthalic acid (1.75 g, 9.6 mmol) was suspended in mixture of water (5 mL) at 0-5 ^{o}C. Dilute HCl (10% wt, 30 mL, 30 mmol) and $NaNO_2$ (701 mg, 10.1 mmol) solutions were added successively, and then the solution was stirred for 1 hr to complete diazotization. Then small amount of sulfamic acid was added to remove excess nitrite. KI (6.37 g, 38.4 mmol) was slowly added, and the mixture was stirred overnight at room temperature. After reaction, the precipitate was collected by filtration, washed with water several times, and dried in vacuo (1.26 g, yield 45%). 1H NMR (300 MHz, $CDCl_3$): δ_H = 8.8 (b, 3H), ^{13}C NMR (75 MHz, $CDCl_3$): δ_C = 172.0, 144.5, 132.0, 130.0, 98.0. m/z (ESI MS) 291.0 (M^-).

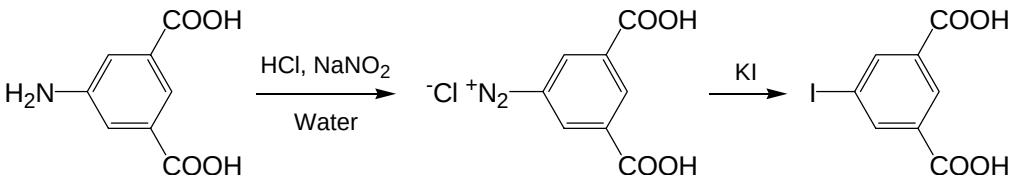

Scheme 4.2. Synthesis of 5-iodoisophthalic acid **2**.

Acetylene dye rotaxane (3): A mixture of 4,4'-diethynylbiphenyl **1** (0.151 g, 0.75 mmol), triethylamine 0.0.46 g (4.5 mmol) and α-cyclodextrin (2.92 g, 3.0 mmol) was suspended in water (10 mL). 5-Iodoisophthalic acid **2** (0.64 g, 2.2 mmol) with potassium carbonate (0.91 g, 6.6 mmol) in water (5 mL) were slowly added, and the resultant mixture was sonicated for 1 hour under nitrogen. Palladium acetate (11 mg, 0.05 mmol), 3,3',3"-phosphinidynetris(benzene sulfonic acid) trisodium salt (29 mg , 0.05 mmol) and copper iodide (48 mg, 0.25 mmol) were added with stirring. The mixture was warmed up to 50 ^{o}C, and then stirred for a day. After reaction, the mixture was diluted with aqueous Na_2CO_3 solution (2 M, 50 mL), and then filtered. The filtrate was collected and acidified to below pH 1 with dilute HCl. Soxhlet extraction was done using acetone for 3 days in order to remove remaining starting materials and/or free dye. The dye rotaxane **3** (RD hereafter) was obtained by filtration, washed profusely with water and dried *in vacuo* overnight. The product was obtained as a yellow powder (132 mg, yield 13 %). δ_H (300 MHz, DMSO) δ = 8.46 (t, 1H), 8.45 (t, 1H), 8.28 (d, 2H), 8.04 (d, 2H), 7.91 (d, 2H), 7.80 (m, 4H), 7.70 (d, 2H), 5.28 (s, 6H), 5.27 (s, 6H), 4.75 (d, 6H), 4.33 (s, 6H), 3.8-3.2 (m, 36H) ; δ_C (75 MHz, DMSO): δ = 165, 139-140, 135, 134.4, 133, 131, 129, 127, 125, 123, 120, 119, 101, 90, 87, 81, 72-71, 59 ppm; m/z (ESI$^-$ MS) 1501 (M^-).

Free dye (FD hereafter) was synthesized following the same routes, but without the addition of α-CD. It was purified by dissolving in absolute ethanol, and then precipitating by small amount of water. It was repeatedly dissolved in aqueous Na_2CO_3 solution (2 M, 50 mL), and then precipitated in acidic condition, as a pale yellow powder (170 mg, yield 50 %). δ_H (300 MHz, DMSO) δ = 8.45 (t, 2H), 8.27 (d, 4H), 7.8 (d, 4H),

7.7 (d, 4H) ; δ_C (75 MHz, DMSO): δ = 165, 139, 135, 132, 131, 129, 126, 123, 121, 90, 88 ppm; m/z (ESI$^-$ MS) 529 (M^-).

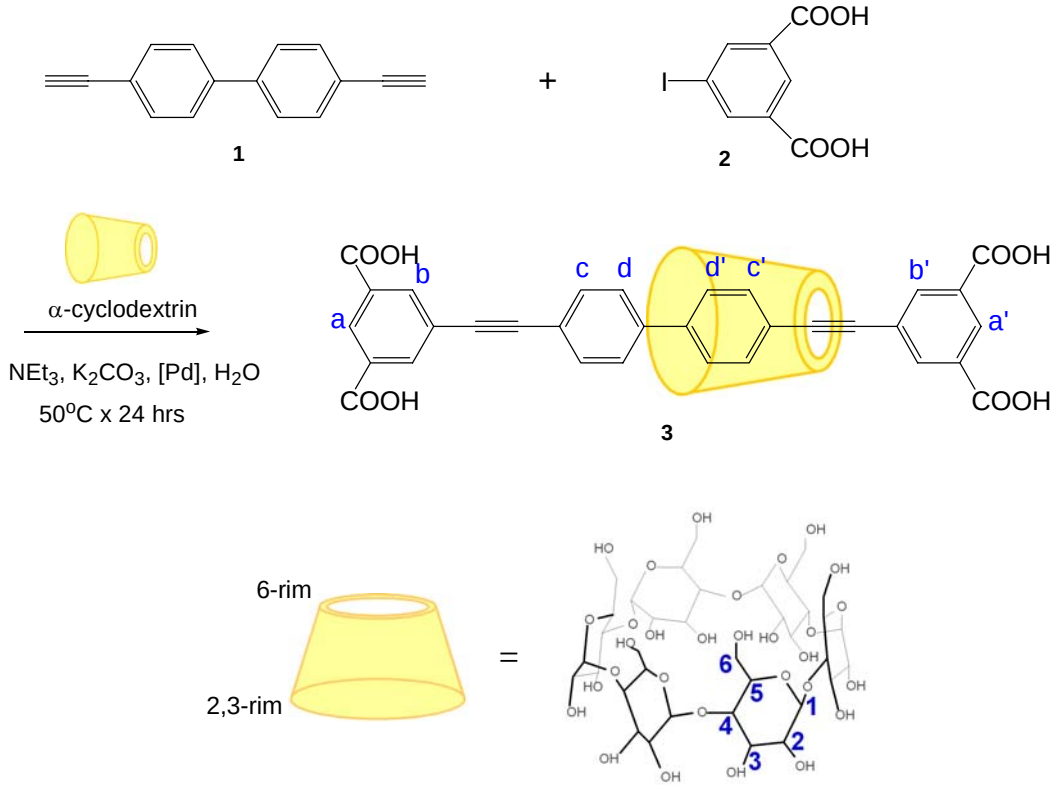

Scheme 4.3. Synthesis of acetylene dye rotaxane.

4.2.2. Property investigation. The fluorescent spectra were collected using a Shimadzu RF-5300PC spectrofluorophotometer. Emission spectra were obtained with excitation at 330 nm, if not specified otherwise. For quantum yield determination, a solution of quinine sulfate in 0.1 N H_2SO_4 was used as a reference. The concentrations were adjusted such that the absorbance was around 0.05. The area of the emission spectrum was calculated from the program and then compared to provide an estimate of the quantum yield using the following equation: $\Phi_s = \Phi_r (A_r F_s / A_s F_r)(n_s^2)(n_r^2)$, where, Φ_s = quantum yield of the sample, Φ_r = quantum yield of the reference (Φ_r = 0.54), A_r =

absorbance of the reference, F_s = integrated fluorescence intensity of the sample, A_s = absorbance of the sample, F_r = integrated fluorescence intensity of the reference, n_s = refractive index of solvent, and n_r = refractive index of 0.1 N H_2SO_4 solution (n_r = 1.35). Absorption spectra were measured on a Lambda 7 spectrometer (Perkin Elmer) in 1 cm cuvette. A Headway Research model PWM32 instrument was used to spin-coat dilute ethanol solutions of dyes onto glass slides for thin film measurements. For fluorescence quenching experiments with various metal ions, both FD and RD were prepared at a concentration of 1.0 x 10^{-6} M in HEPES (4-(2-hydroxyethyl)-1-piperazineethanesulfonic acid) pH 7.2 buffer solutions with 10 mM buffer strength. Buffer solutions with various pHs are prepared, using acetate (pH 3.5~5), phosphate (pH 6~9), and ethanolamine (above pH 9) buffer, respectively, and buffer concentration is maintained at 10 mM.

4.3. Results

The rotaxane formation can readily be characterized by various characterization techniques, such as ^{1}H, ^{13}C NMR and ESI MASS spectroscopies. As seen in Scheme 4.3, FD has symmetrical structure around its biphenyl moiety, and thus shows simple NMR spectra. Once threaded, however, due to the conical shape of α-CD, RD experiences a nonequivalent environment at both ends, leading to more splitting of the aromatic proton peaks. In both ^{1}H and ^{13}C NMR spectra, consequently, RD shows much more complex peaks than FD, aside from additional aliphatic peaks from α-CD. By comparing the relative integrals, threading ratio between dye and CD was determined and found to be 1:1, forming acetylene dye [2]rotaxane. ESI mass measurements clearly show the formation of rotaxane structure.

The ROESY spectrum of RD was shown in Figure 4.1. Strong couplings are observed from the aromatic protons d' and c' of the dumbbell to protons H3 and H4 of the α-CD, from b' to H5 and H6, which indicate that the narrow 6-OH rim of α-CD is closer to the isophthalic acid blocker. This indicates that the α-CD exists over one end of the dye molecule, leaving the other end uncovered. Aromatic protons from uncovered part show their peaks at the same positions as those of FD.

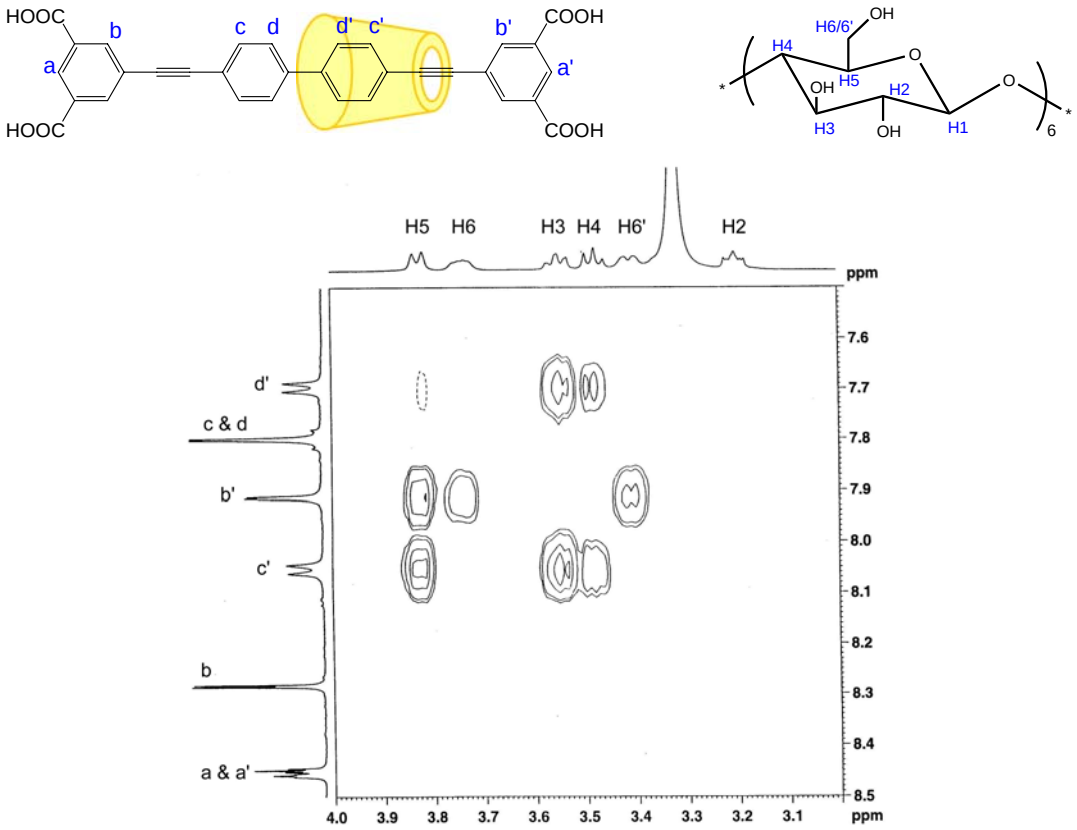

Figure 4.1. ^{1}H ROESY NMR (500 MHz) spectrum of acetylene dye rotaxane (in DMSO-d^6, 298 K).

Hydrated crystals of RD for X-ray crystallographic study were grown from water, by dissolving it in weak alkaline solution containing K_2CO_3 (0.2~0.3 g/L), and then slowly making precipitates by the addition of dilute HCl solution (1 % wt). Important

crystal data are listed in Table 4.1, and resultant side view of RD molecule is shown in Figure 4.2. As shown in NMR study, the α-CD is displaced from the center of the threaded molecule, with its narrower 6-rim closer to the end blocker and wider 2,3-rim over the center of the biphenyl unit. The threaded dye molecule looks quite planar, but its main axis exhibits a slight torsion. In adjacent molecules, the dye molecule is also observed to become unthreaded out of CD cavity during crystal growing.

Table 4.1. Crystal data and structure refinement for RD **3**.[*)]

Empirical formula	C68 H78 O40.92
Formula weight	1550.10
Temperature	173(2) K
Wavelength	0.71073 Å
Crystal system	Monoclinic
Space group	P2(1)
Unit cell dimensions	a = 13.580(2), b = 22.798(4), c = 23.880(4) Å α= 90°, β= 98.241(4)°, γ= 90°
Volume	7317(2) $Å^3$
Z	4
Density (calculated)	1.407 Mg/m^3
Absorption coefficient	0.118 mm^{-1}
Crystal size	0.36 x 0.22 x 0.13 mm^3
Theta range for data collection	1.52 to 23.53°
Index ranges	$-15 \le h \le 15$, $-25 \le k \le 25$, $-26 \le l \le 26$
Reflections collected	46811
Max. and min. transmission	1.00 and 0.428476
Absorption correction	Semi-empirical from equivalents
Refinement method	Full-matrix least-squares on F^2 (Full-matrix least-squares on F = 1.022)
Final R indices [I>2σ(I)]	R_1 = 0.1961, R_{w2} = 0.4422
R indices (all data)	R_1 = 0.2472, R_{w2} = 0.4764

There are two cyclodextrin and two dye molecules per asymmetric unit, with around 700 atoms per unit cell. And there is disorder in one of the dye molecules. Only the higher occupancy coordinates are plotted in Figure 4.2. Refer to Appendix A for complete crystallographic data.

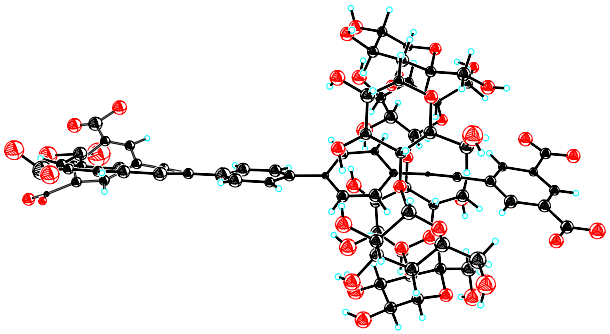

Figure 4.2. X-ray structure of a dye rotaxane **3**.

There is no significant difference in the electronic absorption and emission spectra of these dyes. With rotaxanation, RD shows a slight red shift in solution, compared with free dye (for FD and RD, λ_{max}(abs.) = 326 and 327 nm; λ_{max}(emi.) = 367, 387 and 369, 388 nm in methanol, respectively, Figure 4.3a). It was known that rotaxane encapsulation stabilized the dumbell in both ground and excited states by protecting the threaded chromophore,[3] which is considered to be responsible for a slight red shift of RD. In the solid state, however, the emission spectrum of RD exhibits a different behavior. When spin-cast on the glass slide, RD shows a slight blue shift with a narrowing of the absorption peak (Figure 4.3b). CD encapsulation is known to reduce aggregation of rigid and planar molecules.[5] As a result, RD shows decreased amount of aggregation, compared to FD, in the solid state. These separated dye molecules of RD can lead to a blue shift in their emission. Also CD cavity allows more rotation of a dye moiety even in the solid state, which may be responsible for blue shift in emission to some degree.

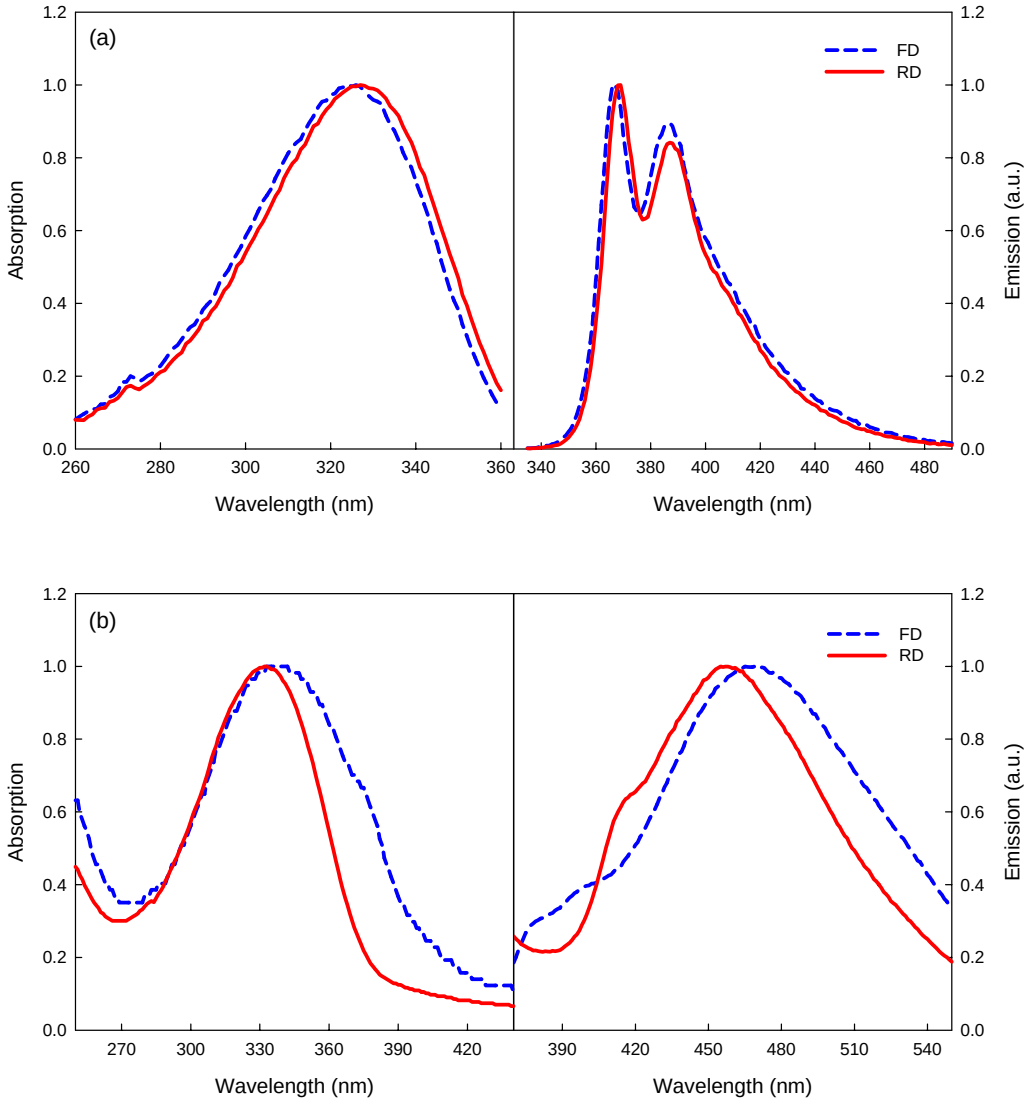

Figure 4.3. Normalized absorption spectra (left) and emission spectra (right) of FD (blue dotted) and RD (red solid); (a) in methanol, (b) in the solid-state thin film. Emission was obtained with excitation at 330 nm.

The relative fluorescence quantum yields in aqueous buffer and methanol are listed in Table 4.2. In both solvents, the fluorescence quantum yields of RD are higher than those of FD. This result is not so surprising, since several papers have already reported that CD encapsulation acts as a way of reducing the quenching effect of a

surrounding environment and reducing the flexibility of the threaded chromophore, thus leading to an enhancement in quantum yield.[1,4]

Table 4.2. Relative fluorescence quantum yields of FD and RD in aqueous buffer solution and methanol [1)].

Solvent	FD	RD
Methanol	0.554	0.669
Aqueous Buffer [2)]	0.548	0.632

[1)] Quinine sulfate in 0.1 N sulfuric acid was used as standard. Absorbance was adjusted at 0.05 ± 0.01,
[2)] Ethanolamine buffer (pH 9.6), buffer conc. 10 mM

The structure of free dye includes four carboxylic acids, and these are responsible for the transition from neutral to anionized form of a dye molecule in various pH range. The emission intensity of FD is observed to be highly pH sensitive (Figure 4.4). In acidic conditions, its emission intensity is negligibly low. This is mainly due to low solubility of the dye. With increasing pH, it exhibits an increase in its emission. It is attributed to the formation of carboxylate (COO^-) groups at these conditions. FD shows a huge fluorescence increase around pH 7. Above pH 8.3, the emission intensity is saturated, and no longer increased. Behavior of RD found to be similar to that of FD, in that the intensity also increases at higher pH. However, its fluorescence intensity increases gradually with pH, without any sudden jump as in FD. This is due to the existence of numerous hydroxyl groups from CDs, from which its aqueous solubility is quite stable even in acidic condition. RD also shows small fluorescence increase from pH 4.5 to pH 5.0, but the difference is not as big as that of FD. Around pH 7, its fluorescence is observed to be saturated.

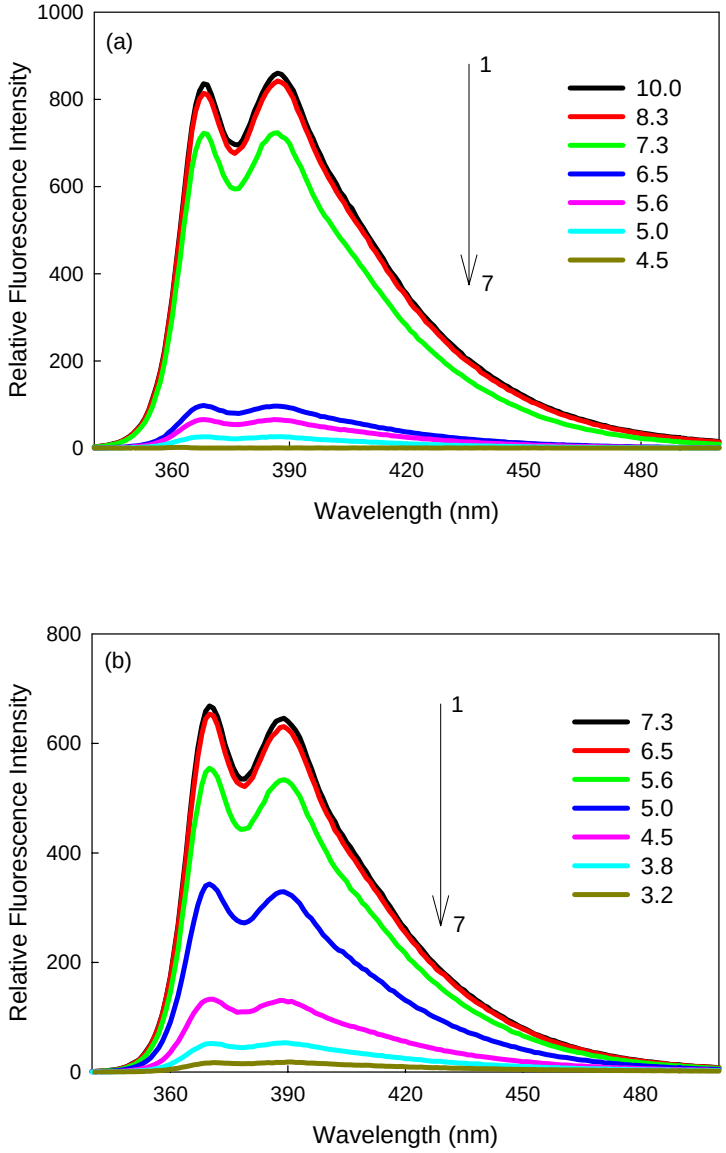

Figure 4.4. Relative fluorescence intensity under different pH conditions. The concentrations of both dyes are 1.0 x 10^{-6} M. Dyes are excited at 330 nm. (a) for FD, legends indicate pHs of the solutions (1→7): 10.0, 8.3, 7.3, 6.5, 5.6, 5.0, 4.5. (b) for RD, legends indicate pHs of the solutions (1→7): 7.3, 6.5, 5.6, 5.0, 4.5, 3.8, 3.2. Arrows indicate decreasing pH of the solutions.

In order to investigate the sensing abilities, the fluorescence intensity of both dyes was measured in the presence of various metal ions as quenchers. The Stern-Volmer equation [eq. (4.1)] is useful in the quantitative measurement of fluorescence quenching; F_o is the initial fluorescence intensity measured without any quenchers, F is the fluorescence intensity at a given concentration of the quencher $[Q]$, and K_{SV} is the Stern-Volmer constant [18, 19].

$$F_o / F = 1 + K_{SV}[Q] \qquad (4.1)$$

The graph of (F_o / F) versus $[Q]$ yields K_{SV} value as a slope. Normally, the more sensitive system gives steeper plot, leading to higher K_{SV} values. Linear Stern-Volmer plots were observed for both dyes when Cu^{2+} was used as a quencher (Figure 4.5). We observe that FD is effectively quenched by copper ion, and its K_{sv} value is determined to be 2.5×10^5 M^{-1} from the slope. Compared to FD, RD shows much smaller K_{SV} value, 2.0×10^3 M^{-1}, with a difference by the order of 10^2. This indicates that RD exhibits much less sensitivity to the existing quencher, Cu^{2+} ion. Similar behavior is observed for all quenching species we tried, including Hg^{2+} (Figure 4.6), Pb^{2+} (Figure 4.7), and methyl viologen hydrate (Figure 4.8). As for Mg^{2+} and Zn^{2+}, both dyes exhibit almost no fluorescence quenching. All K_{SV} values for these various quenchers are calculated and listed in Table 4.3.

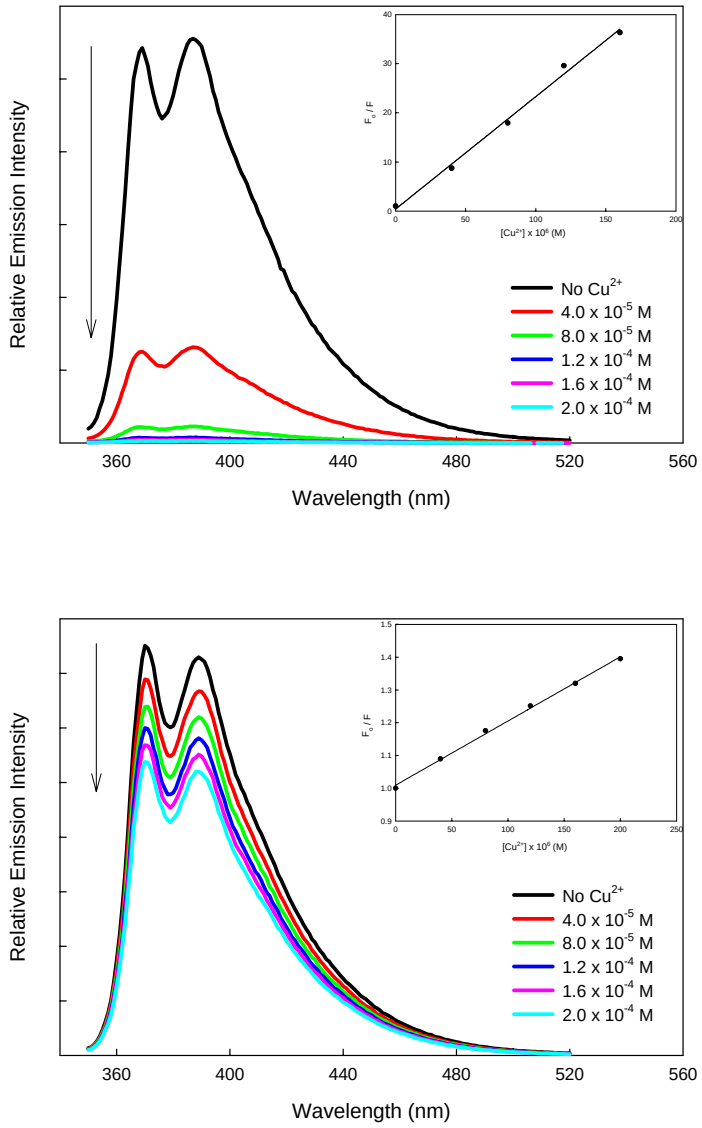

Figure 4.5. Fluorescence emission spectra of FD (upper) and RD (lower) during quenching with $CuSO_4$ in aqueous buffer (HEPES pH 7.2 with 10 mM buffer strength). Concentrations of both dyes are 1.0 x 10^{-6} M. The insets show the Stern-Volmer plot. The Stern-Volmer constant, K_{SV}, were calculated to be 2.5 x 10^5 M^{-1} (FD) and 2.0 x 10^3 M^{-1} (RD), respectively. Arrows indicate increasing amount of $CuSO_4$.

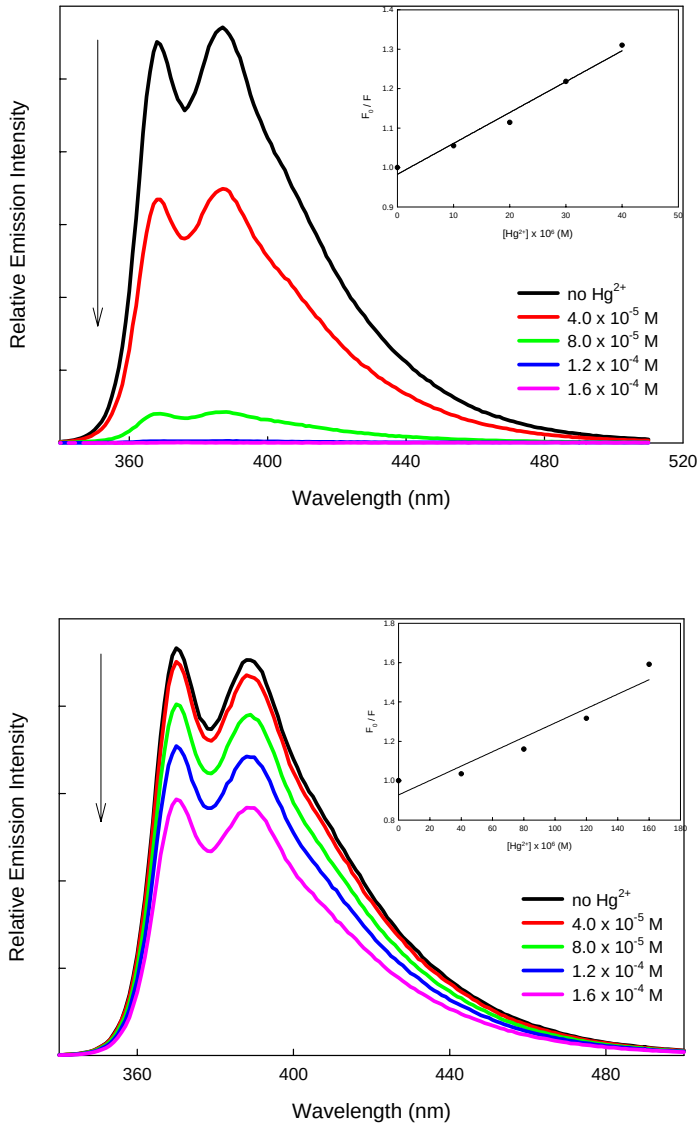

Figure 4.6. Fluorescence emission spectra of FD (upper) and RD (lower) with $Hg(OOCCH_3)_2$. The Stern-Volmer constant, K_{SV}, were calculated to be 7.8 x 10^3 M^{-1} (FD) and 3.7 x 10^3 M^{-1} (RD), respectively. Arrows indicate increasing amount of $Hg(OOCCH_3)_2$.

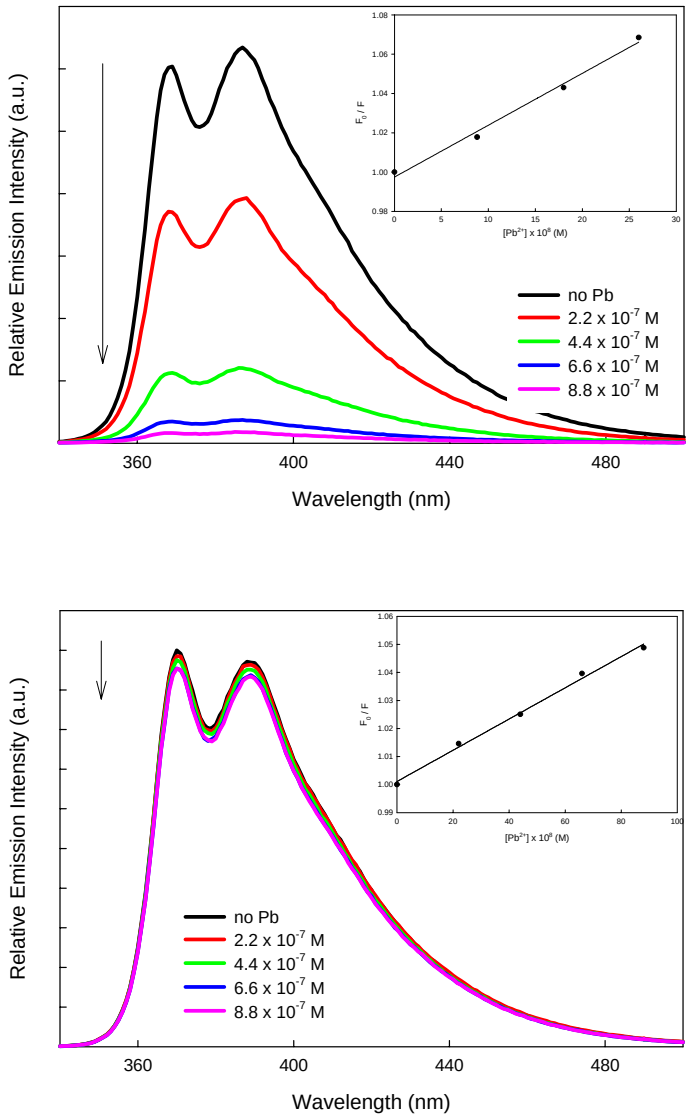

Figure 4.7. Fluorescence emission spectra of FD (upper) and RD (lower) with $PbCl_2$. The Stern-Volmer constant, K_{SV}, were calculated to be 2.6 x 10^5 M^{-1} (FD) and 5.6 x 10^4 M^{-1} (RD), respectively. Arrows indicate increasing amount of $PbCl_2$.

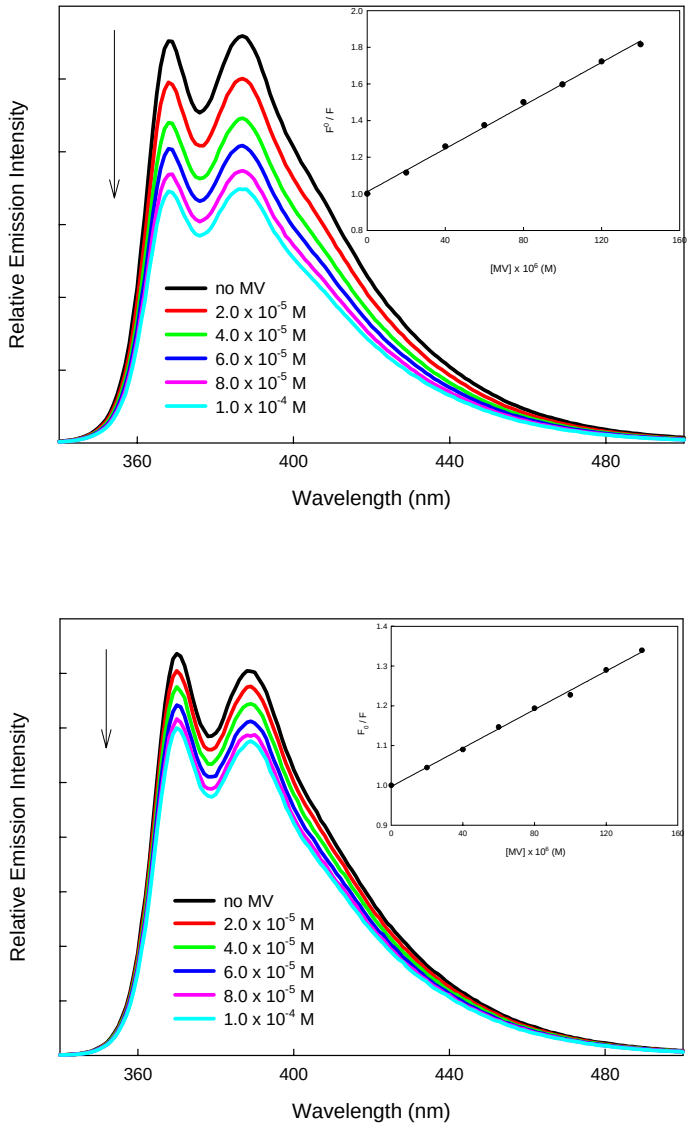

Figure 4.8. Fluorescence emission spectra of FD (upper) and RD (lower) with methyl viologen hydrate. The Stern-Volmer constant, K_{SV}, were calculated to be 5.9 x 10^3 M^{-1} (FD) and 2.4 x 10^3 M^{-1} (RD), respectively. Arrows indicate increasing amount of methyl viologen hydrate.

Table 4.3. K_{SV} (M^{-1}) values measured with the addition of various metal ions.

Quenchers	FD	RD
$CuSO_4$	2.5×10^5	2.0×10^3
$Hg(OOCCH_3)_2$	7.8×10^3	3.7×10^3
$PbCl_2$	2.6×10^5	5.6×10^4
$Pb(NO_3)_2$	4.7×10^5	1.7×10^5
$Mg(OOCCH_3)_2$	NQ [1)]	NQ [1)]
$ZnCl_2$	< 10	< 10
Methyl viologen hydrate	5.9×10^3	2.4×10^3

[1)] NQ : no quenching observed.

4.4. Discussion

Anderson and coworkers have reported numerous papers on the synthesis of fluorescence dye rotaxanes based on Suzuki coupling (Figure 4.9 a).[4,5,20-24] They successfully showed that the combination of aryl iodide stopper, diboronic acid core and macrocycle components can give highly fluorescent CD encapsulated rotaxanes in high yields. This approach is quite different from previous stilbene rotaxanes which have been prepared by aromatic nucleophilic substitution and by slipping macrocycles over preformed dumbbells.[25,26] Here, we adopt Heck-Cassar-Sonogashira-Hagihara type coupling for the synthesis of a fluorescent rotaxane. Its overall synthetic scheme is similar to that of Suzuki Coupling; threading and then capping (Figure 4.9 b). In terms of the threaded dumbbells, however, these two reactions are quite different. Boronic acid derivatives in Suzuki Coupling are generally soluble in aqueous alkaline medium, and thus the reaction proceeds in a homogeneous state in water. This is considered as favorable for the threading of a dumbbell through CD cavity. On the contrary, diethynyl derivative is completely insoluble in water. Also highly aromatic moiety of biphenyl group makes it completely insoluble in water. Therefore, the mixture looks turbid and the

reaction starts in a heterogeneous condition. This is probably unfavorable for obtaining a high inclusion yield. Moreover, in the current case, we should expect a side reaction of forming extended acetylene structure.[27] These are responsible for a low yield (~13%). Unlike Suzuki Coupling, we've not succeeded in the synthesis of polyrotaxane using this scheme. We consider that poor water solubility of the dumbbell is also responsible for this failure.

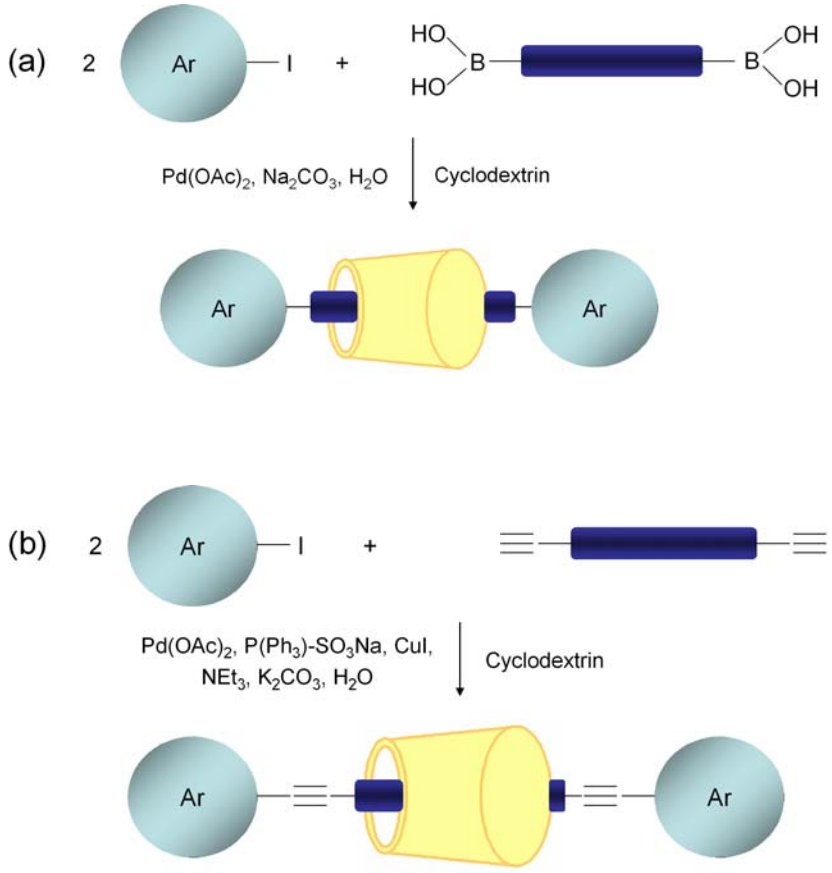

Figure 4.9. Synthetic schemes for fluorescent dye rotaxanes. (a) Suzuki coupling, (b) Heck-Cassar-Sonogashira-Hagihara coupling.

Even though the rotaxane formation could readily be characterized by NMR spectroscopy, there still remains a question as to where CD locates over the dye axis. ROESY technique was found to be very effective for this purpose, since it shows long-

range weak interactions between CD macrocycle and the threaded chromophore. By observing NOEs (Non Overhauser Effects) spectra between protons from acetylene dye and CD, the direction and the position of CD rim over the dye axis are possibly determined. Spectrum shows that only one end of the dye is encapsulated by the CD. This result is consistent with one obtained from the crystal structure of RD (Figure 4.2).

Both dyes, FD and RD, show an increase in fluorescence intensity at higher pH. This is due to the formation of carboxylate (COO^-) which has higher aqueous solubility. Obviously, in strong acidic conditions, FD is sparingly soluble in water, and its fluorescence is negligible. Then, its fluorescence intensity shows a sudden jump from pH 6.5 to 7.3. The broad and red-shifted emission at acidic pH is commonly known for molecules having an electron withdrawing group, such as –COOH, attached to an aromatic nucleus.[28] This red-shifted emission is attributed to an intramolecular charge-transfer (ICT) state, stabilized by hydrogen bonding with the solvent.[28] No such shift between acid (COOH) – base (COO^-) pairs are observed in our case, and spectral shape does not change with pH, either. Thus, deprotonation is considered to occur at ground state.[29,30] RD shows similar behavior, an increase in emission at higher pH, but its increase is gradual. At the same pH, RD's emission intensity is found to be stronger, especially in acidic condition. CDs' pK_a and solubility are previously reported, and α-CD, which is being used as a macrocycle for dye rotaxane, is highly water soluble even at low pH (Table 4.4).[31] It is previously reported that CD complexation shifts the acid-base equilibrium in favor of the free-base form.[32] Therefore, stronger emission of RD comes from its higher solubility mainly aided by CD.

Table 4.4. pKa and water solubility of CDs.

Property	α-CD	β-CD	γ-CD
pK_a	12.33	12.20	12.08
Water solubility (g/100mL, 25°C)	14.5	1.85	23.0

We intended to explore the fluorescence quenching behavior of both FD and RD in the presence of various quenchers, such as metal ions (M^{2+}) and methyl viologen (paraquat, PQ^{2+}). The existence of these electron-acceptors quenches the fluorescence of organic chromophore, since they accept an electron from the excited state of π-conjugate systems. This photoluminescence quenching is of recent interest, since it offers promising end-use as highly sensitive chemical and biological sensors.[11,33,34] The carboxylate terminal groups are one of important functional groups to this sensing concept. Proton dissociation $(R-COOH \longleftrightarrow R-COO^- + H^+)$ makes the negatively charged fluorescent dye water-soluble. As a result, the cationic electron acceptor, such as metal ions (M^{2+}), and the anionic dye form a weak complex via electrostatic interaction. This complex formation leads to large fluorescence quenching, as observed in a large Stern-Volmer constant, K_{SV}, up to 10^6. It is generally accepted that monomeric single fluorophore is less sensitive, showing a low value of K_{SV}, compared to a conjugate polymeric form.[11~14] It is because conjugate polymer system is able to amplify and synchronize its quenching ability.[11~14] However, present FD exhibits exceptionally high sensitivity, showing almost the same K_{SV} values as those of conjugate polymers. It is attributed to the existence of large number of anionic sites, tetra-carboxylic acids. It also has some selectivity, which shows actually no quenching with Mg^{2+} and Zn^{2+}, while showing highest quenching in the case of Cu^{2+}, Pb^{2+} and Hg^{2+}. Heavy metals, such as

copper, lead and mercury, are hazardous due to their long-term toxic effects on natural environment.[12,35] As a consequence, the detection and determination of these heavy metals are of recent interest. This result implies that even monomeric acetylene dye can exhibit such a high degree of sensitivity, revealing the promising use for metal sensing application.

We further explored the fluorescence quenching behavior of RD, in order to examine the effect of cyclodextrin on the photo-induced electron transfer to metal ions. Obviously, once rotaxanated, RD experiences much less fluorescence quenching, consequently, with lower values of K_{SV}. Table 4.2 shows that all quenchers exhibit a higher quenching effect on FD. RD does show some quenching by these metals, since its molecular structure is still the same as that of FD, but its degree of quenching is much smaller. The K_{SV} difference is huge in the case of Cu^{2+} and Pb^{2+}, to which FD is highly sensitive, and especially for Cu^{2+}, it amounts up to the order of 10^2.

There are two possible processes for fluorescence quenching, namely static and dynamic quenching.[19] In static quenching, less soluble aggregates are formed between fluorescent dye and quenchers in the ground state, and this leads to decreased fluorescence intensity upon irradiation. It is sometimes called as Chelation Enhanced Fluorescent Quenching effect (CHEQ).[19] In dynamic quenching, electron-acceptors approach and quench the excited state of the fluorophore by diffusion. A linear Stern-Volmer plot, as observed in cases of FD and RD, occurs when either one of these processes is predominant.[12] From its high sensitivity, FD is thought to form aggregates with metal ions even under very dilute conditions. As seen Figure 4.6, FD has higher intensity of the 0-1 band in fluorescence spectra, while RD has higher intensity of 0-0

band. It implies that, according to Franck-Condon principle, RD has smaller geometry change between the excited state and the ground state, compared with FD.[36] With the addition of quenchers, the spectral shapes of both dyes remain unchanged, even though overall fluorescence intensity is decreased. This indicates that the geometry of the ground and the excited state of dyes are unaffected by the existence of external quenchers. Therefore, in the present case, it is believed that static quenching is the dominant mechanism.

4.5. Conclusion

In summary, a novel acetylene dye rotaxane with α-CD is synthesized using Heck-Cassar-Sonogashira-Hagihara type reaction. Its structure is characterized using ^{1}H, ^{13}C and ROESY NMR techniques. X-ray structure shows that the α-CD is located at one side end, with its narrower 6-rim closer to the end blocker. In fluorescence measurements, rotaxane dye shows a slight red shift in solution, and a blue shift in the solid-state. From its higher quantum yield, the shielding effect of cyclodextrin encapsulation against surrounding environment is assumed. Free dye is found to be highly sensitive to various metal ions, showing high Stern-Volmer constants, K_{SV}. It is attributed to the existence of tetra-carboxylic acids. However, as CD encapsulation protects and stabilizes the threaded chromophore against outside quencher, rotaxane dye exhibits much less quenching against various quenchers.

REFERENCES

[1] Buston J. E. H.; Young, J. R.; Anderson, H. L. "Rotaxane-encapsulated cyanine dyes: enhanced fluorescence efficiency and photostability", *Chem. Comm.* **2000**, (11), 905.

[2] Matsuzawa, Y.; Tamura, S.; Matsuzawa, N.; Ata, M. "Light-stability of a β-cyclodextrin (cyclomaltoheptaose) inclusion complex of a cyanine dye", *J. Chem. Soc., Faraday Trans.* **1990**, *90*, 3517.

[3] Buston J. E. H.; Marken, F.; Anderson, H. L. "Enhanced chemical reversibility of redox processes in cyanine dye rotaxanes", *Chem. Comm.* **2001**, (11), 1046.

[4] Stanier, C. A.; O'Connell, M. J.; Clegg, W.; Anderson, H. L. "Synthesis of fluorescent stilbene and tolan rotaxanes by Suzuki coupling", *Chem. Comm.* **2001**, (8), 493.

[5] Cacialli, F.; Wilson J. S.; Michels, J. J.; Daniel, C.; Silva, C.; Friend, R. H.; Severin, N.; Samori, P.; Rabe, J. P.; O'Connell, M. J.; Taylor, P. N.; Anderson, H. L. "Cyclodextrin-threaded conjugated polyrotaxanes as insulated molecular wires with reduced interstrand interactions", *Nature Materials* **2002**, 1, 160.

[6] Tan, C.; Atas, E.; Muller, J. G.; Pinto, M. R.; Kleiman, V. D.; Schanze, K. S. "Amplified quenching of a conjugated polyelectrolyte by cyanine dyes", *J. Am. Chem. Soc.* **2004**, *126*, 13685.

[7] Swager, T. M.; Gil, C. J.; Wrighton, M. S. "Fluorescence studies of poly(p-phenyleneethylene)s: The effect of anthracene substitution", *J. Phys. Chem.* **1995**, *99*, 4886.

[8] Yamamoto, T. "conjugated polymers bearing electronic and optical functionalities. Preparation by organometallic polycondensations, properties, and their applications", *Bull. Chem. Soc. Jpn.* **1999**, *72*, 621.

[9] Bunz, U. H. F. "Poly(aryleneethynylene)s: synthesis, properties, structure, and applications", *Chem. Rev.* **2000**, *100*, 1603.

[10] Casalnuovo, A. L.; Calabrese, J. C. "Palladium-catalyzed alkylations in aqueous media", *J. Am. Chem. Soc.* **1990**, *112*, 4324.

[11] Li, C.-J., Slaven IV, W. T.; John, V. T.; Banerjee, S. "Palladium catalysed polymerization of aryl diodides with acetylene gas in aqueous medium: a novel synthesis of areneethylene polymers and oligomers", *Chem. Comm.* **1997**, (12), 1569.

[12] Zhou, Q.; Swager, T. M. “Fluorescent chemosensors based on energy migration in conjugated polymers: the molecular wire approach to increased sensitivity”, *J. Am. Chem. Soc.* **1995**, *117*, 12593.

[13] Kim, I. B.; Erdogan, B.; Wilson, J. N.; Bunz, U. H. F. “Sugar-poly(*para*-phenylene ethynylene) conjugate as sensory materials: efficient quenching by Hg^{2+} and Pb^{2+} ions”, *Chem. Eur. J.* **2004**, *10*, 6247.

[14] Haskins-Glusac, K.; Pinto, M. R.; Tan, C.; Schanze, K. S. “Luminescence quenching of a phosphorescent conjugated polyelectrolyte”, *J. Am. Chem. Soc.* **2004**, *126*, 14964.

[15] Fan, Q. L.; Lu, S.; Lai, Y. H.; Hou, X. Y.; Huang, W. “Synthesis, characterization, and fluorescence quenching of novel phenyl-substituted poly(*p*-phenyleneethynylene)s”, *Macromolecules* **2003**, *36*, 6976.

[16] Wilson, J. N.; Bunz, U. H. F. “Switching of intramolecular charge transfer in cruciforms: metal ion sensing”, *J. Am. Chem. Soc.* **2005**, *127*, 4124.

[17] Wang, J.; Wang, D.; Miller, E. K.; Moses, D.; Bazan, G. C.; Heeger, A. J. “Photoluminescence of water-soluble conjugated polymers: origin of enhanced quenching by charge transfer”, *Macromolecules.* **2000**, *33*, 5153.

[18] Turro, N. J. *Modern Molecular Photochemistry*, Benjamin Cummings, Menlo Park, CA, **1978**.

[19] Lakowicz, J. R. *Principles of Fluorescence Spectrscopy*, Plenum Press, New York, **1986**.

[20] Stanier, C. A.; Alderman, S. J.; Claridge, T. D. W.; Anderson, H. L. “Unidirectional photoinduced shuttling in a rotaxane with a symmetric stilbene dumbbell”, *Angew. Chem. Int. Ed.* **2002**, *41*, 1769.

[21] Stanier, C. A.; O’Connell, M. J.; Clegg, W.; Anderson, H. L. “Synthesis of fluorescent stilbene and tolan rotaxanes by Suzuki coupling”, *Chem. Comm.* **2001**, (8), 493.

[22] Taylor, P. N.; O’Connell, M. J.; McNeill, L. A.; Hall, M. J.; Aplin, R. T.; Anderson, H. L. “Insulated molecular wire: Synthesis of conjugated polyrotaxanes by Suzuki coupling in water”, *Angew. Chem. Int. Ed.* **2000**, *39*, 3456.

[23] Anderson, S.; Aplin, R. T.; Claridge, T. D. W.; Goodson III, T.; Maciel, A. C.; Rumbles, G.; Ryan, J. F.; Anderson, H. L. “An approach to insulated moleculare wires: synthesis of water-soluble conjugated rotaxanes”, *J. Chem. Soc. Perkin Trans. I* **1998**, 2384.

[24] Terao, J.; Tang, A.; Michels, J. J.; Krivokapic, A.; Anderson, H. L. "Synthesis of poly(para-phenylenevinylene) rotaxanes by aqueous Suzuki coupling", *Chem. Comm.* **2004**, 56.

[25] Kunitake, M.; Kotoo, K.; Manabe, O.; Muramatsu, T.; Nakashima, N. "Synthesis and spectral characterization of a rotaxane of beta-cyclodextrin threaded by a 4,4'-diaminostilbene", *Chem. Lett.*.**1993**, (6), 1003.

[26] Easton, C. J.; Lincoln, S. F.; Meyer, A. G.; Onagi, H. "Synthesis and conformational analysis of an alpha-cyclodextrin [2]-rotaxane", *J. Chem. Soc. Perkin Trans. I* **1999**, 2501.

[27] Umezawa, H.; Okada, S.; Oikawa, H.; Matsuda, H.; Nakanishi, H. "Synthesis and non-linear optical properties of new ionic species: tolan and diphenylbutadiyne with trimethylammonio and dimethylamino groups", *J. Phys. Org. Chem.* **2005**, *18*, 468.

[28] Sainz-Rozas, P. R.; Isasi, J. R.; Sanchez, M.; Tardajos, G.; Gonzalez-Gaitano, G. "Effects of natural cyclodextrins on the photophysical properties of dibenzofuran-2-carboxylic acid", *J. Phys. Chem.A* **2004**, *108*, 392.

[29] Grabowski, Z. R.; Rubaszewska, W. "Generalized Forster cycle – Thermodynamic and extrathermodynamic relationships between proton-transfer, electron-transfer and electronic excitation" *J. Chem. Soc. Faraday Trans.*, **1977**, *73*, 11.

[30] Galian, R. E.; Veglia, A. V.; de Rossi, R. H. "Cyclodextrin enhanced fluorimetric method for the determination of tryptamine" *Analyst*, **1998**, *123*, 1587.

[31] Connors, K. A. "The stability of cyclodextrin complexes in solution", *Chem. Rev.* **1997**, *97*, 1325.

[32] Mosinger, J.; Deumie, M.; Lang, K.; Kubat, P.; Wagnerova, D. M. "Supramolecular sensitizer: complexation of meso-tetrakis(4-sulfonatophenyl)porphyrin with 2-hydroxypropyl-cyclodextrins", *J. Photochem. Photobio. A* **2000**, *130*, 13.

[33] Swager, T. M. "The molecular wire approach to sensory signal amplification", *ACC. Chem. Res.* **1998**, *31*, 201.

[34] Zhou, Q.; Swager, T. M. "Methodology for enhancing the sensitivity of fluorescent chemosensors: Energy migration in conjugated polymers", *J. Am. Chem. Soc.* **1995**, *117*, 7017.

[35] Hutchinson, T. C.; Meema, K. M., *Lead, Mercury, Cadmium and Arsenic in the Environment*, John Wiley, New York, **1987**.

[36] Michels, J. J.; O'Connell, M. J.; Taylor, P. N.; Wilson, J. S.; Cacialli, F.; Anderson, H. L. "Synthesis of conjugated polyrotaxanes", *Chem Eur. J.* **2003**, *9*, 6167.

CHAPTER 5

CYCLODEXTRIN-TEMPLATED FLUORESCENT ANISOTROPIC STRUCTURE

5.1. Introduction

γ-Cyclodextrin (γ-CD) consisting of eight glucose units has a large cavity with a diameter of ca. 9 Å. This large cavity size allows the inclusion of more than one molecule and the proximity of the molecules can lead to electronic interaction among them. There have been several reports of fluorescent dye inclusion in CD with a 2:1 stoichiometry.[1-4] It was shown that pyrene (Py) molecules enter the γ-CD cavity to form a 2:1 Py:γ-CD inclusion complex, resulting in excimer fluorescence emission.[5] In other reports, γ-CD complexation caused excimer formation of appended anthracene[6] and charge-transfer complexes.[7] Different stoichiometric ratio, such as 2:2 Py:γ-CD, of inclusion complexes have also been reported, and depending on stoichiometry, different fluorescent behaviors are observed.[8] 2,5-Diphenyloxazole (PPO) as a guest has been studied quite extensively, since it shows a very long fluorescence lifetime on complexation due to excimer formation.[9,10] PPO was found to self-assemble to form extended molecular aggregates, held together by inclusion in γ-CD.[11] Oxadiazole derivatives showed similar behavior as PPO, forming extended aggregates at high concentration, and the fluorescent emission of these rod-like aggregates was found to be highly polarized.[12]

In this chapter we describe unusual anisotropic behavior observed in the complex of acetylene dye **3** with γ-CD. It is apparent that dye **3** is a linear molecule. When mixed with γ-CD, dye **3** forms an anisotropic liquid, as observed using a polarized light microscope. We have used various fluorescence measurements in order to investigate the

nature of the complex formed in aqueous solution. Emission intensity and steady state fluorescence anisotropy were measured as a function of temperature. Stability constant was calculated using the modified Benesi-Hildebrand equation.[13] NMR titration method was used to study the stoichiometry of the complex. Wide angle X-ray scattering (WAXD) and differential scanning calorimetry (DSC) were used to characterize the complex formed. Fluorescence lifetime of the complex was also measured.

5.2. Experimental

5.2.1 Preparation of acetylene dye. All chemicals were purchased (Aldrich) and used without purification. γ-CD was obtained from Wacko Chemicals, and recrystallized twice from water. Overall synthetic scheme is shown (scheme 5.1).

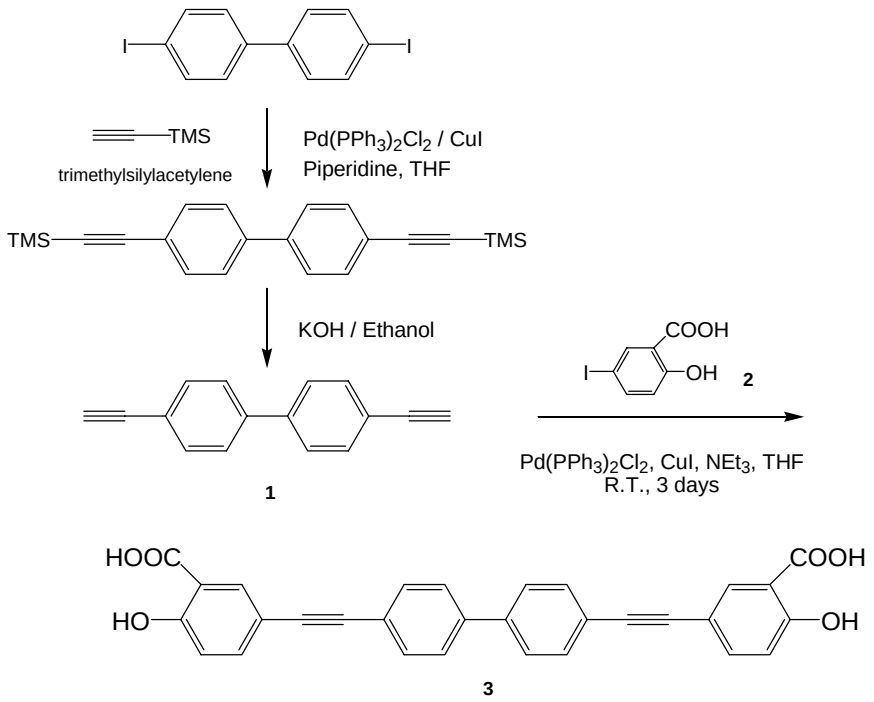

Scheme 5.1. Synthesis of acetylene dye **3**.

4,4'-Diethynylbiphenyl (1): 4,4'-Diiodobiphenyl (10 g, 24.6 mmol) was dissolved in THF (50 mL) with piperidine (5 mL), $(Ph_3P)_2PdCl_2$ (0.35 g, 0.5 mmol), CuI 0.475 g (2.5 mmol), and trimethylsilylacetylene (8.7 mL, 61.6 mmol) was slowly added under nitrogen. The mixture was warmed to 40^{o}C for 30 minutes, and then stirred overnight at room temperature. Excess hexane was added and all salts including Pd catalyst were removed by filtering the mixture through silica gel. The filtrate was collected, and evaporated. The residue was dissolved in methanol (1 L) and purified by recrystallization, to collect the precipitate. To remove the silyl protection groups, the filtrate was dissolved in ethanol (500 mL) in the presence of KOH (10 g), and stirred overnight. Two-thirds of solvent was removed by evaporation, and gradual addition of water gave a pale brownish precipitate. Aqueous layer was extracted with CH_2Cl_2 to give the product **1**. (4.48 g, yield 90%). ^{1}H NMR (300 MHz, $CDCl_3$): δ_H = 7.4 (b, 8H), 3.1 (s, 2H), ^{13}C NMR (75 MHz, $CDCl_3$): δ_C = 136.3, 132.6, 127.0, 121.2, 84.0, 79.0. m/z (ESI MS) 201.1 (M^-).

Acetylene diacid (3): 4,4'-Diethynylbiphenyl **1** (0.77 g, 3.8 mmol) was dissolved with 2-hydroxy-5-iodo-benzoic acid **2** (2.11 g, 8.0 mmol) in THF (10 mL) in the presence of piperidine (2 mL), $(Ph_3P)_2PdCl_2$ (56 mg, 0.08 mmol), CuI (74 mg, 0.39 mmol). The reaction was carried out overnight at room temperature under nitrogen. The mixture was diluted with aqueous Na_2CO_3 solution (2 M, 100 mL), filtered, then acidified to below pH 1 with dilute HCl. The precipitate **3** was collected by filtration, washed profusely with water and dried *in vacuo* overnight at room temperature (1.03 g, yield 57 %). 1H NMR (300 MHz, DMSO-d6): δ_H = 7.8 (d, 2H), 7.7 (d, 4H), 7.5 (d, 4H), 7.4 (q, 2H), 6.6 (d, 2H); 13C NMR (300 MHz, DMSO-d6): δ_C = 172.0, 159.5, 139.0, 136.3, 135.1, 131.6, 127.0, 121.1, 119.0, 116.4, 115.0, 90.6, 89.2. m/z (negative MALDI-TOF) 473.1 (M^-).

5.2.2. Formation of complex. After mixing specific amounts of dye **3** and γ-CD in phosphate buffer solution (pH 8.0, buffer concentration 100 mM), the aqueous solutions were sonicated for 3 hours, and then allowed to stand overnight. To ensure complete mixing, the mixtures of higher concentrations (over 25 mM) were heated directly on a hot-plate at above 90^{o}C, followed by sonication.

5.2.3. Property investigation. The mixture was separated into two distinct parts by centrifugation (5000 rpm, 1 hr); upper isotropic part and lower anisotropic part. Relative volume of lower anisotropic part was measured as a function of the total solid concentration. The steady-state fluorescent spectra were collected using Shimadzu RF-5300PC spectrofluorophotometer. PTI (Photon Technology International) was used for fluorescence intensity measurement as a function of temperature. The same instrument was used for polarization anisotropy measurement, with two polarizers equipped for excitation and emission, respectively.

Rubbed polyimide was used as a substrate for aligning the anisotropic, liquid crystalline phase. One part PI 2556 (HD MicroSystems) was diluted with two parts N-methyl-2-pyrrolidone. The dilute polyimide solution was applied on the cleaned surface, after being washed with acetone, of glass slide, and spin-coated at 2000 rpm for 5 minutes. Coated glass was dried at 100 ^{o}C to remove solvent and baked at 220 ^{o}C in air for 5 hrs. Both polyimide surfaces were rubbed in one direction with clean tissue. Several drops of inclusion complex mixture were applied between two slides, and the resulting texture was observed using polarized optical microscopy. A Leica DMRX microscope was used to make the observation of the texture of the anisotropic phase.

The stoichiometric ratio of the dye and γ-CD inclusion complexes was determined by using the continuous variation technique (Job's plot).[14-16] For this purpose, several different mixtures in D_2O were prepared with different molar ratios of dye/γ-CD, maintaining total concentrations constant at 10.0 mM. Chemical shifts relative to H3 signal in CD at 3.81 ppm were measured using Mercury Vx 300 (Varian, 300MHz). Water in aqueous mixture of acetylene dye and γ-CD was removed by evaporation at room temperature, and then crude powder was vacuum-dried for DSC measurements. The measurements were done at a heating rate of 10 ^{o}C/min from 25 to 250 ^{o}C on a TA Instruments differential scanning calorimeter (DSC Q100). Wide angle X-ray diffraction analysis (WAXD) was conducted on finely ground powder using Rigaku 2D SAXS/WAXS Diffraction System (Rigaku Micromax-007, 45 kV, 66 mA, λ=1.54 Å). The diffraction patterns were analyzed using AreaMax Ver. 1.00 and MDI Jade 6.1. Fluorescence lifetime was measured using Single Photon Decay Spectrometer (PTI), with excitation at 330 nm and emission at 390 nm.

5.3. Results

Anisotropy observation. The formation of anisotropic structure can be observed using polarized optical microscope (POM). In mixtures of low concentrations, for example [**3**] = 1.0 mM and [γ-CD] = 2.0 mM, a clear solution is observed. As concentration increases, the solution becomes turbid, and anisotropic structure begins to appear. At this point, huge striation is visible even with bare eyes. When the mixture is heated above 90 ^{o}C, the anisotropic phase disappears, leading to a clear isotropic solution. However, when cooled down to room temperature, the anisotropy reappears (Figure 5.1

left). When sandwiched between glass surfaces with rubbed polyimide, the anisotropic mixture exhibits preferential alignment, as is expected for a liquid crystalline material on aligning surfaces (Figure 5.1 right).[17,18]

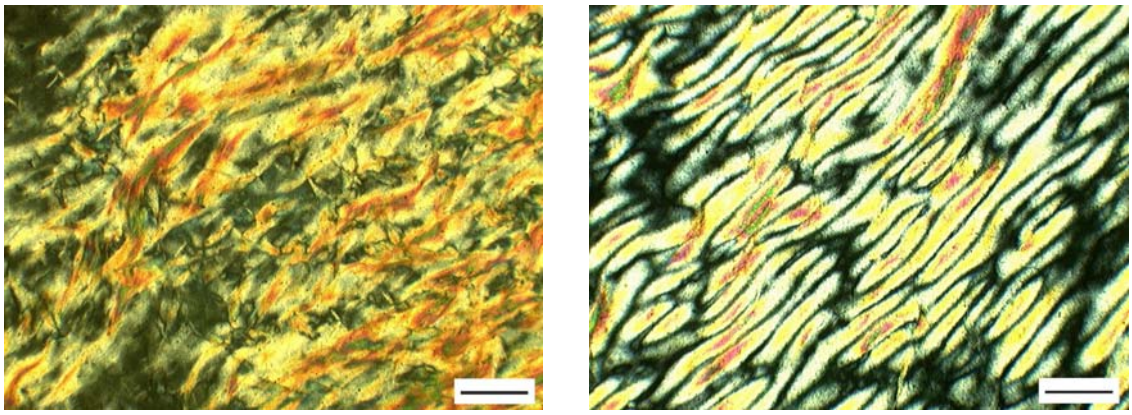

Figure 5.1. Images from polarized optical microscope of inclusion complex between dye **3** and γ-CD; on glass slide without any treatment (left) and between glass slides with rubbed polyimide (right). [Dye] = 75 mM and [γ-CD] = 150 mM in phosphate buffer solution (pH=8.0). Scale bar is 300μm.

The relative volume of the lower anisotropic part was obtained as a function of the total solid concentration by measuring a volume fraction of anisotropic part after centrifuge, and the result is given in Figure 5.2. When the total concentration (dye **3** + γ-CD) is below 0.8 wt % (corresponding to [**3**] = 2.5 mM + [γ-CD] = 5.0 mM), the mixture does not show phase separation. As the total concentration increases above this point, an anisotropic phase precipitates out on centrifugation. This leads to a biphasic region with a upper isotropic phase and a lower anisotropic phase. The volume of the lower phase increases with the total mixture concentration, until at weight 43 % (corresponding to [**3**] = 130 mM + [γ-CD] = 260 mM), the upper isotropic phase disappears completely and the whole mixture shows complete anisotropy.

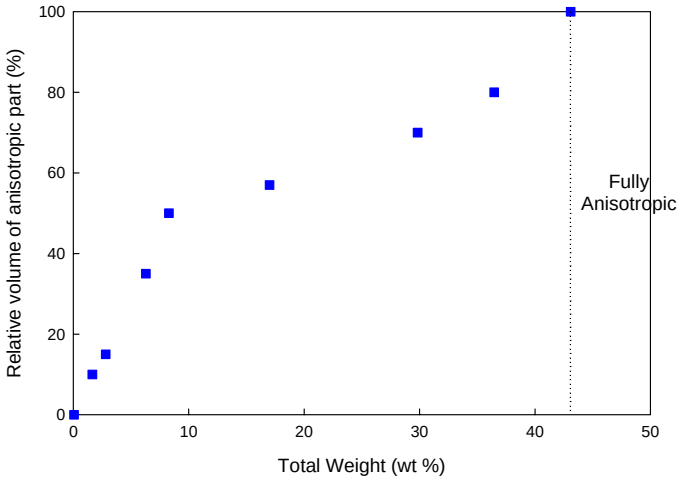

Figure 5.2. Relative volume of the lower anisotropic part as a function of the total solid concentration. A molar ratio between dye **3** and γ-CD (1:2) is maintained.

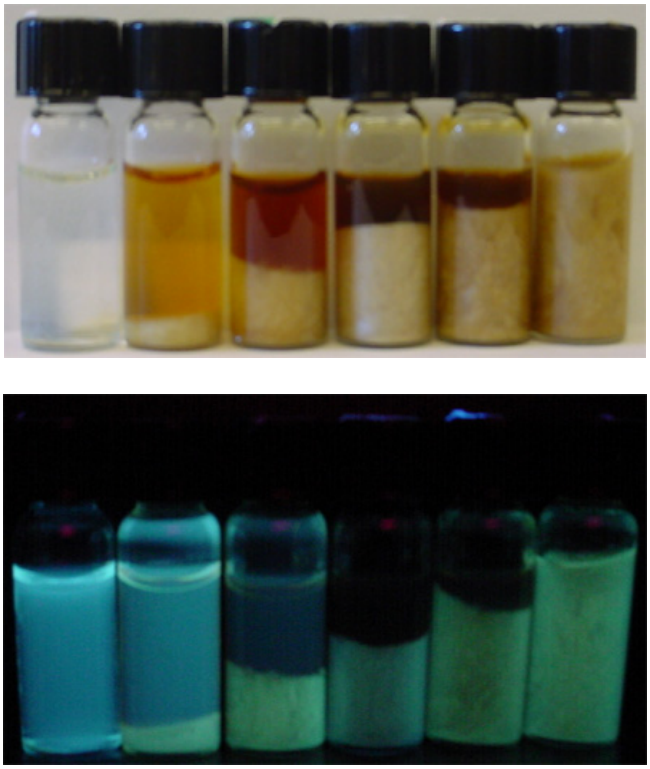

Figure 5.3. Phase separation of acetylene dye **3** with γ-CD after centrifuge (5000 rpm, 1 hr). Under normal light (upper), and under fluorescent light (lower). From left to right, the sample concentrations are 1.6, 2.8, 8.3, 29.8, 36.5, 43.1 wt %, respectively. These correspond to the dye concentrations of 5.0, 8.5, 25.0, 90.0, 110, 130 mM, respectively. A molar ratio between dye and γ-CD (1:2) is maintained for all samples.

Absorption measurement and pH titration. The pH dependence of acetylene dye **3** was examined (Figure 5.4). As pH increases, its absorbance is observed to increase. It is due to an increase in dye solubility, from deprotonation of terminal salicylic acids. When the relative absorbance values at 330 nm are plotted, we notice that deprotonation occurs as a two step process. The apparent pK_a values are evaluated from the pH-titration curve, giving pK_a^1 = 5.0 and pK_a^2 = 8.0. At pH 7.9, dye **3** exists in a couple of forms, including monomer (330 nm) and aggregates (from a shoulder at 390 nm).

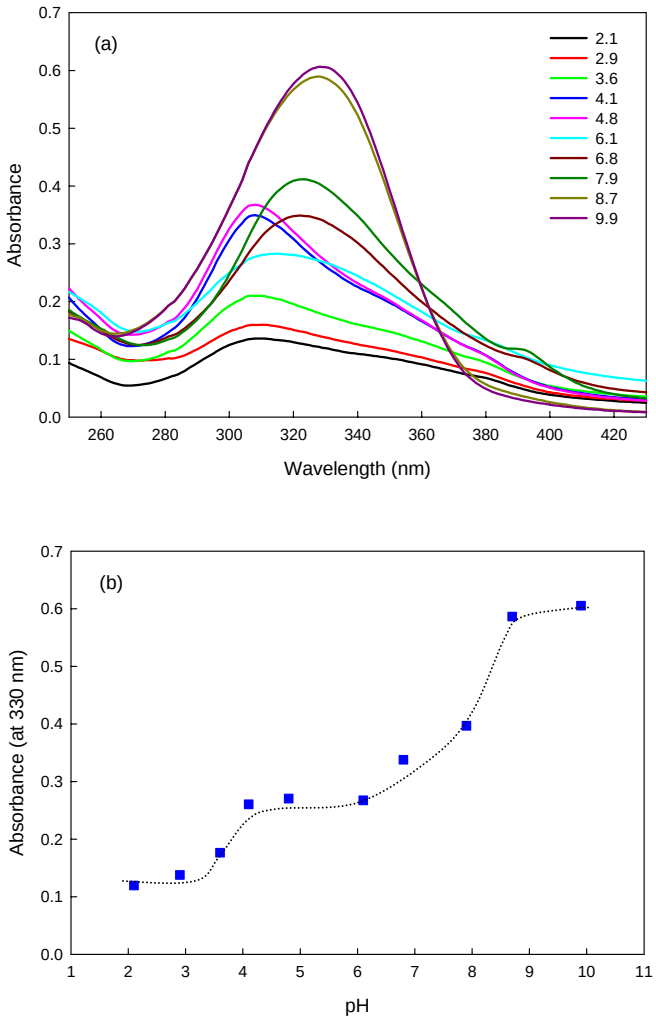

Figure 5.4. (a) Absorption spectra, (b) absorbance values at 330 nm of acetylene dye **3** under different pHs. Legends indicate pHs of the solution. Dye Concentrations are [dye **3**] = 1.0 x 10^{-5} M.

The pH dependence of absorbance of dye-CD complex is found to be rather simple (Figure 5.5). The pH titration shows that absorbance increases sharply from pH 4.8 to pH 6.1, giving approximately apparent $pK_a^{complex}$ = 5.5. Evidently, an absorbance increase occurs only at one step. This result is reminiscent of the fact that binding to CD shifts the acid-base equilibrium in favor of the free-base form.[19] The absorption spectra in Figure 5.5 show that below pH 4.8, the neutral and deprotonated forms of dye **3** exist as a mixture. Above pH 6.1, both forms are converted into the inclusion complex, giving a sharp increase in its absorbance. When dye **3** is included in γ-CD, a complex exhibits single absorption maximum, with λ_{max} at 334 nm.

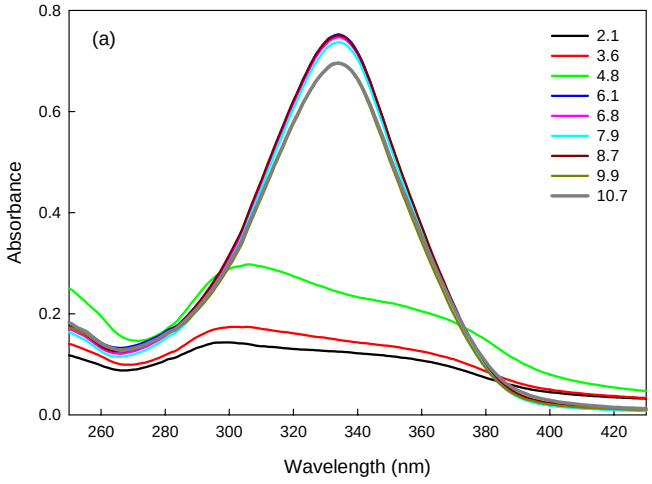

Figure 5.5. (a) Absorption spectra of acetylene dye **3** and γ-CD complex under different pHs. Legends indicate pHs of the solution. Dye Concentrations are [dye **3**] = 1.0 x 10^{-5} M. The molar ratio between dye and γ-CD (1:2) is maintained.

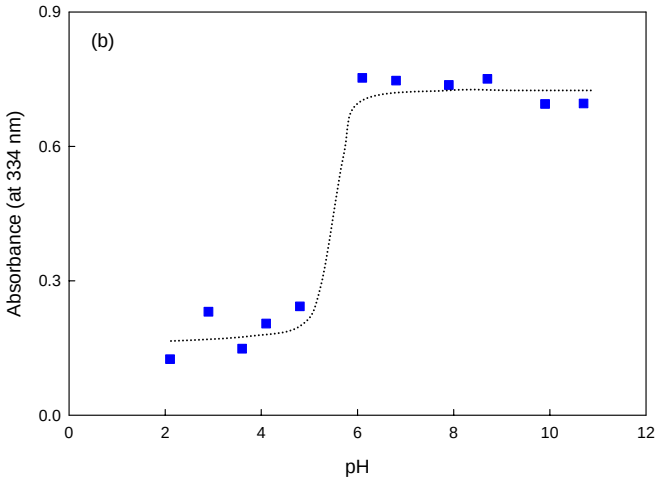

Figure 5.5. (continues) (b) Absorbance values at 334 nm of acetylene dye **3** and γ-CD complex under different pHs.

Fluorescence shift with concentration. Emission spectra of acetylene dye **3** and its inclusion complex with γ-CD were measured as a function of concentration (Figure 5.6). Emission characteristics are found to be dependent on the concentrations of both components. In both cases, the emission spectra shift to longer wavelength as concentration increases, exhibiting a red shift. However, in the presence of γ-CD, the complex shows a large red shift by 30 nm from the concentration of 1.0 to 5.0 mM, while dye **3** shows a red shift only by 5 nm. These shifts are believed to be closely related to aggregational behaviors of dye molecules in the presence of γ-CD. Fluorescence intensity decreases at higher concentrations. We attribute this mainly to scattering losses due to the formation of anisotropic phase in the fluid mixture.

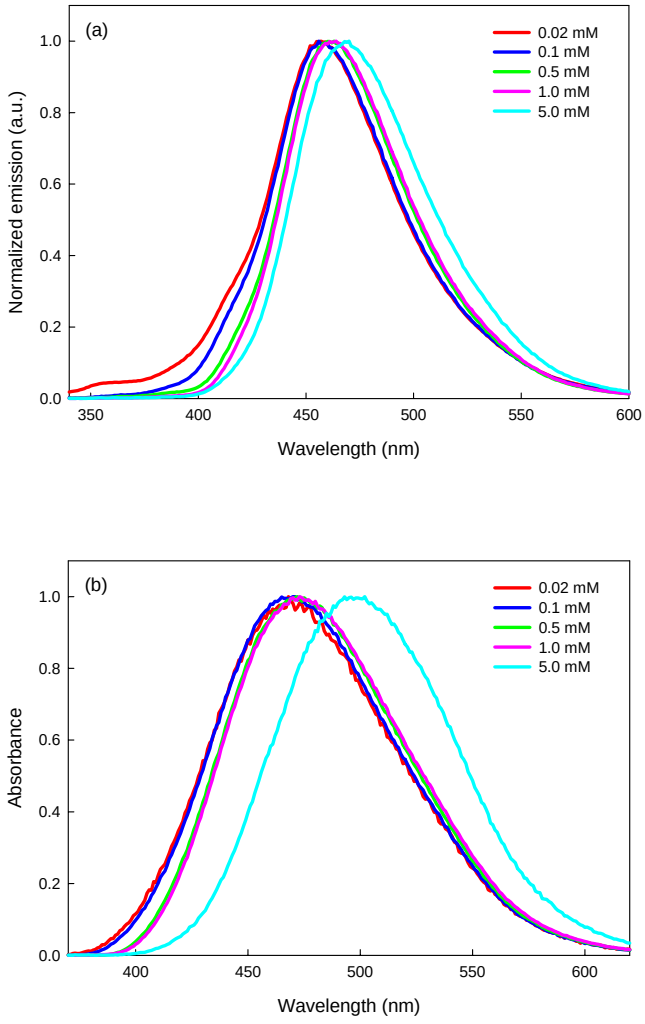

Figure 5.6. Emission spectra of (a) acetylene dye **3** and (b) its complex with γ-CD. The molar ratio between dye and γ-CD (1:2) is maintained for all dye-CD complexes. Legends indicate dye's concentration. The intensities in (a) and (b) are normalized in arbitrary units. Emission was obtained with excitation at 330 nm.

Fluorescence anisotropy. When excited with polarized light, the emission from the sample is also polarized. The emission can be depolarized by a number of reasons, and one common cause is rotational diffusion of fluorophores.[20] The polarization or anisotropy measurement reveals the average angular displacement of the fluorophores, depending on the rate of rotational diffusion during the lifetime of the excited state.[20]

Emission polarization is normally determined by anisotropy r:[20,21]

$$r = \frac{I_{VV} - GI_{VH}}{I_{VV} + 2GI_{VH}} \qquad (5.1)$$

where I_{VV} and I_{VH} are the emission intensities when the emission polarizer has a vertical and horizontal orientation, respectively, when the excitation polarizer is oriented vertically. Similarly, polarization P is defined as:[20,21]

$$P = \frac{I_{VV} - GI_{VH}}{I_{VV} + GI_{VH}} \qquad (5.2)$$

G-factor is an instrumental correction factor, and is defined as:

$$G = \frac{I_{HV}}{I_{HH}} \qquad (5.3)$$

where I_{HV} and I_{HH} are the emission intensities where the emission polarizer has a vertical and horizontal orientation, respectively, when the excitation polarizer is fixed horizontally. Measurements are schematically shown in Figure 5.7.

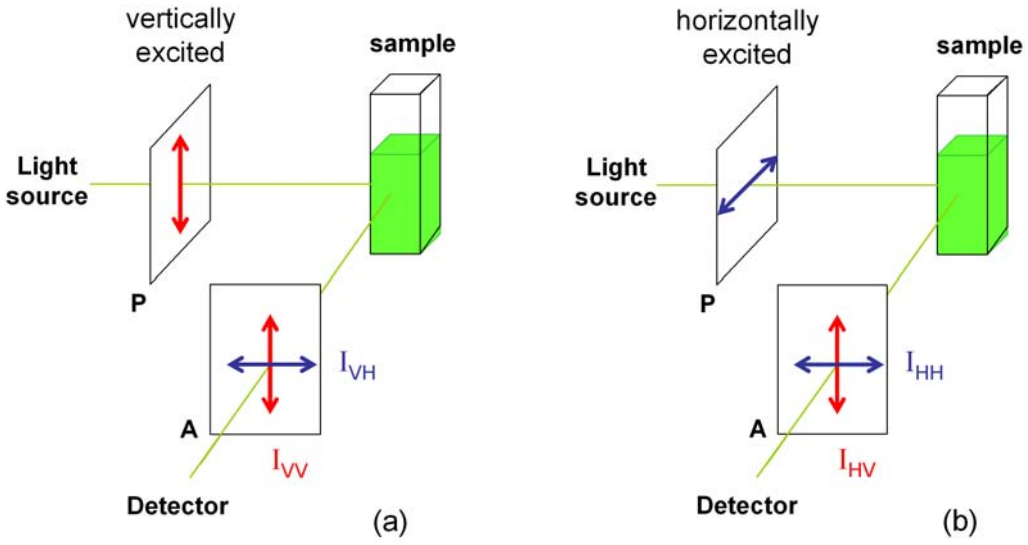

Figure 5.7. Schematic diagram for measurements of fluorescence anisotropy. **P** and **A** indicate polarizer and analyzer, respectively. (a) and (b) shows vertically and horizontally excited cases, respectively (from ref 20).

Following Perrin plot (equation 5.4), for a spherical object, anisotropy is directly related to temperature, medium viscosity, and rotating volume.[20]

$$\frac{1}{r} = \frac{1}{r_0} + \frac{\tau RT}{r_0 \eta V} \qquad (5.4)$$

where r_0 is limiting anisotropy which indicates the anisotropy of the fluorophore in a frozen state, τ is the fluorescence lifetime, η is the viscosity of the medium, R is the ideal gas constant, T is the absolute temperature, and V is the volume of the rotating unit. When rotational diffusion is considered as a source for depolarization, we can obtain the apparent volume V by measuring anisotropy at various temperatures.

In order to understand the rotational diffusion behavior of acetylene dye **3** and γ-CD complex, steady state fluorescence anisotropy was measured. At a very dilute concentration ([dye **3**] = 0.005 mM), the absorption and emission spectra, and their corresponding fluorescence anisotropy values are shown in Figure 5.8. Anisotropy of the dye-γCD complex remains almost constant at low temperature, and then, above 50 ^{o}C, increases by 2-fold, and approaches the value of r exhibited by the free dye. Generally, however, anisotropy r is expected to decrease since it is lost by increased rotational diffusion at higher temperature. We attribute the increase in anisotropy with increasing temperature to unthreading of inclusion complex at higher temperature. Anisotropy values of free and complexed dye become almost identical at 70 ^{o}C. At this temperature, we assume that dye **3** becomes completely unthreaded out of CD cavity. The lifetime of dye **3** is measured to be shorter in a free state (0.33 ns) than in CD cavity (2.71 ns) (Table 5.1).

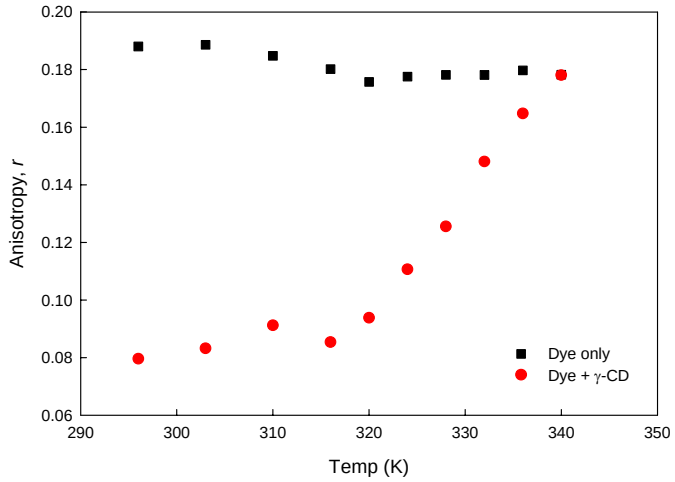

Figure 5.8. Fluorescence anisotropy of dye **3** (black square) and **3**-γ-CD mixture (red circle) as a function of temperature. [**3**] = 0.005 mM and [γ-CD] = 0.01 mM. Excited at 330 nm and emission collected at 460 nm.

Table 5.1. Lifetime of acetylene dye **3** in the absence and presence of γ-CD.

Concentration	Analysis	Lifetime (ns)		χ^2
		τ_1	τ_2	
[**3**] 0.005 mM	Biexp.	0.33	2.49	1.16
[**3**] 0.005 mM + [γ-CD] 0.01 mM	Single exp.	2.71	-	1.07

χ^2 indicates a correlation factor, when curve fitting of fluorescence decay is carried out based on the equation $I(t) = I_o(t) \exp(-t/\tau)$ (for single exponential) and $I(t) = I_{01}(t) \exp(-t/\tau_1) + I_{02}(t) \exp(-t/\tau_2)$ (for biexponential).

At increased concentration ([**3**] = 0.1 mM), dye **3** are considered to form aggregates, by the formation of hydrogen bonding between terminal salicylic acids. Anisotropy of dye **3** without CD is observed to increase with temperature (Figure 5.9). This is attributed to, so-called, hydrophobic effect,[22] resulting from the liberation of water molecules surrounding molecules. However, anisotropy of dye-CD complex is observed to decrease up to 53 ^{o}C. This comes from the fact that liberation of water is retarded

within CD cavity. Thus, anisotropy decreases with temperature due to increased rotational diffusion at higher temperature, as expected in equation (5.4).

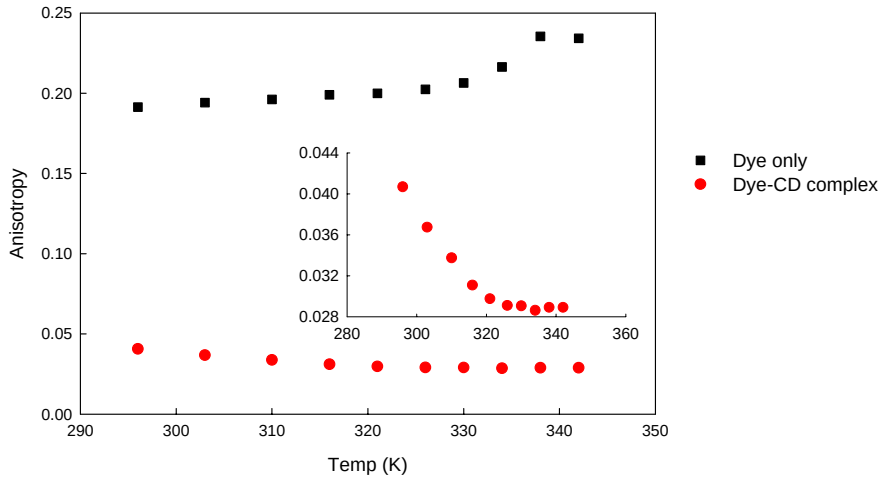

Figure 5.9. Fluorescence anisotropy of dye **3** (black square) and **3**-γ-CD mixture (red circle) as a function of temperature. Inset shows the magnified part of dye-CD complex. Concentrations are [dye **3**] = 0.1 mM and [γ-CD] = 0.2 mM. For dye only, excited at 395 nm and emission collected at 455 nm. For dye-CD complex, excited at 378 nm and emission collected at 465 nm.

Regardless of concentrations, it is observed that I_{HV} is higher than I_{VV} at all temperature. Intensities, both I_{VV} and I_{HV}, are observed to decrease with temperature.

Temperature effect on fluorescence. Temperature dependence of fluorescence emission intensity is shown in Figure 5.10. The fluorescence intensity decreases with increasing temperature, accompanied by a blue shift of 24 nm (from 527 nm at 23 ^{o}C to 503 nm at 70 ^{o}C). This observation is attributed to the fact that the heating gradually increases the thermally activated intramolecular rotations and leads to a fluorescence decrease.[22,23] When this temperature dependence of the fluorescence intensity is fitted using an Arrhenius-type equation, $I = I_0 \exp(\Delta E / \kappa T)$, where I and I_0 are the fluorescence intensities at temperature T and at infinite temperature, respectively, and k is

the Boltzmann constant, it is found that a non-linear plot results with a change of slope around 52 ^{o}C. The activation energies (ΔE) are estimated to be about 2.24 KJ/mol (3.72 x 10^{-21} J, 23.2 meV, below 52 ^{o}C) and 17.0 KJ/mol (2.83 x 10^{-20} J, 177 meV, above 52 ^{o}C), respectively. This suggests that a partial disassembling of the aggregates occurs around 52 ^{o}C. It may cause unthreading of the included dye molecules, leading to a decrease in emission. Breakdown of the aggregates prevents molecular coupling, leading to a slight blue shift in emission. This transition temperature is almost identical to the temperature where we observe a sudden change in anisotropy measurement.

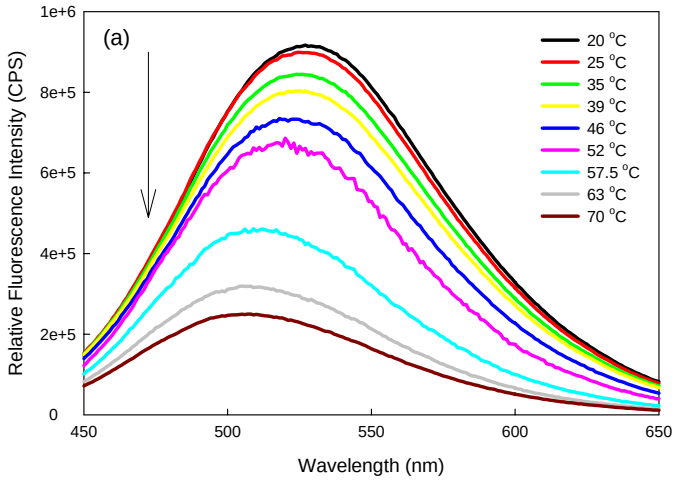

Figure 5.10. Steady state fluorescence spectra for dye **3** and γ-CD complex. (a) Emission spectra at different temperatures. Excited at 370 nm. [**3**] = 10.1 mM and [γ-CD] = 20.2 mM. Arrow indicates increasing temperature (from 20 ^{o}C to 70 ^{o}C).

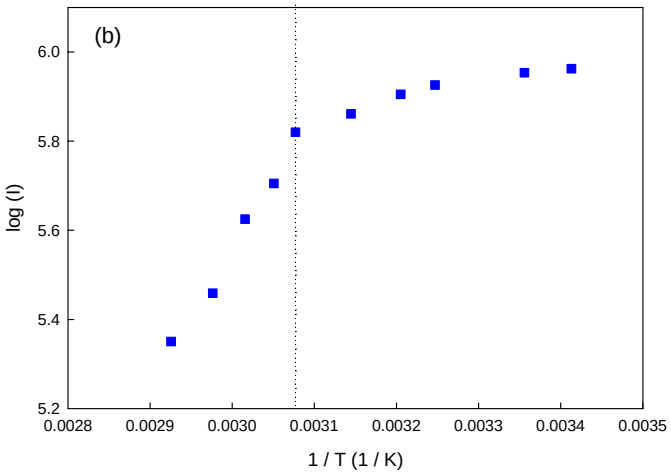

Figure 5.10. (continued) (b) Arrhenius-type plot of intensity with temperature. Intensities were collected at the wavelength of 530 nm. All data were obtained with excitation at 370 nm and emission at 530 nm.

Stability constant. The effect of γ-CD concentration on the inclusion complex was examined (Figure 5.11). Fluorescence enhancement was observed on the addition of γ-CD. At a fixed dye concentration, the larger the amount of γ-CD, the higher the fluorescence intensity. The fluorescence behavior of dye-CD system could be analyzed using Benesi-Hildebrand equations.[13,23,24] For a simple 1:1 complex, the equilibrium can be expressed as (5.5). Then equilibrium constant *K* is expressed as given in (5.6), which implies that a Benesi-Hildebrand plot of 1 / *(F-F$_0$)* versus *[γCD]* should give a straight line, and from the slope and intercept of which we can estimate binding constant K_1.

$$\mathrm{Dye} + \mathrm{CD} \xleftrightarrow{K_1} \mathrm{Dye(CD)} \qquad (5.5)$$

$$\frac{1}{F - F_0} = \frac{1}{K_1(F_1^{'} - F_0)[\gamma CD]} + \frac{1}{F_1^{'} - F_0} \qquad (5.6)$$

where F, F_0, F_1' and $[\gamma CD]$ are observed fluorescence intensity, initial fluorescence intensity of dye without γ-CD, fluorescence intensity of the dye-γ-CD complex, and concentration of γ -CD, respectively.

In the present case, where a 1:2 complex forms, additional stepwise equilibrium needs to be considered:

$$\mathrm{Dye(CD)} + \mathrm{CD} \xleftrightarrow{K_2} \mathrm{Dye(CD)_2} \qquad (5.7)$$

From this equilibrium, we obtain a modified equation.[25]

$$\frac{1}{F - F_0} = \frac{1}{K(F' - F_0)[\gamma CD]^2} + \frac{1}{F' - F_0} \qquad (5.8)$$

where K equals to K_1K_2, and K_2 is the stepwise association constant of $Dye(CD)_2$. Figure 5.8 shows the linear plot of $1 / (F\text{-}F_0)$ vs $[\gamma CD]^2$ following equation (5.8). From the slope and intercept, the stability constant K was calculated as 9.7×10^9 $(M)^{-2}$.

The fluorescence quantum yield of dye **3** was measured as a function of γ-CD concentration. Dye concentrations were adjusted such that the absorbance was around 0.05. A solution of quinine sulfate in 0.1 N H_2SO_4 was used as a reference. Measurement shows that dye **3** itself has a very low quantum yield ($\Phi = 0.013$) and that the presence of γ-CD does not change quantum yields of dye **3** ($\Phi = 0.015 \pm 0.005$).

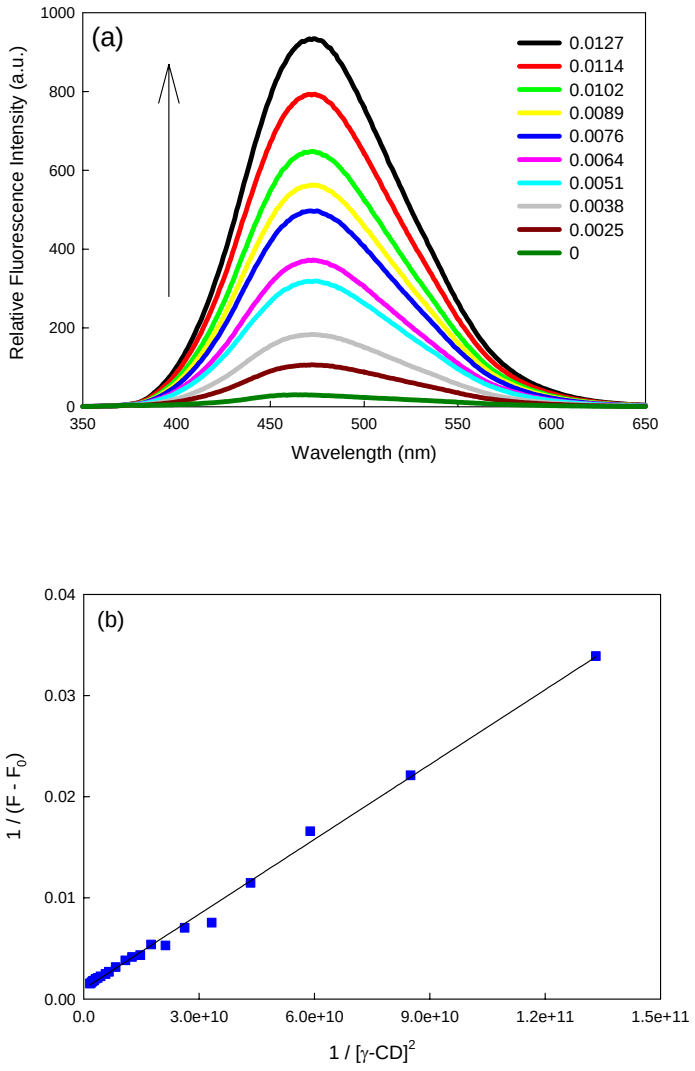

Figure 5.11. (a) Emission spectra of acetylene dye **3** with different amount of γ-CD. The concentration of the dye is fixed at 0.005 mM. Legends indicate the amount of γ-CD added in mM. Arrow indicates increasing amount of γ-CD. (b) modified Benesi-Hildebrand plot of 1 / $(F\text{-}F_0)$ vs 1 / $[\gamma CD]^2$ of acetylene dye **3** in the presence of γ-CD.

Job's plot. The method of continuous variations, so-called Job's method, is one of the experimental mixing techniques commonly used in determining stoichiometric ratio of each component involved.[14-16] This is based on the assumption that if a physical property of the solution is a linear function of the concentration for each species, the

deviation of this property can be used to estimate unknown concentration. Using continuous variation method, it is shown that complex consists of one dye and two γ-CD molecules (Figure 5.12). This was obtained from the observation that the maximum chemical shift occurred when [γ-CD]/([γ-CD]+[Dye]) = 0.67, which corresponds to 1:2 stoichiometry ([Dye]:[γ-CD]). This result agrees well with what we obtained from modified Benesi-Hildebrand equation.

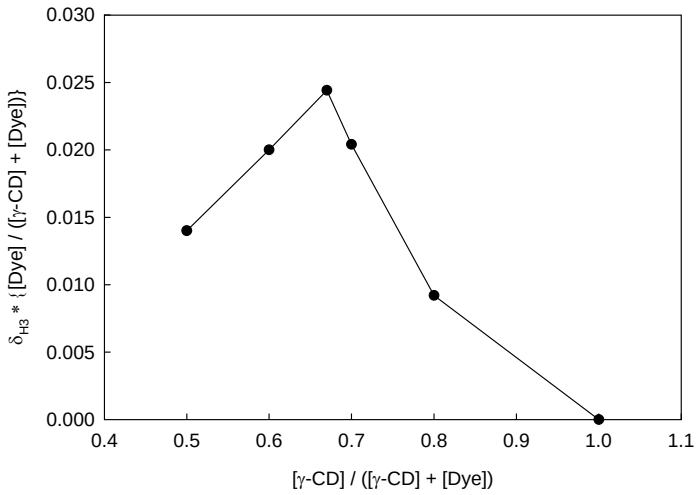

Figure 5.12. Job's plot with chemical shift of H3 proton of γ-CD for acetylene dye/γ-CD complexes in aqueous solution (phosphate buffer pH 8.0, buffer strength 100 mM).

Powder WAXD measurement. X-ray powder diffraction patterns are shown (Figure 5.13). The inclusion complex of dye **3** and γ-CD exhibits a different crystalline structure from those of two starting materials. Also, the diffraction patterns of the inclusion complex are not simple superposition of those of dye and γ-CD. Obviously, both acetylene dye and γ-CD show very sharp diffraction patterns due to higher crystallinity. In comparison, the mixture is found to be less crystalline, with two broad

peaks observed at 16° and 22° (2θ), which correspond to the d-spacings of 5.5 Å and 4.0 Å.

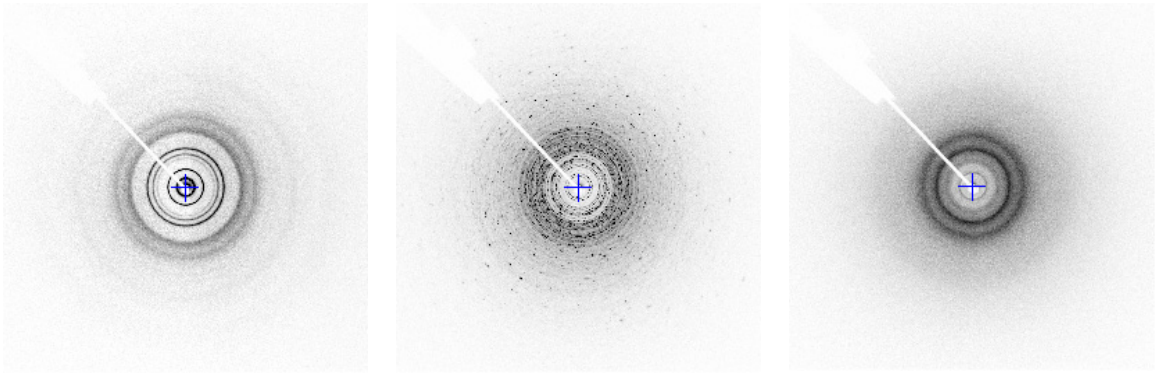

<Dye> <γ-CD> <Dye + γ-CD>

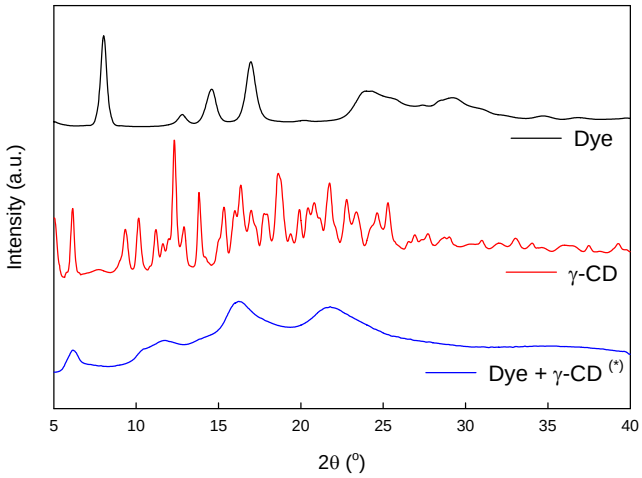

Figure 5.13. X-ray powder diffraction patterns of acetylene dye **3**, γ-CD and their mixtures. The mixture powder was from dye 75 mM and γ-CD 150 mM in phosphate buffer (pH 8.0, 100 mM buffer strength).

DSC measurement. The DSC thermograms of the acetylene dye, γ-CD, and the mixture are presented in Figure 5.14. The dye does not show any sharp thermal transitions in the range of 25 – 250 °C, while γ-CD shows a sharp endothermic peak at 140 °C. The mixture powder shows a broad transition which is not seen in either dye or γ-CD alone. The broad peak corresponds to the release of water from CD cavity on

heating.[26] In addition, the transition peak shifts towards lower temperature compared to that of each component.

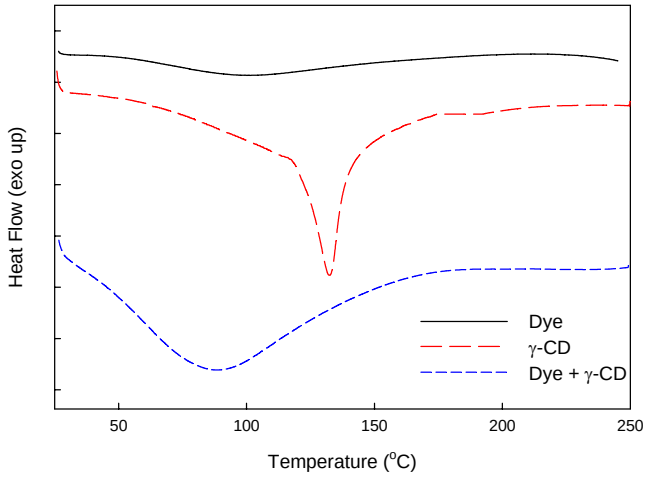

Figure 5.14. DSC diagrams of acetylene dye, γ-CD and their mixtures. These samples are prepared by vacuum-drying at room temperature. Thermograms are obtained on 1st heating. The mixture powder was from dye 75 mM and γ-CD 150 mM.

CD effect on fluorescence lifetime. To further characterize the properties of the inclusion complex of dye **3** and γ-CD, the fluorescence life-time was measured with the addition of different amount of γ-CD. Typical fluorescence decay profiles are shown in Figure 5.15. The fluorescence decay of free acetylene dye is biexponential with lifetime of 1.1 and 48.8 ns in a given condition. Meanwhile, in the presence of γ-CD, dye mixture shows single exponential decay with a longer emission lifetime, with lifetimes around 5.0 to 5.2 ns. The lifetime of these complexes are listed in Table 5.2.

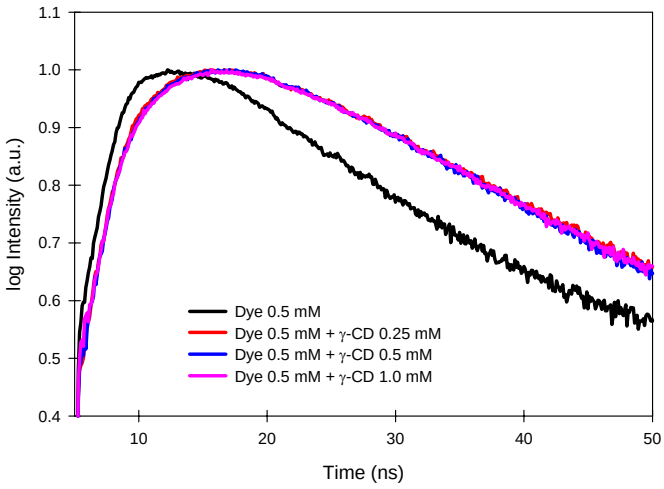

Figure 5.15. Fluorescence decay profiles of acetylene dye **3** in the absence and presence of γ-CD in aqueous conditions, λ_{ex} = 330 nm and λ_{emi} = 390 nm.

Table 5.2. Lifetime of acetylene dye with different amount of γ-CD. [Dye] = 0.50 mM.

[γ-CD]	Analysis	Lifetime (ns)		χ^2
		τ_1	τ_2	
0	Biexp.	1.1	48.8	1.3
0.25 mM	Single exp.	5.2	-	1.5
0.50 mM	Single exp.	5.2	-	1.2
1.0 mM	Single exp.	5.0	-	1.5

χ^2 indicates a correlation factor.

5.4. Discussion

From absorption spectra, we see that when dye **3** is included in γ-CD, the complex mostly exists in a single state. It is known that complexation to CD prevents aggregation of a guest at low concentrations, and this gives a uniform inclusion complex.[27] As concentration increases, dye **3** is thought to align linearly in the presence of CDs. The possible formation of hydrogen bonding between terminal salicylic acids plays a favorable role in the formation of linear aggregates. Upon further increase in

concentrations, dye **3** molecules are considered to be densely stacked, possibly with the aid of CD crystalline packing. These extended aggregates with dense packing are responsible for the appearance of anisotropic structure.

At high concentration, for example [**3**] = 10 mM, free dye **3** makes a precipitate in water, since its aqueous solubility is very low. On the contrary, CD-dye complex forms an anisotropic phase, exhibiting huge striations. From this, we see that self-assembly of extended molecular array forms, held together by inclusion complexes. Previously, several reports show the formation of extended molecular aggregates between fluorescent guests and γ-CD,[9-12] and they are characterized by highly polarized emission.[12] In this case, however, acetylene dye **3**-γ-CD complex is found to exhibit a low anisotropy value in its emission, even lower than that of free dye, and this will be discussed in detail later.

The increase in concentrations of both dye **3** and γ-CD causes a red shift in emission spectra of complexes. A red shift is caused either by the restriction of vibrational motions from the inclusion of dye molecules in a CD cavity or by the formation of aggregates which enables intermolecular energy migrations.[12] Regardless of the reason, a continuous red shift in emission occurs in the presence of γ-CD. As observed, these extended aggregates are expected to show low fluorescence compared to that of the single guest complex. As reported earlier, it is due to the fact that the planarizable nature of the conjugated materials promotes face-to-face stacking, resulting in strong intermolecular interactions that usually lead to low luminescent efficiencies.[28,29]

At first sight, it looks surprising that the fluorescence anisotropy is much smaller in the presence of CD. Since rotational motions of **3** should be hindered in the CD cavity, CD-dye complex is expected to exhibit higher anisotropy. It is attributed to the fact that

the lifetime of dye **3** is shorter in a free state than in CD complex (Table 5.1). A short lifetime leads to an increase in anisotropy (according to equation 5.4). Energy migration in CD complex is also responsible for lower anisotropy, and it will be discussed later.

When any molecule is put in water, water molecules are known to form a rigid hydration shell, forming arrays of six and seven water molecules around atoms.[22,30,31] It forms solvent-accessible surface (SAS), the effective surface of the molecule that is hydrated. At higher temperature, these waters in hydrogen-bonded networks begin to be liberated. It enables to overcome the inherently low entropy of bound water molecules. As a result, a molecule seemingly exhibits a higher anisotropy without a bulky hydrated surface. This hydrophobic effect is often observed in biological macromolecules.[22] Networks of hydrogen-bonded waters have been found to sit in the minor grooves of DNAs.[22] At higher temperature, when the molecules are liberated, the anisotropy of DNAs is observed to increase.[22] When an inclusion complex forms, several water molecules are often included within the CD cavity, together with guest molecules. It is known that the translational mobility of the trapped water molecules is restricted and that water liberation from the cavity is severely hindered.[32] Therefore, we observe an anisotropy decrease with temperature on CD complexation (as shown in Figure 5.9).

It is interesting to notice the effect of concentration on anisotropy (Figure 5.16). With the formation of aggregate, dye **3** showed a slight increase in anisotropy. Similarly, the J-aggregate of porphyrin complex was previously reported to show high fluorescence anisotropy.[33] On the contrary, CD complex shows a decrease in anisotropy with concentration. We can think of rapid depolarization of fluorescence by energy transfer in these aggregates as a likely explanation.[20,33] Radiationless energy transfer occurs only in

concentrated solution, where the average distance between the fluorophore molecules are close.[20] This energy transfer results in angular displacement of the emission oscillator and hence lower anisotropies.[20] Therefore, in a concentrated viscous solution, anisotropy is observed to decrease. Another cause of depolarization can be light scattering. As mentioned earlier, CD mixture at higher concentrations shows an anisotropic structure. The turbid structure results in scattering of both the incident light and of the emitted photons. The scattered incident light causes re-excitation, and the emitted photons can be scattered off before detection, leading to a decrease in anisotropy.[20] However, in the present case, an anisotropy decrease is observed in dye-CD complexes, and thus energy migration is considered as a main cause for depolarization.

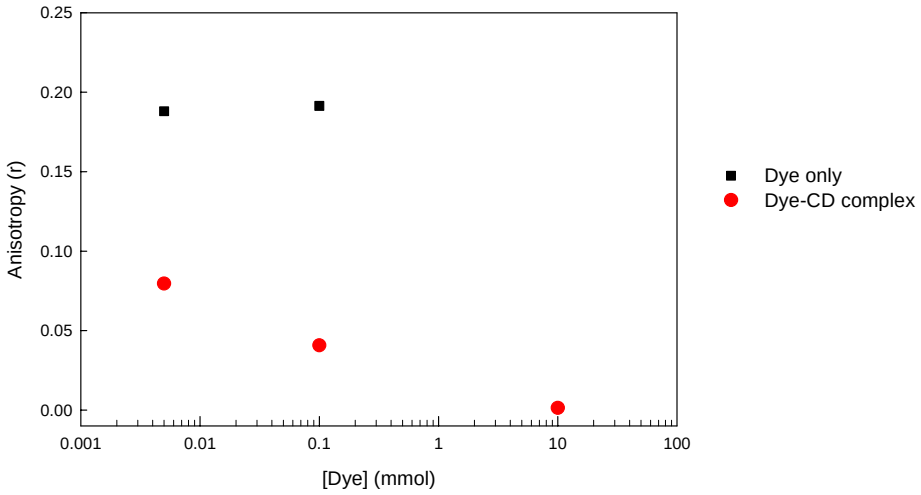

Figure 5.16. Anisotropy change as a function of concentration. All measurements are done at 23 ^{o}C. In dye-CD complexes, a molar ratio between dye **3** and γ-CD (1:2) is maintained. Dye **3** is found to be almost non-fluorescent at the concentration of 10 mM, and no anisotropy value could be obtained.

Fluorescence enhancement with the addition of γ-CD is attributed to the formation of inclusion complex (Figure 5.11). CD complexation increases dye solubility, leading to

higher absorption. At given conditions, no peak shift in emission is observed. It is also observed that the presence of γ-CD does not change quantum yields of dye **3** (Φ = 0.015 ± 0.005). From a relationship $I_{emi} = k\Phi P_0 A$, where I_{emi} is emission intensity, k is a geometric instrumental factor, Φ is the quantum yield, P_0 is the radiant power of the excitation source, and A is absorbance, respectively,[34] therefore, an increased absorbance causes an enhancement in emission.

The γ-CD dependence of the acetylene dye fluorescence enables the calculation of binding constant. The linearity in the plot reflects the formation of 1:2 complex between dye and γ-CD, and from the slope and intercept, the binding constant *K* is found to be 9.7 x 10^9 $(M)^{-2}$. The high magnitude of *K* indicates that the binding of the complex is very strong, and the hydrophobic interactions between the host and guest are maximized when the cavity if filled with dye molecules.[24] Figure 5.17 shows Benesi-Hildebrand plot for dye **3** complexed to γ-CD, according to equation (5.6). The plot of 1 / *(F-F_0)* vs *[γCD]* is better described by two linear segments. The initial linear plot at higher γ-CD concentrations may contain K_2 for the 1:2 (Dye:CD) complex, while the latter linear portion at low γ-CD concentrations may contain K_1 for the 1:1 (Dye:CD) complex. In this case, two individual equilibrium constants can be evaluated from the slopes and the intercepts for the two segments. At lower concentrations where the 1:1 (Dye:CD) complex is dominantly formed, binding constant K_1 value is calculated as 2.1 x 10^3 M^{-1} using equation (5.6). From the relationship $K = K_1 K_2$, using *K* and K_1 values binding constant, K_2 can also be obtained as 4.6 x 10^6 M^{-1}. The result strongly implies the dominant formation of 1:2 inclusion complex between dye **3** and γ-CD at high γ-CD

concentrations. This agrees well with the stoichiometric estimation obtained by NMR titration method.

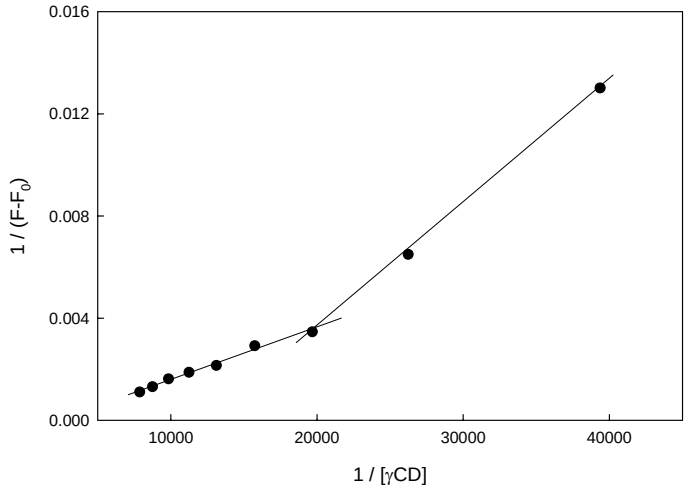

Figure 5.17. A plot of 1 / *(F-F$_0$)* vs 1 / *[γCD]* following equation (5.6).

^{1}H NMR shift titration, as a method of continuous variations, is being frequently used in determining stoichiometric ratio of CD inclusion complexes. When aromatic dye moieties are included in CD cavity, both H3 and H5 protons of glucose units, which are located inside CD cavity, exhibit upfield shifts. It is known to come from the ring current shielding the effect of the aromatic portions of the included dyes.[16,35] The shift, $\Delta\delta_{H3}$, showed its maximum value when two γ-CD molecules had one dye molecule, from which we concluded the stoichiometry of the inclusion complexes to be 1:2 ([Dye]:[γ-CD]). The diameter of γ-CD cavity is around 9.0 Å which is almost twice as large as that of α-CD (4.5 Å). But the height of γ-CD is identical to those of α-CD and β-CD (8 Å), which corresponds to half the length of acetylene dye. Therefore, this result, two CD molecules per one dye molecule, seems quite reasonable.

CD molecules pack within the crystal lattice in the solid state.[36,37] It has been reported that CD inclusion complexes can adopt three different structures, including channel-type and cage-type structure (Figure 5.18).[37] In the cage-type structure, CD molecules are arranged in a herringbone type, and both ends are generally blocked by neighboring CDs. It is well-known that γ-CD exists in a hydrated form, γ-CD.7H_2O, and that its diffraction pattern is typically that of a cage herringbone structure.[38] In the channel-type structure, CD units are formed with head-to-head or head-to-tail orientations. The crystalline structure obtained from dye-CD complex is very similar to those of the inclusion complexes between γ-CD and polyisobutylene,[39] poly(ε-carprolactone),[40] poly(1,3-dioxolane)[41] and other polymers,[42,43] which have been reported to have a channel type structure. Moreover, the peak at $2\theta \sim 22^{o}$ in WAXD is well-known as a characteristic peak for the channel structure of CDs, including long guest molecules, polymers in particular.[44] Therefore, we believe that the inclusion complex of acetylene dye with γ-CD is based on a channel type structure rather than a cage-type structure. It was previously believed that this kind of structure can generally be formed when a long polymer is included as a guest compounds.[39-44] This result is noteworthy in that unlike previous reports which came from polymer-γ-CD inclusion complexes, present complex formation is based on the extended linear aggregates of small molecular acetylene dye with γ-CD.

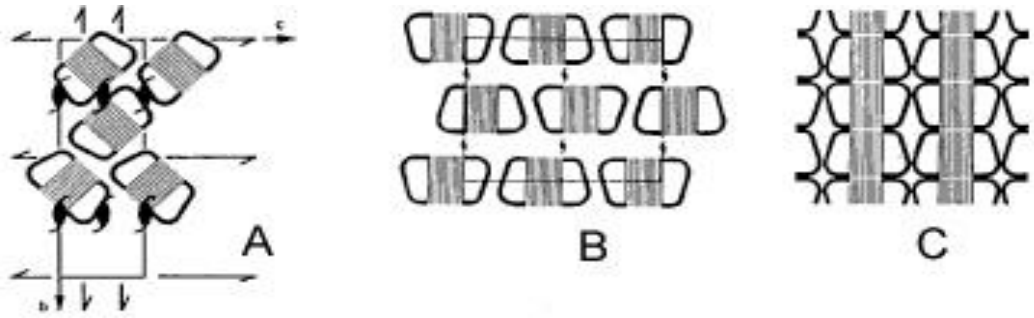

Figure 5.18. Cage herringbone (A), cage brick (B), and channel (C) type crystal formed by CD inclusion complexes (from ref 37).

Since CD does not have any thermal transitions in the range of 25 – 300 ^{o}C, but decomposes around 320 ^{o}C, the transition at 140 ^{o}C corresponds to dehydration.[26] It is known that γ-CD.7H_2O has its included water statistically distributed among several possible sites.[45] Thus, its dehydration shows one-step liberation of the entire water content. On the other hand, CD inclusion complex shows a very broad peak in its DSC thermogram, centered at 90 ^{o}C and extended from 50 to 150 ^{o}C. It seems that the escape of water molecules is hindered due to the existence of included dye molecules, which leads to a broad endothermic peak. It also causes lower transition temperature. It is sometimes related to melting point depression by the complex formation of large aggregates.[46] Similar results were previously reported in the case of antioxidants when mixed with β-CD.[47]

Two decay lifetimes indicate that free dye exists in a couple of different forms. The short lifetime (τ_1) can be assigned to the monomeric state of single dye molecule, while the longer one is attributed to the intermolecular interaction of dye molecules as aggregates. With the addition of γ-CD, decay lifetime is observed to increase, and its decay becomes single exponential. This implies the existence of different kind of

environment or excited-state species, which is completely bound to γ-CD. Regardless of γ-CD concentrations, the increase in the lifetime of acetylene dye is observed, and as previously reported, it is attributed to a strong hindrance of rotation of the included fluorescence chormophore, phenyl acetylene moieties, within CD cavity.[24]

5.5 Conclusion

In summary, here we report the formation of anisotropic structure from the inclusion complexes of acetylene dye and γ-CD. From absorption measurements, the pH dependence of absorbance of dye-CD complex is found to be simpler than that of free dye. The inclusion complex gives a sharp increase in its absorbance as pH increases, exhibiting a lower pK_a value. From fluorescence measurements, the structure is found to be dependent on the concentrations of both components. In emission spectra, a continuous red shift occurs with concentrations. It is found that dye-CD complex exhibits lower anisotropy than free dye, due to longer emission lifetime. From anisotropy measurement at various temperatures, we see that dye molecules remain included inside CD cavity by the formation of aggregates, and that the aggregates are strong enough to hold each other up to 53 ^{o}C. Emission intensities are observed to decrease with temperature, and its Arrhenius-type plot shows non-linear relationship with a transition temperature. Around 52 ^{o}C, unthreading of dye molecule is believed to occur, forming a free dye. From the linear plot in the modified Benesi-Hildebrand equation, binding constant, *K*, of the complex is calculated. From the high *K* value, it was confirmed that the binding nature of the complex is very strong, and 1:2 (Dye:CD) complex is dominantly formed. In NMR spectra, the stoichiometric ratio is confirmed to be 1:2

(Dye:CD). From X-ray powder diffraction patterns, these extended aggregates of inclusion complexes are found to be based on the channel-type structure of γ-CD. The increase in fluorescence lifetime is observed with the formation of Dye-CD complex.

REFERENCES

[1] Edwards, H. E.; Thomas, J. K. "A flurorescence-probe study of the interaction of cycloheptaamylose with arenes an amphiphilic molecules", *Carbohydr. Res.* **1978**, *65*, 173.

[2] Yorozu, T.; Hoshino, M.; Imamura, M. "Fluorescence studies of pyrene inclusion complexes wih α-, β- and γ-cyclodextrins in aqueous solutions. Evidence of formation of pyrene dimer in γ-cyclodextrin cavity", *J. Phys. Chem.* **1982**, *86*, 4426.

[3] Arad-Yellln, R.; Eaton, D. F. "Excited-state reactivity changes induced by complexation with cyclodextrins: Inclusion of 2,2-bis(α-naphthylmethyl)-1,3-dithiane into β- and γ-cyclodextrins", *J. Phys. Chem.* **1983**, *87*, 5051.

[4] Herkstroeter, W. G.; Martic, P. A.; Evans, T. R.; Farid, S. "Cyclodextrin inclusion complexes of 1-pyrenebutyrate: The role of coinclusion of amphiphiles", *J. Am. Chem. Soc.* **1986**, *108*, 3275.

[5] Kano, K.; Takenoshita, I.; Ogawa, T. "γ-Cyclodextrin-enhanced excimer fluorescence of pyrene an effect of n-butyl alcohol", *Chem. Lett.* **1982**, 321.

[6] Ueno, A.; Moriwaki, F.; Osa, T.; Hamada, F.; Murai, K. "Association, photodimerization, and induced-fit types of host-guest complexation of anthracene-appended γ-cyclodextrin derivatives", *J. Am. Chem. Soc.* **1988**, *110*, 4323.

[7] Kano, K.; Takenoshita, I.; Ogawa, I. "Fluorescence quenching of pyrene and naphthalene in aqueous cyclodextrin solutions-evidence of 3-component complex formation", *J. Phys. Chem.* **1982**, *86*, 1833.

[8] Kobayashi, N.; Saito, R.; Hino, H.; Hino, Y.; Ueno, A.; Osa, T. "Fluorescence and induced circular-dichroism studies on host-guest complexaton between γ-cyclodextrin and pyrene", *J. Chem. Soc. Perkin Trans. 2* **1983**, 1031.

[9] Berlman, I. B. "Transient dimer formation by 2,5-diphenyloxazole", *J. Chem. Phys.* **1961**, *34*, 1083.

[10] Ware, W. R.; Watt, D. J.; Holmes, J. D. "Exciplex photophysics. I. The α-cyanonaphthalene-olefin system", *J. Am. Chem. Soc.* **1974**, *96*, 7853.

[11] Agbaria, R. A.; Gill, D. "Extended 2,5-diphenyloxazole-γ-cyclodextrin aggregates emitting 2,5-diphenyloxazole excimer fluorescence", *J. Phys. Chem.* **1988**, *92*, 1052.

[12] Agbaria, R. A.; Gill, D. "Non-covalent polymers of oxadiazole derivatives induced by γ-cyclodextrin in aqueous solutions-fluorescence study", *J. Photochem. Photobio. A: Chem.* **1994**, *78*, 161.

[13] Hirai, H.; Toshima, N.; Uenoyama, S. "Inclusion complex formation of γ-cyclodextrin. On host-two guest complexation with water-soluble dyes in ground state", *Bull. Chem. Soc. Jpn.* **1985**, *58*, 1156.

[14] Schneider, H.; Hacket, F.; Rudiger, V. "NMR studies of cyclodextrins and cyclodextrin complexes", *Chem. Rev.* **1998**, *98*, 1755.

[15] Polyakov, N. E.; Leshina, T. V.; Konovalova, T. A.; Hand, E. O.; Kispert, L. D. "Inclusion complexes of carotenoids with cyclodextrins; ^{1}H NMR, EPR, and optical studies", *Free Rad. Bio. Med.* **2004**, *36*, 872.

[16] Rekharsky, M. V.; Goldberg, R. N.; Schwarz, F. P.; Tewari, Y. B.; Ross, P. D.; Yamashoji, Y.; Inoue, Y. "Thermodynamic and nuclear-magnetic-resonance study of the interactions of α-cyclodextrin and β-cyclodextrin with model substances-phenethylamine, ephedrines, and related substances", *J. Am. Chem. Soc.* **1995**, *117*, 8830.

[17] Chandrasekhar, S. *Liquid crystals*, Cambridge university press, Cambridge, 1977.

[18] Gennes, P. de. *The physics of liquid crystals*, Oxford university press, Oxford, 1993.

[19] Mosinger, J.; Deumie, M.; Lang, K.; Kubat, P.; Wagnerova, D. M. "Supramolecular sensitizer: complexation of meso-tetrakis(4-sulfonatophenyl)porphyrin with 2-hydroxypropyl-cyclodextrins", *J. Photochem. Photobio. A.* **2000**, *130*, 13.

[20] Lakowicz, J. R. *Principles of Fluorescence Spectroscopy*, Plenum, New York, 1999.

[21] Weber, G. in Hercules, D. M (ed.) *Fluorescence and phosphorescence Analysis*, Wiley, New York, 1966.

[22] van Holde, K. E.; Johnson, W. C.; Ho, P. S., *Principles of physical biochemistry*, Prentice Hall, New Jersey, 1998.

[23] Selvaraju, C.; Thiagarajan, V.; Ramamurthy, P. "Interaction of 1,8-acridinedione dye with urea dimmer in methanol", *Chem. Phys. Lett.* **2003**, *379*, 437.

[24] Indirapriyadharshini, V. K.; Karunanithi, P.; Ramamurthy, P. "Inclusion of resorcinol-based acridinedione dyes in cyclodextrins: Fluorescence enhancement", *Langmuir* **2001**, *17*, 4056.

[25] Perdomo-Lopez, I.; Rodriguez-Perez, A. I.; Yzquierdo-Peiro, J. M.; White, A.; Estrada, E. G.; Villa, T. G.; Torres-Labandeira, J. J. "Effect of cyclodextrins on the solubility and antimycotic activity of sertaconazole: Experimental and computational studies", *J. Pharm. Sci.* **2002**, *91*, 2408.

[26] Rusa, C. C.; Bullions, T. A.; Fox, J.; Porbeni, F. E.; Wang, X.; Tonelli, A. E. "Inclusion compound formation with a new columnar cyclodextrin host", *Macromolecules* **2002**, *18*, 10016.

[27] Balzani, V.; Scandola, F. *Suprmolecular Chemistry*, Ellis Horwood, New York, 1991.

[28] Wagner, B. D.; Stojanovic, N.; Leclair, G.; Jankowski, C. K. "A spectroscopic and molecular modeling study of the nature of the association complexes of Nile Red with cyclodextrins", *J. Inc. Phen. Mac. Chem.* **2003**, *45*, 275.

[29] Cornil, J; Heeger, A. J.; Bredas, J. L. "Effects of intermolecular interaction on the lowest excited state in luminescent conjugated polymers and oligomers", *Chem. Phys. Lett.* **1997**, *272*, 463.

[30] Wayne, R. P. *Chemistry of atmospheres*, Oxford University Press, Oxford, 1991.

[31] Kassner, J. L.; Hagen, D. E. "Clustering of water hydrated protons in a supersonic free jet expansion-comment", *J. Chem. Phys.* **1976**, *64*, 1860.

[32] Nandi, N.; Bhattacharyya, K.; Bagchi, B. "Dielectric relaxation and salvation dynamics of water in complex chemical and biological systems", *Chem. Rev.* **2000**, *100*, 2013.

[33] Maiti, N. C.; Mazumdar, S., Periasamy, N. "J- and H-aggregates of porphyrin-surfactant complexes: time-resolved fluorescence and other spectroscopic studies", *J.Phys. Chem. B* **1998**, *102*, 1528.

[34] Kasha, M., *Spectroscopy of the excited state*, Plenum Press, New York, 1976.

[35] Yoshida, N. "Dynamic aspectes in host-guest interaction, 4. Kinetic and ^{1}H NMR evidence for multistep directional binding in the molecular recognition of some 2-naphthylazophenol guests with α-cyclodextrin", *J. Chem. Soc. Perkin Trans. 2* **1995**, 2249.

[36] Harata, K. *Crystallographic Studies Vol. 3*, Pergamon, Oxford, **1996**.

[37] Saenger, W.; Steiner, T. "Cyclodextrin inclusion complexes: host-guest interactions and hydrogen-bonding networks", *Act. Cryst.* **1998**, *A54*, 798.

[38] Szejtli, J. *Cyclodextrin and their inclusion compounds*, Academiai Kiado, Budapest, **1982**.

[39] Harada, A; Suzuki, S.; Okada, M.; Kamachi, M. "Preparation and characterization of inclusion complexes of polyisobutylene and cyclodextrins", *Macromolecules* **1996**, *29*, 5611.

[40] Kawaguchi, Y.; Nishiyama, T.; Okada, M.; Kamachi, M.; Harada, A. "Complex formation of poly(ε-carprolactone) with cyclodextrins", *Macromolecules* **2000**, *33*, 4472.

[41] Li, J.; Yan, D. "Inclusion complexes formation between cyclodextrins and poly(1,3-dioxolane)", *Macromolecules* **2001**, *34*, 1542.

[42] Rusa, C. C.; Fox, J.; Tonelli, A.E. "Competitive formation of polymer-cyclodextrin inclusion compounds", *Macromolecules* **2003**, *36*, 2742.

[43] Shuai, X.; Porbeni, F. E.; Wei, M.; Bullions, T.; Tonelli, A. E. "Formation of inclusion complexes of poly(3-hydroxybutyrate)s with cyclodextrins. 1. Immobilization static poly(R,S-3-hydroxybutyrate) and miscibility enhancement between poly(R,S-3-butyrate) and poly(ε-carprolactone)", *Macromolecules* **2002**, *35*, 3126.

[44] Huang, L.; Tonelli, A. E. "Polymer inclusion compounds", *J. Macromol. Sci. Rev. Macromol. Chem. Phys.* **1998**, *38*, 781.

[45] Usha, M. G.; Wittebort, R. J. "Structural and dynamical studies of the hydrate, exchangeable hydrogens, and included molecules in β- and γ-cyclodextrins by powder and single-crystal deuterium magnetic resonance", *J. Am. Chem. Soc.* **1992**, *114*, 1541.

[46] Mielcarek, J. "Studies on inclusion complexes of felodipine with β-cyclodextrin", *J. Inclu. Phenom. Mol.* **1998**, *30*, 243.

[47] Wen, X.; Tan, F.; Jing, Z.; Liu, Z., "Preparation and study the 1:2 inclusion complex of carvedilo with β-cyclodextrin", *J.Pharm. Biomed. Anal.* **2004**, *34*, 517.

CHAPTER 6

ANISOTROPIC SUPRAMOLECULES WITH METHYL ORAGNE AND GAMMA-CYCLODEXTRIN

6.1. Introduction

The aggregation behavior of organic dyes, especially in the presence of host molecules, has drawn great interests. Various experimental methods have been used to study the nature of their aggregations, which include UV/Vis, NMR spectroscopy, conductivity measurement and scattering techniques.[1-4]

Complex formation with cyclodextrins (CDs) usually accompanies some change in UV-Visible absorption spectra. Some azo dyes, mostly those used as indicators, exhibit significant spectral changes, thus make them suitable for determining and understanding their complexing behavior with CDs.[5-19] Several spectrophotometric studies have been done on the formation of inclusion complexes of α-cyclodextrin (α-CD) and β-cyclodextrin (β-CD) with acid and anion forms of azo dyes, such as methyl yellow and *p*-methyl red.[5-7] According to spectrophotometric and conductance measurements, the inclusion complexes of these dyes were found to be based on 1:1 stoichiometry.[6-10] Crystal violet and methylene blue are found to form 2:1 (guest:host) inclusion complexes with γ-cyclodextrin (γ-CD) owing to its larger cavity size,[11,12] and several azo dyes that have a tight fit in the CD cavity exhibit exciton interaction between two molecules of the chromophoric dye included in the complexes.[13] There are studies on the complex formation of methyl orange and orange II with γ-CD.[14-17] Interestingly enough, orange II and γ-CD were reported to form liquid crystalline structure.[18] They were found to form

2:1 complex, leading to the formation of a pine needle-like self-assembly when observed in optical microscope.[19]

In this chapter, we report the complex formation of methyl orange (MO) with γ-CD, which forms similar liquid crystalline phase, as early reported earlier. At high concentration above 0.02 M, the complex is found to exhibit a biphasic anisotropic structure, which can be observed under polarized optical microscope. It seems to be related to the formation of extended linear aggregate with γ-CD, in which MOs are included in CD cavity.[20,21] In order to understand the nature of this association, we use UV-Visible spectrophotometric method. Under different pH conditions, its color change in the presence of γ-CD was measured and compared to that without γ-CD. The change in anisotropy of the inclusion complex was observed using polarized optical microscope.

6.2. Experimental

Methyl Orange was purchased (Sigma-Aldrich), and purified by recrystallization in absolute ethyl alcohol. γ-CD, donated from Wacko Chemicals, was recrystallized twice from water. Buffer solutions were made using corresponding phosphate salts (weak acid~neutral) and ethanolamine (alkaline) in deionized water (with 18 mΩ resistance), and buffer concentration was maintained at 10 mM. The solutions below pH 3.2 were made by adjusting the pH with dilute HCl. UV-Vis absorption spectra were recorded on Lambda 7 (Perkin Elmer) in 1 cm cuvette. Polarized optical microscope DMRX (Leica) was used to observe the anisotropic phase. The stability constant (K_f) for a 2:1 (MO:γ-CD) complex was calculated based on original Benesi-Hildebran method and its modified one.[11,22] Transmission electron microscopy (TEM) image was obtained on JEOL 100 at

100 kV. The sample for TEM measurement was prepared by dipping a carbon-coated copper grid in the sample solution and then air-drying overnight. The conductance of solutions was measured at 25 ^{o}C with an Accumet AR20 conductivity meter using an electrode with a cell constant of 1.0 cm^{-1}.

6.3. Results

The absorption spectra of MO (5 x 10^{-5} M) in the presence of γ-CD with its concentration ranging from 1 x 10^{-4} to 2.5 x 10^{-4} M are shown (Figure 6.1). The buffer was prepared using combination of Na_2HPO_4 and NaH_2PO_4, and its pH was adjusted to 7.5 at 25 ^{o}C. It shows a slight decrease in maximum absorbance with the addition of γ-CD, coupled with a gradual blue shift. No fixed isosbestic point was observed, which indicates that more than one environment of MO exists, such as uncomplexed MO, 1:1 complex and 2:1 complex with γ-CD.

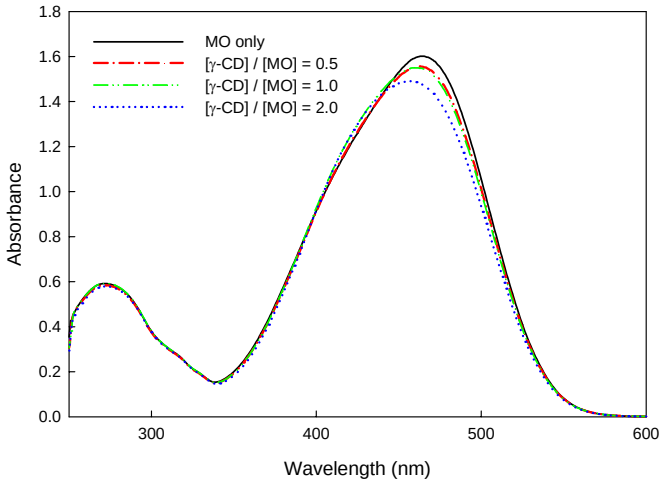

Figure 6.1. Absorption spectra of MO in the presence of γ-CD. Absorbances were measured under pH 7.5. MO concentration is 0.00125M. Legends indicate the concentration ratio of γ-CD / MO.

Absorbance values at 505 nm are measured with various molar ratios between MO and γ-CD under different pH conditions (Figure 6.2). This wavelength, 505 nm, is the characteristic of MO's red color in acidic condition. As seen in Figure 6.2, absorbance value at this wavelength is observed to increase at lower pH. This is due to the dominant formation of azonium tautomer in acidic condition (see Scheme 6.1 below). More importantly, it is also observed that absorbance slightly decreases with increasing [γ-CD] / [MO]. It means that the presence of γ-CD oppresses the formation of azonium tautomer. From this, we see that the formation of azonium tautomer is retarded within CD cavity.[23]

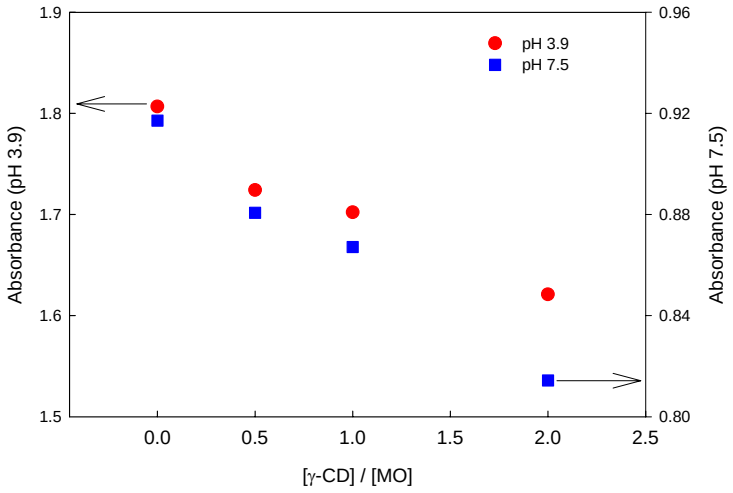

Figure 6.2. Absorption spectra of MO in the presence of γ-CD under pH 3.9 and pH 7.5 Absorbances were measured at 505 nm.

The change in conductivity is measured with different amounts of γ-CD (Figure 6.3). The addition of γ-CD leads to a decrease in solution conductivity, and it is the evidence of complex formation. In neutral condition, a sharp inflection point is observed at [γ-CD] / [MO] = 0.5, while in acidic condition only gradual decrease in conductivity is

observed. It is believed that around this point a different complex begins to form, making the conductance decrease more gradually.

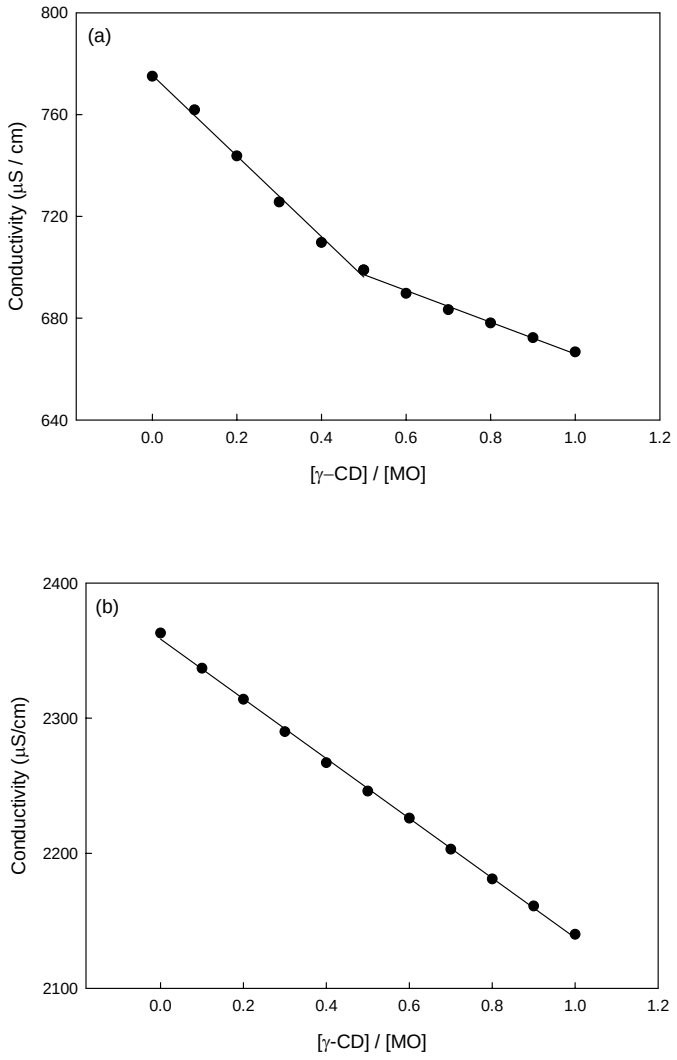

Figure 6.3. Conductivity measurement under different ratio of γ-CD and MO. MO concentration is 0.02M; (a) pH 7.5 (upper), (b) pH 3.9 (lower).

No birefringence is observed when only MO or γ-CD exists. When MO is mixed with γ-CD at high concentrations above 0.02 M, it is observed to form a biphasic anisotropic phase. This anisotropy can be observed under polarized optical microscope (Figure 6.4). However, in acidic condition, anisotropy disappears. Thus, the appearance

and disappearance of anisotropic structure, which strongly depends on the solution pH, could be directly observed. It is assumed that this change is related to tautomeric behavior of MO under different pH conditions.

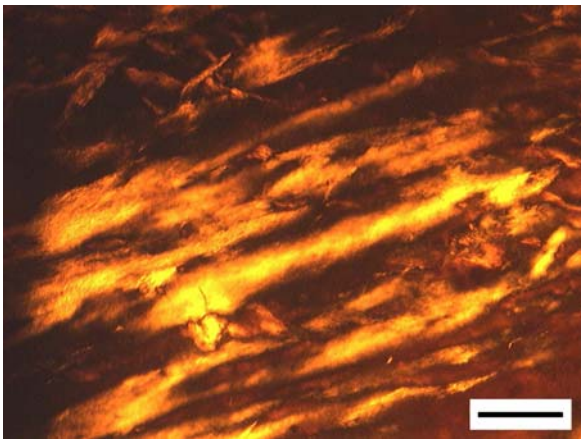

Figure 6.4. Optical microscope images under crossed polarizers. The concentrations of both MO and γ-CD are 0.03 M. The scale bar is 300 μm.

Figure 6.5 shows the TEM image for the inclusion complex of MO and γ-CD. The image reveals a number of stripes with the width of each stripe ranging from 70 to 80 nm. This reminds us of crystal packing mode of γ-CD complex, where γ-CD molecules stack in columns, forming large channel-type structures.[24]

Figure 6.5. TEM image for the inclusion complex of MO and γ-CD. The concentrations of both MO and γ-CD are 0.03 M. The scale bar is 500 nm.

The absorbance ratio at 505 nm versus 460 nm is shown (Figure 6.6). At low pH, MO absorbance at 505nm increases while one at 460nm decreases, and as a result, the ratio between the two becomes larger. Again, this is due to the dominant formation of azonium tautomer at low pH. At the same pH condition, a slight decrease in ratio was observed at higher CD concentrations. This comes from the fact that the formation of azonium tautomer is hindered inside CD cavity.

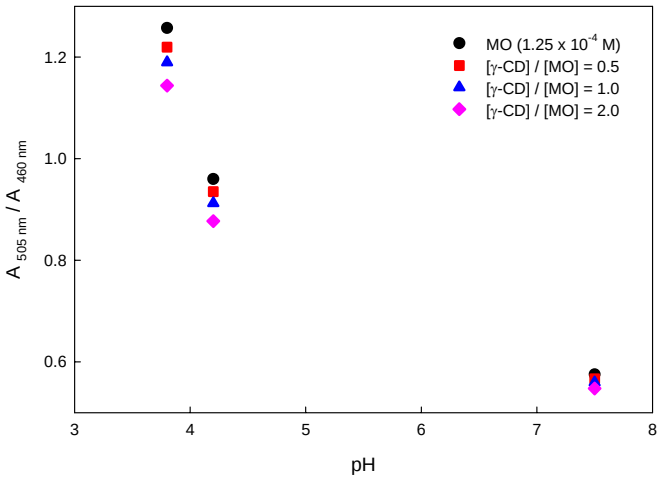

Figure 6.6. Absorbance ratio at 505 nm over at 460 nm, $A_{505\ nm} / A_{460\ nm}$, in different pHs. Legends indicate the concentration ratio of γ-CD / MO.

Benesi-Hildebrand method is frequently used to estimate the formation of dye inclusion complex with CD.[22] For 1:1 (CD : dye) complex, the stability constant (K_f) is calculated using equation 6.1.[22]

$$\frac{lC_0S_0}{\Delta A} = \frac{1}{K_f \Delta\varepsilon} + \frac{C_0}{\Delta\varepsilon} \qquad (6.1)$$

where l is the optical path length of the cell used, C_0 and S_0 are molar concentrations of γ-CD and MO, respectively. ΔA is the change in the absorbance of MO by the addition of γ-CD, $\Delta\varepsilon$ is the difference in molar absorptivities between free and complexed MO, and K_f

is the stability constant of the inclusion complex. In a linear plot of ($lC_0S_0/\Delta A$) against C_0, $\Delta\varepsilon$ and K_f are determined from the slope and intercept, respectively.

In our case, where 2:1 (CD:dye) complex is expected to form, the modified Benesi-Hildebrand, equation (6.2), is used.[11] Similarly, $\Delta\varepsilon$ and K_f are determined from the plot of ($lC_0S_0^2/\Delta A$) against $2C_0S_0$.

$$\frac{lC_0S_0^{\ 2}}{\Delta A} = \frac{1}{K_f \Delta\varepsilon} + \frac{2C_0S_0}{\Delta\varepsilon} \qquad (6.2)$$

The linear plot in Figure 6.7 indicates the formation of 2:1 complex between MO and γ-CD. The stability constant K_f was calculated to be 4.0 x 10^7 mol^{-2} dm^6. From a high K_f value, we see that binding nature of the complex is very strong.

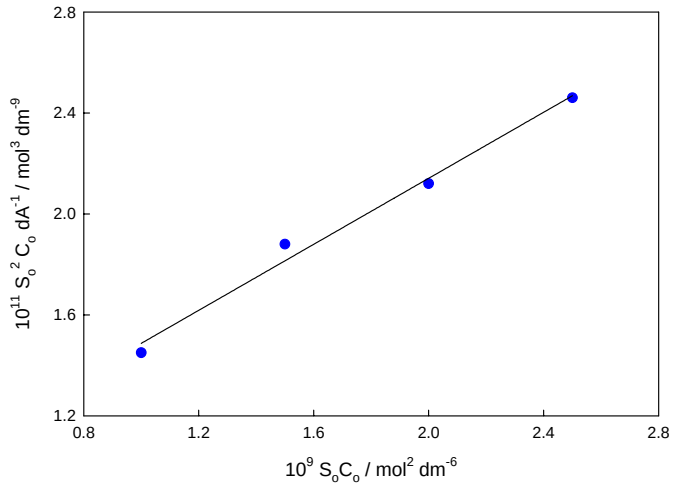

Figure 6.7. The stability constant, K_f, was calculated for 2:1 complex under pH 7.5. Absorbance values were measured at 460 nm.

6.4 Discussion

Methyl Orange (MO) is a well-known pH indicator. It exists as unprotonated in alkaline solutions and protonated in acidic media.[25] Orange color with λ_{max} at 460 nm is attributed to ammonium (AM) tautomer, and red color at 505 nm is to azonium (AZ) tautomer (Figure 6.8). Due to the existence of a delocalized positive charge (AZ1↔AZ2), azonium tautomer generally exhibits a red shift and higher tinctorial strength (Table 6.1).[26] Under acidic condition, MO shows a strong peak at 505 nm due to the dominant existence of azonium tautomer (Scheme 6.1).

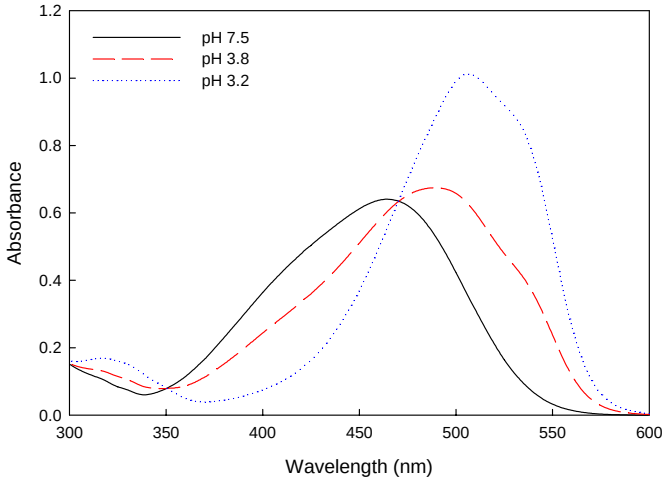

Figure 6.8. Absorption spectra of MO in different pHs. Phosphate buffer with concentration of 10 mM is used for pH 7.5 and pH 3.8. pH 3.2 is adjusted by dilute HCl solution. MO concentration is 5 x 10^{-5} M.

Table 6.1. Absorption properties of MO in different pHs.

pH	λ_{max}	ε_{max}
3.2	505 nm	20,234
3.8	490 nm	13,490
7.5	460 nm	12,810

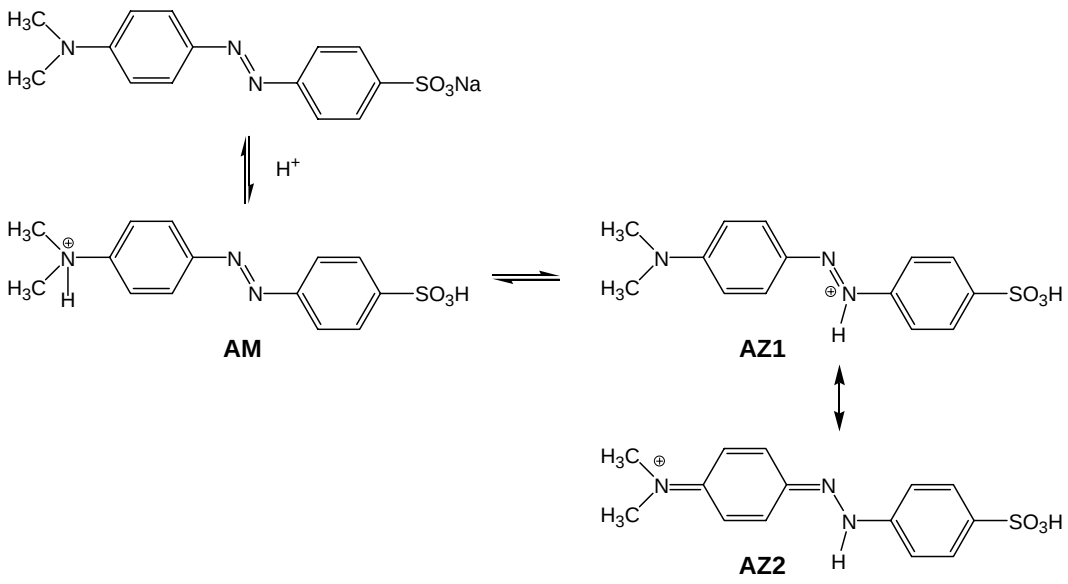

Scheme 6.1. Tautomeric equilibrium of MO under different pH conditions.

MO forms an inclusion complex in the presence of γ-CD. Obviously, the complex becomes less soluble, and consequently less conductive in aqueous medium. This leads to the decrease in the conductivity. It is consistent with the nonelectrolyte nature of the complexes.[27] Similar behavior, a change in conductance with the complex formation, is often observed in metal-ligand complexes.[28] The conductivity measurements show a sharp inflection point around [CD]/[MO] = 0.5 at neutral pH. After this point, the change in conductivity becomes much smaller. This clearly shows that different types of complex exist around this molar ratio. Also the inflection point, where the molar ratio is [MO]:[γ-CD]=2:1, shows the existence of dimeric inclusion, i.e. two dye molecules are included in the cavity of γ-CD.[6,29] Under acidic condition, however, there is no inflection point, as observed in neutral condition. It implies that there exists only one kind, monomeric inclusion complex. Dimeric inclusion seems to be hindered at low pH,

because azonium tautomer makes dimeric inclusion difficult due to its steric hindrance from extra hydrogen atom on azo group inside CD.

It was reported previously that three mechanistic steps were considered in complex formation between MO and γ-CD;[30,31]

$$MO + \gamma\text{-}CD \xleftrightarrow{K_1} MO(\gamma\text{-}CD) \qquad \text{fast}$$

$$MO + MO(\gamma\text{-}CD) \xleftrightarrow{K_2} MO_2(\gamma\text{-}CD) \qquad \text{slow}$$

$$\gamma\text{-}CD + MO_2(\gamma\text{-}CD) \xleftrightarrow{K_2} MO_2(\gamma\text{-}CD)_2 \qquad \text{fast}$$

where it was found that K_2 is on the order of 10^6 in slightly alkaline condition (pH 9). Therefore, this result agrees well to the current K_f calculations, even though there is some discrepancy, which mainly results from different experimental conditions. As mentioned earlier, high stability of the dimeric inclusion complex, MO_2 (γ-CD), compared to that of the monomeric inclusion complex, MO (γ-CD), is closely related to the larger diameter of γ-CD cavity. Interestingly, MO_2 $(\gamma\text{-CD})_2$, also contains dimer, included by both γ-CD molecules, but its stability is not as high as that of MO_2 (γ-CD). These results strongly suggest the formation of an aggregate-like compound in the γ-CD nanocavity.[31]

Under neutral pH, MO forms stable anisotropic complexes which come from dimeric inclusion within large cavity of γ-CD. It shows the thread-like texture and it also causes the increase in its viscosity. On standing still several days, the mixture separates into an isotropic upper layer and an anisotropic lower layer. This phenomenon is almost identical to that of Orange II.[18] Unlike the γ-CD complex, in complex with α-CD and β-CD, no anisotropy is observed. Both CDs have smaller cavities than that of γ-CD, and no dimeric inclusion is considered. Therefore, monomeric inclusion may not be strong

enough to hold the extension of dye aggregates. This can be related to the disappearance of anisotropy at low pH, in which monomeric inclusion is considered to be dominant. Obviously, the existence of both components, dye and γ-CD, is indispensable in the appearance of anisotropy.

Several other azo dyes are found to show similar anisotropy, and they are shown in Figure 6.9 (dye **1** - dye **3)**. In their chemical structures, several common factors are noticed; they have one sulfonate group as solubilizing group and it exists at the *p*-position to azo chromophore. Interestingly, most azo dyes do not form anisotropic structure, even though they have similar chemical structures. When looking closely into them, we clearly see that the position of solubilizing group is very important. Acid Alizarin Violet N (**4**) and Crocein Orange G (**5**) don't show an anisotropy even though they have a $-SO_3H$ group. It is also observed that the number of solubilizing group plays an important role. Dyes with more than one sulfonate group, such as Biebrich Scarlet (**6**) and Sunset Yellow FCF (**7**), don't show any anisotropy either. Higher solubility, from multiple sulfonate groups, of these dyes may hinder the formation of inclusion complex, and hence large aggregates. Water-insoluble dyes, such as Sudan I (**8**) and Para Red (**9**), don't show anisotropy, mainly due to their limited accessibility to host material. From these results, we conclude that azo dyes with one sulfonate group at p-position to azo group, which leads to the extended linear structure, can form anisotropic phases in the presence of γ-CD.

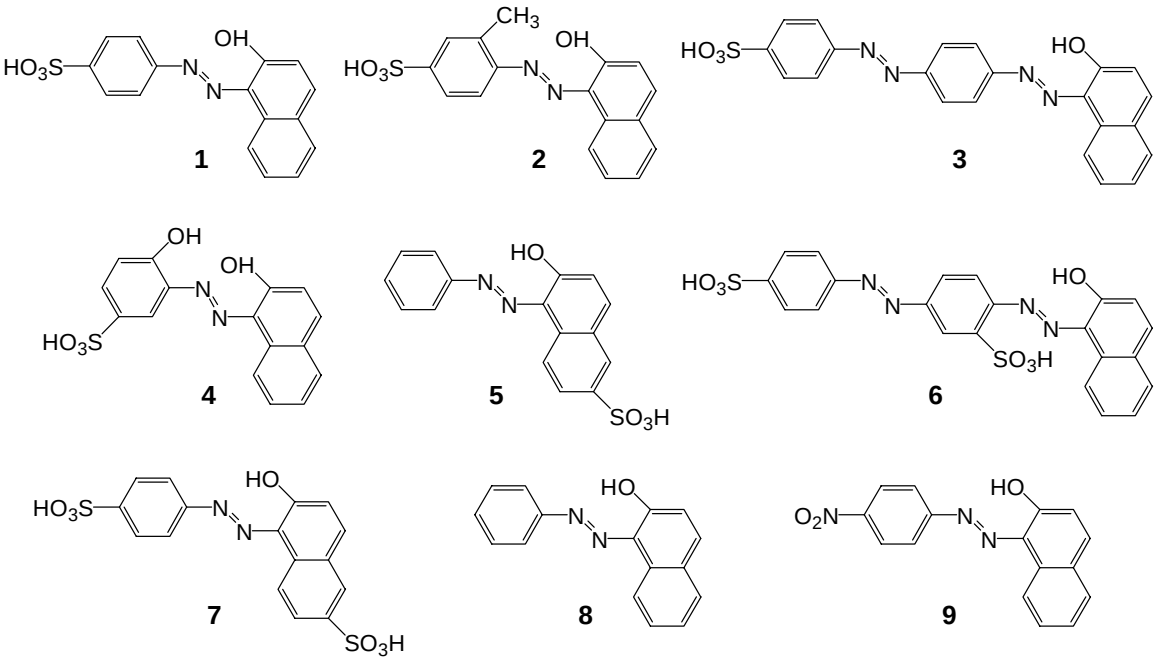

Figure 6.9. Azo dyes showing anisotropy in the presence of γ-CD; Orange II (**1**), C.I. Acid Orange 8 (**2**), CI acid red 151 (**3**), and azo dyes showing no anisotropy with γ-CD; Acid Alizarin Violet N (**4**), Crocein Orange G (**5**), Biebrich Scarlet (**6**), Sunset Yellow FCF (**7**), Sudan I (**8**), Para Red (**9**).

6.5. Conclusion

In summary, MO is found to form dimeric inclusion complexes with γ-CD based on 2:1 (MO:CD) molar ratio in neutral conditions. At high concentration above 0.02 M, an anisotropic structure is observed. It is postulated that MO dimers are included in the channel type structure of γ-CD in aqueous solution, resulting in the formation of stable anisotropic aggregates. Under acidic condition, monomeric inclusion of azonium tautomer is dominant, and no anisotropy is observed. It is found that azo dyes with one sulfonate group at p-position to azo group, which leads to the extended linear structure, can form anisotropic phases in the presence of γ-CD.

REFERENCES

[1] Spencer W.; Sutter, J. R. "Kinetic study of the monomer-dimer equilibrium of methylene blue in aqueous solution", *J. Phys. Chem.* **1979**, *83*, 1573.

[2] Hamada, K.; Take, S.; Iijima, T.; Amiya, S. "Effects of electrostatic repulsion on the aggregation of azo dyes in aqueous-solution", *J. Chem. Soc. Fara. Trans. 1* **1986**, *82*, 3141.

[3] Rawarah, K. M.; Wazwaz, A. A. "Conductance study of the binding of methyl orange, o-methyl red and p-methyl red anions by α-cyclodextrin in water", *J. Chem. Soc. Faraday Trans.* **1989**, *89*, 1729.

[4] Wojtyk, J.; McKerrow, A.; Kazmaier, P.; Buncel, E. "Quantitative investigations of the aggregation behavior of hydrophobic aniline squaraine dyes through UV/Vis spectroscopy and dynamic light scattering", *Can. J. Chem.* **1999**, *77*, 903.

[5] Cramer, F.; Saenger, W.; Spartz, H.-Ch. "Inclusion compounds. XIX. The formation of inclusion compounds of α-cyclodextrin in aqueous solutions. thermodynamics and kinetics", *J. Am. Chem. Soc*.**1967**, 89, 14.

[6] Suzuki, M.; Ohmori, H.; Kajtar, M.; Szejtli, J.; Vikmon, M. "The association of inclusion complexes of cyclodextrins with azo dyes", *Inclu. Phenom. Mol. Recog. Chem.***1994**, *18*, 255.

[7] Buvari, A.; L. J. Barcza, "Color-change and tautomerism of some azo-indicators on complex-formation with cyclodextrins", *Inclu. Phenom. Mol. Recog. Chem.* **1989**, *7*, 313.

[8] Yoshida, N.; Seiyama, A.; Fujimoto, M. "Stability and structure of the inclusion complexes of alkyl-substituted hydroxyphenylazo derivatives of sulfanilic acid with α- and β-cyclodextrins", *J. Phys. Chem.* **1990**, *94*, 4254.

[9] Mwakibete, H.; Bloor, D. M.; Wynjones, E. "Electrochemical studies of cationic drug inclusion complexes with α-cyclodextrins and β-cyclodextrins", *Inclu. Phenom. Mol. Recog. Chem.* **1991**, *10*, 497.

[10] Rohrbach, R. P.; Rodriguez, L. J.; Eyring, E. M. "An equilibrium and kinetic investigation of salt-cycloamylose complexes", *J. Phys. Chem.* **1977**, *81*, 944.

[11] Hirai, H.; Toshima, N.; Uenoyama, S. “Inclusion complex formation of γ-cyclodextrin. On host-two guest complexation with water-soluble dyes in ground state”, *Bull. Chem. Soc. Jpn.* **1985**, *58*, 1156.

[12] Clarke, R. J.; Coates, J. H.; Lincoln, S. F. “Complexation of roccellin by β-cyclodextrin and γ-cyclodextrin”, *J. Chem. Soc. Fara. Trans.* **1986**, *82*, 2333.

[13] Suzuki, M.; Kajrar, M.; Szejtli, J.; Vikmon, M.; Fenyvesi, E. “Inclusion compounds of cyclodextrins and azo dyes. 10. Induced circular-dichroism spectra of complexes of cyclomaltooligosaccharides an azo dyes containing naphthalene nuclei”, *Carbohyd. Res.* **1992**, *223*, 71.

[14] Suzuki, M.; Sasaki, Y. “Inclusion compounds of cyclodextrin and azo dye. 1. Methyl-Orange”, *Chem. Pharm. Bull.* **1979**, *27*, 609.

[15] Suzuki, M.; Sasaki, Y. “Inclusion compounds of cyclodextrin and azo dyes. 2. ^{1}H nuclear magnetic resonance and circular dichroism spectra of cyclodextrin and azo dyes with a naphthalene nucleus”, *Chem. Pharm. Bull.* **1979**, *27*, 1343.

[16] Suzuki, M.; Sasaki, Y.; Sugiura, M. “Inclusion compounds of cyclodextrin and azo dyes. 3. ^{13}C nuclear magnetic resonance spectra of cyclodextrin and azo dyes with a naphthalene nucleus”, *Chem. Pharm. Bull.* **1979**, *27*, 1797.

[17] Suzuki, M.; Sasaki, Y. “Nuclear magnetic resonance and circular dichroism spectra of γ-cyclodextrin and orange-II in the solution state”, *Chem. Pharm. Bull.* **1984**, *32*, 832.

[18] Suzuki, M.; Sasaki, Y. “Inclusion compounds of cyclodextrin and azo dyes – formation of a liquid crystal”, *Chem. Pharm. Bull.* **1981**, *29*, 585.

[19] Suzuki, M.; Ohmori, H.; Kajtar, M.; Szejtli, J.; Vikmon, M. “The association of inclusion complexes of cyclodextrins with azo dyes”, *J. Inclus. Phenom. Mol.* **1994**, *18*, 255.

[20] Agbaria, R. A.; Gill, D. “Extended 2,5-diphenyloxazole-γ-cyclodextrin aggregates emitting 2,5-diphenyloxazole excimer fluorescence”, *J. Phys. Chem.* **1988**, *92*, 1052.

[21] Agbaria, R. A.; Gill, D. “Non-covalent polymers of oxadiazole derivatives induced by γ-cyclodextrin in aqueous solutions-fluorescence study”, *J. Photochem. Photobio. A: Chem.* **1994**, *78*, 161.

[22] Benesi, H. A.; Hildebrand, J. H. “A spectrophotometric investigation of the interaction of iodine with aromatic hydrocarbons”, *J. Am. Chem. Soc.* **1949**, *71*, 2703.

[23] Clarke, R. J.; Coates, J. H.; Lincolin, S. F. “Kinetic and equilibrium studies of cyclomalto-octaose(γ-cyclodextrin)-methyl orange inclusion complexes”, *Carbohydr. Res.* **1984**, *127*, 181.

[24] Steiner, T.; Saenger, W. “Channel-type crystal packing in the very rare space group P42(1)2 with Z’=3/4: Crystal structure of the complex γ-cyclodextrin-methanol-n-hydrate”, *Acta Crystallogr. Sect. B.* **1998**, *54*, 450.

[25] Gordon, P. F.; Gregory, P. *Organic Chemistry in Colour*, Spinger-Verlag Berlin Herdleberg, Germany, 1987.

[26] Cox, R. A.; Buncel, E. *Azo-hydrazone tautomerism of aromatic azo compounds*, London, John Wiley and Sons, **1975**.

[27] Tawarah, K. M.; Wazwaz, A. A. “Conductance study of the binding of methyl orange, o-methyl red and p-methyl red anions by α-cyclodextrin in water”, *J. Chem. Soc. Faraday Trans.* **1993**, *89*, 1729.

[28] Chandra, S.; Gupta, L. K.; Jain, D. “Spectroscopic studies on Mn(II), Co(II), Ni(II), and Cu(II) complexes with N-donor tetradentate (N-4)macrocyclic ligan derived from ethylcinnamate moiety”, *Spectrochimica Acta Part A* **2004**, *60*, 2411.

[29] Tawarah, K. M.; Khouri, S. J. “Determination of the stability and stoichiometry of p-methyl red inclusion complexes with γ-cyclodextrin”, *Dyes Pigments* **2000**, *40*, 229.

[30] Takei, M.; Yui, H.; Hirose, Y.; Sawada, T. “Femtosecond time-resolved spectroscopy of photoisomerization of methyl orange in cyclodextrins”, *J. Phys. Chem. A* **2001**, *105*, 11395.

[31] Clarke, R. J.; Coates, J. H.; Lincoln, S. F. “Kinetic and equilibrium studies of cyclodmalto-octaose(γ-cyclodextrin)-methyl orange inclusion complexes”, *Carbohydr. Res.* **1984**, *127*, 181.

CHAPTER 7

CONCLUSIONS AND RECOMMENDATIONS FOR FUTURE WORK

7.1. Conclusions

The present thesis covers the study of inclusion complexes of CDs and chromophore dyes, largely in two ways, rotaxane and pseudorotaxane, and the important results of the study are summarized as follows.

The stable rotaxane structure is achieved with the synthesis of dye rotaxane. As a result of the azo dye molecule being encapsulated in cyclodextrin, a cyclic sugar molecule, a number of physical properties change. This change in physical properties can be accomplished without synthesizing a different set of dyes. We have shown that for a azo dye rotaxane, the introduction of CD ring around a chromophore provides a simple way to improve the solubility and stability of azo dye. It is found that CD presence does not interfere with tautomeric equilibrium of threaded aminoazobenzene dye. When 8-hydroxyquinoline is incorporated as a coupling component, azoxine dye rotaxane exhibits a high sensitivity to pH and metal ions. The results show that azo dye rotaxane can be used to develop new sensory applications.

We have described the synthesis of novel acetylene dye rotaxane using the Pd-catalyzed reaction of Heck-Cassar-Sonogashira-Hagihara type. Its fluorescence properties in the solid state as well as in solutions have been examined and compared with those of free dye. Free dye, which has tetra-carboxylic groups, shows high fluorescence quenching to various metal ions. It reveals high Stern-Volmer constants, K_{SV}, exhibiting almost the same K_{SV} values as those of conjugate polymers. On the contrary, acetylene dye rotaxane exhibits much less quenching against these quenchers. It is attributed to the

fact that CD encapsulation protects and stabilizes the threaded chromophore against outside quencher.

The appearance of fluorescent anisotropic structure has been observed by the formation of inclusion complex between acetylene dye and γ-CD. Its structural nature has been studied by various techniques, including fluorescence, fluorescence anisotropy, wide angle X-ray scattering (WAXD) and differential scanning calorimetry (DSC) measurements. Using the Benesi-Hildebrand equation, binding constant, *K*, of the complex is calculated, which shows that the binding nature of the complex is very strong. Emission intensities are observed to decrease with temperature, and its Arrhenius-type plot shows non-linear relationship with a transition temperature. Methyl orange, an acid azo dye, forms an inclusion complex with γ-CD, resulting in the formation of stable anisotropic aggregates. For azo dyes which form anisotropic supramolecule in the presence of γ-CD, their structural similarity has been discussed in terms of the number and position of solubilizing groups.

7.2. Recommendations for future work

- As noted, Azoxine dye rotaxane (AzoxRD) is sensitive to various conditions, which include pHs and solvents as well as metal ions. Sensitivity we have obtained only resulted from a specific condition (solvent mixture with DMF/pH6.0 Buffer in volume ration of 2:8). Therefore, in sensitivity measurement of AzoxRD with metal ions, numerous factors are to be considered.

- For study about fluorescent anisotropic structure from acetylene dye and γ-CD; (1) Structural study needs to be done using various techniques, such as X-ray measurements in a fluid. (2) Rheological properties need to be investigated by measuring G' (elastic) and G" (loss modulus) of the anisotropic solutions. (3) Time-resolved fluorescence measurement is beneficial in understanding a diffusional behavior of the aggregates.

- I would like to make several suggestions for obtaining a high yield in the synthesis of dye rotaxane. They are mostly from an author's experience. (1) Complexing behavior between a thread and cyclodextrin is heavily affected by physical reaction conditions, such as stirring speed, temperature, and starting concentrations. Thus, for rotaxane synthesis, it would be better to use constant experimental conditions; use the same hot plate, reaction vessel, and so on. (2) Before use, cyclodextrins needs to be dried in vacuum, in order to remove residual moisture as much as possible. (3) Water-soluble thread needs to be used for a higher inclusion yield. Diazonium salt for azo dye rotaxane, and boronic acid derivatives for Suzuki coupling seems to be ideal in this sense. (4) Reaction temperature around 50~60 ^{o}C is preferred, in order to obtain homogeneous solutions.

APPENDIX A

COMPLETE CRYSTALLOGRAPHIC DATA OF ACETYLENE DYE ROTAXANE

Table A.1. Atomic coordinates (x 10^4) and equivalent isotropic displacement parameters ($Å^2$ x 10^3) for RD **3**. U(eq) is defined as one third of the trace of the orthogonalized U^{ij} tensor.

	x	y	z	U(eq)
C(1)	6579(13)	3288(8)	11129(8)	50(5)
C(2)	6489(9)	3796(5)	11420(5)	14(3)
C(3)	6457(10)	3779(6)	11994(6)	26(3)
C(4)	6434(10)	3236(6)	12252(6)	24(3)
C(5)	6522(10)	2696(7)	11966(6)	28(3)
C(6)	6569(14)	2721(9)	11392(8)	53(5)
C(7)	6608(15)	2198(9)	11069(8)	60(5)
C(8)	6712(15)	1787(10)	10731(9)	64(5)
C(9)	6684(13)	1306(8)	10382(8)	48(4)
C(10)	6422(17)	698(10)	10594(9)	70(6)
C(11)	6383(18)	237(12)	10229(11)	87(7)
C(12)	6509(10)	302(6)	9648(6)	26(3)
C(13)	6890(18)	823(11)	9470(10)	81(7)
C(14)	6890(17)	1311(11)	9875(10)	77(7)
C(15)	6389(11)	-163(6)	9225(6)	29(3)
C(16)	6489(17)	-738(10)	9417(10)	75(6)
C(17)	6420(20)	-1180(13)	9016(11)	95(8)
C(18)	6211(10)	-1117(6)	8439(6)	23(3)
C(19)	6112(13)	-529(8)	8273(8)	46(4)
C(20)	6147(14)	-104(9)	8676(8)	56(5)
C(21)	6230(13)	-1567(8)	8049(7)	45(4)
C(22)	6267(11)	-1953(7)	7711(6)	33(4)
C(23)	6330(11)	-2432(7)	7302(6)	34(4)
C(24)	6739(10)	-2961(6)	7472(6)	23(3)
C(25)	6769(9)	-3426(6)	7101(5)	17(3)
C(26)	6300(10)	-3358(7)	6548(6)	29(3)
C(27)	5879(9)	-2805(6)	6367(5)	19(3)

C(28)	5963(12)	-2390(7)	6760(6)	37(4)
C(29)	7222(10)	-4019(6)	7264(5)	22(3)
C(30)	5470(12)	-2733(7)	5765(7)	37(4)
C(31)	6343(10)	3175(6)	12882(6)	23(3)
C(32)	6537(12)	4375(8)	11153(7)	43(4)
C(33)	1328(13)	-939(8)	6723(7)	47(4)
C(34)	1134(13)	-1457(8)	7021(7)	46(4)
C(35)	1072(10)	-1997(7)	6722(6)	29(3)
C(36)	1209(9)	-2024(6)	6160(5)	20(3)
C(37)	1442(10)	-1509(6)	5889(6)	24(3)
C(38)	1487(11)	-979(7)	6154(6)	31(3)
C(39)	1690(10)	-458(6)	5863(6)	26(3)
C(40)	1765(8)	-36(5)	5553(5)	9(2)
C(41)	1809(10)	468(6)	5210(6)	25(3)
C(42)	2039(9)	429(6)	4645(5)	19(3)
C(43)	1955(11)	908(7)	4314(6)	33(4)
C(44)	1691(9)	1468(6)	4509(5)	17(3)
C(45)	1488(12)	1492(8)	5045(7)	42(4)
C(46)	1514(13)	1009(8)	5368(7)	46(4)
C(47)	1641(11)	1974(7)	4109(6)	32(3)
C(48)	1294(12)	1909(8)	3542(7)	42(4)
C(49)	1255(14)	2363(8)	3155(8)	54(5)
C(50)	1567(16)	2923(10)	3370(9)	64(6)
C(51)	1902(13)	2984(9)	3901(8)	50(5)
C(52)	1891(11)	2508(6)	4284(6)	30(3)
C(61)	973(12)	-1428(8)	7605(7)	40(4)
C(62)	1274(12)	-2601(7)	5869(7)	38(4)
C(65)	5502(11)	740(6)	5913(6)	28(3)
C(66)	5441(13)	1432(8)	5944(8)	48(4)
C(67)	4401(11)	1590(7)	6036(6)	31(4)
C(68)	4134(11)	1324(7)	6592(7)	35(4)
C(69)	4327(12)	640(7)	6539(7)	40(4)
C(70)	4235(13)	375(8)	7145(7)	49(5)
C(71)	2958(13)	1659(8)	7149(7)	47(4)
C(72)	2252(12)	2233(8)	6981(7)	44(4)
C(73)	1327(13)	1997(8)	6630(8)	50(5)

C(74)	817(13)	1506(8)	6930(7)	47(4)
C(75)	1591(15)	1043(9)	7202(9)	59(5)
C(76)	1237(17)	657(10)	7634(9)	72(6)
C(77)	-826(12)	1135(7)	6549(7)	37(4)
C(78)	-1428(12)	1388(7)	6100(6)	37(4)
C(79)	-1302(13)	1174(8)	5541(7)	44(4)
C(80)	-1434(13)	498(8)	5561(7)	47(4)
C(81)	-890(12)	203(7)	6069(6)	36(4)
C(82)	-1261(15)	-413(9)	6116(9)	61(5)
C(83)	-1785(17)	-50(10)	4634(9)	70(6)
C(84)	-1616(17)	64(10)	4049(10)	72(6)
C(85)	-606(13)	-8(8)	3947(7)	44(4)
C(86)	-418(11)	-686(7)	4029(7)	36(4)
C(87)	-621(12)	-874(7)	4626(7)	37(4)
C(88)	-613(14)	-1521(8)	4724(8)	51(5)
C(89)	863(14)	-1261(9)	3673(8)	54(5)
C(90)	1276(15)	-1064(9)	3225(9)	61(5)
C(91)	2258(11)	-725(7)	3375(6)	33(4)
C(92)	2981(10)	-1073(6)	3838(6)	24(3)
C(93)	2449(10)	-1380(6)	4266(6)	25(3)
C(94)	3054(11)	-1900(7)	4565(6)	32(4)
C(95)	4631(10)	-794(6)	4241(6)	26(3)
C(96)	5268(11)	-300(6)	4131(6)	29(3)
C(97)	5147(12)	217(7)	4524(6)	34(4)
C(98)	5232(13)	50(7)	5146(7)	40(4)
C(99)	4659(12)	-502(7)	5222(6)	35(4)
C(100)	4875(13)	-759(8)	5808(7)	44(4)
C(101)	123(18)	7396(11)	10431(10)	77(7)
C(102)	248(17)	7234(11)	11014(10)	75(6)
C(103)	1304(12)	7160(8)	11277(7)	41(4)
C(104)	1965(12)	7670(8)	11139(7)	42(4)
C(105)	1697(12)	7928(7)	10544(7)	39(4)
C(106)	2095(15)	8548(9)	10453(8)	55(5)
C(107)	3758(13)	7762(8)	11496(7)	48(4)
C(108)	4487(13)	7338(8)	11837(7)	43(4)
C(109)	4868(11)	6921(7)	11419(6)	35(4)

C(110)	5400(11)	7255(7)	11013(6)	33(4)
C(111)	4705(11)	7769(6)	10727(6)	30(3)
C(112)	5266(16)	8216(10)	10422(9)	72(6)
C(113)	6622(12)	6877(7)	10516(7)	37(4)
C(114)	6975(13)	6224(7)	10556(7)	41(4)
C(115)	6527(14)	5875(8)	10080(7)	49(4)
C(116)	6585(13)	6160(8)	9500(7)	44(4)
C(117)	6187(11)	6800(6)	9496(6)	27(3)
C(118)	6282(13)	7133(8)	8973(7)	47(4)
C(119)	6264(12)	5651(7)	8590(6)	36(4)
C(120)	6130(13)	4960(8)	8555(7)	44(4)
C(121)	5045(11)	4863(7)	8486(7)	36(4)
C(122)	4478(12)	5207(8)	8034(7)	45(4)
C(123)	4818(11)	5868(7)	8008(6)	30(3)
C(124)	4421(12)	6192(7)	7489(7)	39(4)
C(125)	2766(13)	5047(8)	7644(8)	51(5)
C(126)	1943(19)	4661(11)	7835(11)	83(7)
C(127)	1520(20)	4898(12)	8253(11)	88(7)
C(128)	1044(19)	5584(12)	8110(11)	86(7)
C(129)	1851(16)	5915(10)	7834(9)	65(6)
C(130)	1375(15)	6462(9)	7515(8)	59(5)
C(131)	-90(20)	6197(12)	8540(12)	92(8)
C(132)	-640(20)	6038(12)	8953(11)	93(8)
C(133)	-206(16)	6183(9)	9546(9)	63(6)
C(134)	20(20)	6829(12)	9517(11)	90(8)
C(135)	710(20)	6925(13)	9092(11)	93(8)
C(136)	1120(30)	7681(17)	9027(17)	149(14)
C(53A)	1702(19)	3462(11)	3076(11)	30
C(54A)	1670(30)	3879(17)	2761(16)	66(10)
C(55A)	1640(20)	4366(14)	2316(12)	56(8)
C(56A)	1250(30)	4270(20)	1847(12)	74(11)
C(57A)	1240(19)	4746(12)	1365(11)	30
C(58A)	1676(18)	5193(11)	1515(10)	30
C(59A)	2069(18)	5314(11)	2067(10)	30
C(60A)	2135(18)	4925(11)	2505(10)	30
C(63A)	2490(40)	5880(20)	2260(20)	109(15)

C(64A)	1210(30)	4550(20)	902(19)	82(13)
O(13A)	3010(30)	6158(16)	1854(16)	123(11)
O(14A)	2860(20)	5986(13)	2787(12)	87(8)
O(15A)	940(30)	4988(16)	413(15)	118(11)
O(16A)	330(40)	4150(20)	680(20)	172(17)
C(53B)	1400(30)	3329(17)	2804(17)	30
C(54B)	1410(30)	3629(17)	2438(16)	30
C(55B)	1370(30)	3954(18)	1994(16)	30
C(56B)	1450(30)	3747(17)	1424(15)	30
C(57B)	1390(30)	4046(17)	979(15)	30
C(58B)	890(30)	4721(19)	944(18)	30
C(59B)	970(30)	4989(18)	1533(16)	30
C(60B)	1170(30)	4628(18)	1978(16)	30
C(63B)	930(20)	5612(15)	1548(14)	23
C(64B)	1420(40)	3880(30)	360(20)	70(15)
O(13B)	1220(16)	5863(10)	1961(9)	20(5)
O(14B)	460(20)	5798(14)	1101(13)	53(8)
O(15B)	1210(30)	4174(18)	-45(16)	77(11)
O(16B)	1710(30)	3341(16)	355(15)	69(10)
O(1)	6180(8)	3681(5)	13115(5)	45(3)
O(2)	6415(9)	2742(6)	13142(5)	54(3)
O(3)	6713(9)	4824(6)	11433(5)	58(3)
O(4)	6329(15)	4361(9)	10627(8)	111(6)
O(5)	6930(9)	-4437(6)	6944(5)	54(3)
O(6)	7808(9)	-4052(5)	7708(5)	49(3)
O(7)	5100(8)	-2283(5)	5550(5)	44(3)
O(8)	5436(8)	-3227(5)	5462(5)	44(3)
O(9)	1355(10)	-2580(6)	5363(6)	62(4)
O(10)	1131(9)	-3070(6)	6121(5)	58(3)
O(11)	782(11)	-1899(7)	7860(6)	73(4)
O(12)	1082(9)	-930(6)	7853(5)	55(3)
O(17)	5275(8)	490(5)	6431(5)	44(3)
O(18)	5741(10)	1681(6)	5470(5)	59(3)
O(19)	4334(8)	2210(5)	6083(5)	46(3)
O(20)	5012(13)	575(8)	7539(8)	99(5)
O(21)	3167(8)	1418(5)	6640(4)	38(3)

O(22)	2508(9)	1302(6)	7461(5)	58(3)
O(23)	2740(10)	2630(6)	6668(6)	66(4)
O(24)	635(10)	2457(6)	6511(6)	68(4)
O(25)	1142(13)	935(8)	8136(7)	94(5)
O(26)	159(8)	1231(5)	6502(4)	38(3)
O(27)	-1060(9)	527(5)	6593(5)	50(3)
O(28)	-1361(10)	2030(7)	6128(6)	73(4)
O(29)	-1909(11)	1393(7)	5049(6)	77(4)
O(30)	-2278(13)	-453(8)	6148(7)	91(5)
O(31)	-1115(9)	275(6)	5041(5)	54(3)
O(32)	-1625(10)	-673(6)	4719(6)	66(4)
O(33)	-1838(13)	721(8)	3946(7)	97(5)
O(34)	-474(11)	69(7)	3381(6)	73(4)
O(35)	-1260(10)	-1833(6)	4317(6)	68(4)
O(36)	605(8)	-786(5)	4017(4)	39(3)
O(37)	1497(8)	-1655(5)	4041(4)	39(3)
O(38)	645(12)	-698(8)	2814(7)	88(5)
O(39)	2719(10)	-584(6)	2929(6)	68(4)
O(40)	3103(7)	-2370(5)	4199(4)	35(2)
O(41)	3654(6)	-647(4)	4107(4)	24(2)
O(42)	4885(8)	-952(5)	4827(4)	40(3)
O(43)	5066(10)	-166(6)	3532(5)	59(3)
O(44)	5829(9)	653(6)	4390(5)	55(3)
O(45)	4241(9)	-1257(5)	5862(5)	54(3)
O(46)	4909(7)	544(4)	5441(4)	31(2)
O(47)	632(10)	7970(6)	10386(6)	67(4)
O(48)	-433(17)	6763(11)	11097(10)	135(8)
O(49)	1470(11)	7031(7)	11852(6)	79(4)
O(50)	1753(11)	8938(7)	10808(6)	73(4)
O(51)	2949(8)	7456(5)	11207(5)	44(3)
O(52)	4271(8)	8097(5)	11140(5)	45(3)
O(53)	3987(10)	6997(7)	12218(6)	71(4)
O(54)	5584(9)	6517(5)	11717(5)	52(3)
O(55)	5994(8)	8526(5)	10791(5)	48(3)
O(56)	5686(7)	6884(4)	10608(4)	27(2)
O(57)	6750(8)	7108(5)	9964(5)	47(3)

O(58)	6920(11)	5995(7)	11091(6)	71(4)
O(59)	6835(11)	5254(7)	10049(6)	74(4)
O(60)	7306(9)	7178(6)	8900(5)	58(3)
O(61)	5960(7)	5841(5)	9087(4)	35(2)
O(62)	5839(7)	5914(4)	8103(4)	30(2)
O(63)	6664(9)	4668(5)	9029(5)	52(3)
O(64)	4778(9)	4254(6)	8399(5)	57(3)
O(65)	4518(9)	5903(6)	6998(5)	53(3)
O(66)	3431(8)	5179(5)	8100(5)	44(3)
O(67)	2266(8)	5590(5)	7427(5)	47(3)
O(68)	2443(13)	4126(8)	8091(8)	100(5)
O(69)	722(16)	4565(10)	8450(9)	127(7)
O(70)	646(10)	6286(6)	7052(6)	63(4)
O(71)	810(12)	5824(7)	8567(7)	84(5)
O(72)	93(17)	6819(11)	8560(10)	134(8)
O(73)	-811(15)	5411(9)	8990(8)	112(6)
O(74)	-775(13)	6028(8)	9974(7)	93(5)
O(75)	320(17)	7957(10)	8905(9)	120(7)
O(76)	489(12)	6980(7)	10114(7)	83(4)
O(1W)	4285(11)	7780(7)	3135(7)	80(4)
O(2W)	6659(11)	8219(7)	4542(6)	78(4)
O(3W)	8748(16)	4046(10)	1044(9)	42(5)
O(4W)	3503(11)	6678(7)	6180(6)	71(4)
O(5W)	8020(20)	8388(13)	864(12)	66(8)
O(6W)	4766(15)	8856(9)	2683(8)	33(5)
O(7W)	8344(16)	4981(10)	8017(9)	42(5)
O(8W)	8682(17)	4847(11)	88(10)	49(6)
O(9W)	3160(30)	3695(19)	6939(17)	69(11)

Table A.2. Bond lengths [Å] and angles [°] for RD **3**.

C(1)-C(2)	1.37(2)	C(27)-C(28)	1.33(2)
C(1)-C(6)	1.44(3)	C(27)-C(30)	1.47(2)
C(2)-C(3)	1.379(18)	C(29)-O(6)	1.235(16)
C(2)-C(32)	1.47(2)	C(29)-O(5)	1.249(18)
C(3)-C(4)	1.39(2)	C(30)-O(7)	1.223(19)
C(4)-C(5)	1.42(2)	C(30)-O(8)	1.336(19)
C(4)-C(31)	1.534(19)	C(31)-O(2)	1.162(17)
C(5)-C(6)	1.38(2)	C(31)-O(1)	1.313(17)
C(6)-C(7)	1.42(3)	C(32)-O(3)	1.23(2)
C(7)-C(8)	1.26(3)	C(32)-O(4)	1.25(2)
C(8)-C(9)	1.37(3)	C(33)-C(38)	1.41(2)
C(9)-C(14)	1.28(3)	C(33)-C(34)	1.42(3)
C(9)-C(10)	1.53(3)	C(34)-C(35)	1.42(2)
C(10)-C(11)	1.36(3)	C(34)-C(61)	1.44(2)
C(11)-C(12)	1.43(3)	C(35)-C(36)	1.381(19)
C(12)-C(13)	1.39(3)	C(36)-C(37)	1.398(19)
C(12)-C(15)	1.46(2)	C(36)-C(62)	1.50(2)
C(13)-C(14)	1.48(3)	C(37)-C(38)	1.36(2)
C(15)-C(20)	1.31(2)	C(38)-C(39)	1.42(2)
C(15)-C(16)	1.39(3)	C(39)-C(40)	1.227(18)
C(16)-C(17)	1.38(3)	C(40)-C(41)	1.417(18)
C(17)-C(18)	1.38(3)	C(41)-C(46)	1.37(2)
C(18)-C(21)	1.39(2)	C(41)-C(42)	1.431(18)
C(18)-C(19)	1.40(2)	C(42)-C(43)	1.34(2)
C(19)-C(20)	1.36(3)	C(43)-C(44)	1.42(2)
C(21)-C(22)	1.20(2)	C(44)-C(45)	1.35(2)
C(22)-C(23)	1.48(2)	C(44)-C(47)	1.49(2)
C(23)-C(28)	1.32(2)	C(45)-C(46)	1.34(2)
C(23)-C(24)	1.37(2)	C(47)-C(52)	1.32(2)
C(24)-C(25)	1.386(19)	C(47)-C(48)	1.38(2)
C(25)-C(26)	1.390(19)	C(48)-C(49)	1.38(2)
C(25)-C(29)	1.512(18)	C(49)-C(50)	1.42(3)
C(26)-C(27)	1.426(19)	C(50)-C(51)	1.29(3)

C(50)-C(53A)	1.44(3)	C(79)-O(29)	1.43(2)
C(50)-C(53B)	1.62(4)	C(79)-C(80)	1.55(2)
C(51)-C(52)	1.42(2)	C(80)-O(31)	1.46(2)
C(61)-O(12)	1.28(2)	C(80)-C(81)	1.49(2)
C(61)-O(11)	1.28(2)	C(81)-O(27)	1.498(19)
C(62)-O(9)	1.230(19)	C(81)-C(82)	1.50(3)
C(62)-O(10)	1.26(2)	C(82)-O(30)	1.40(2)
C(65)-O(46)	1.364(17)	C(83)-O(31)	1.44(2)
C(65)-O(17)	1.434(18)	C(83)-O(32)	1.45(3)
C(65)-C(66)	1.58(2)	C(83)-C(84)	1.47(3)
C(66)-O(18)	1.38(2)	C(84)-C(85)	1.44(3)
C(66)-C(67)	1.50(2)	C(84)-O(33)	1.54(3)
C(67)-O(19)	1.422(18)	C(85)-O(34)	1.40(2)
C(67)-C(68)	1.55(2)	C(85)-C(86)	1.57(2)
C(68)-O(21)	1.352(18)	C(86)-O(36)	1.412(18)
C(68)-C(69)	1.59(2)	C(86)-C(87)	1.55(2)
C(69)-O(17)	1.391(19)	C(87)-O(32)	1.49(2)
C(69)-C(70)	1.59(2)	C(87)-C(88)	1.49(2)
C(70)-O(20)	1.39(2)	C(88)-O(35)	1.41(2)
C(71)-O(22)	1.31(2)	C(89)-C(90)	1.35(3)
C(71)-O(21)	1.40(2)	C(89)-O(36)	1.43(2)
C(71)-C(72)	1.64(2)	C(89)-O(37)	1.45(2)
C(72)-O(23)	1.40(2)	C(90)-O(38)	1.47(3)
C(72)-C(73)	1.51(2)	C(90)-C(91)	1.54(2)
C(73)-O(24)	1.41(2)	C(91)-O(39)	1.35(2)
C(73)-C(74)	1.55(3)	C(91)-C(92)	1.58(2)
C(74)-O(26)	1.41(2)	C(92)-O(41)	1.423(16)
C(74)-C(75)	1.56(3)	C(92)-C(93)	1.508(19)
C(75)-O(22)	1.44(2)	C(93)-O(37)	1.469(17)
C(75)-C(76)	1.49(3)	C(93)-C(94)	1.56(2)
C(76)-O(25)	1.38(3)	C(94)-O(40)	1.391(18)
C(77)-O(26)	1.375(18)	C(95)-O(41)	1.361(16)
C(77)-C(78)	1.38(2)	C(95)-O(42)	1.437(17)
C(77)-O(27)	1.43(2)	C(95)-C(96)	1.47(2)
C(78)-C(79)	1.45(2)	C(96)-O(43)	1.449(19)
C(78)-O(28)	1.47(2)	C(96)-C(97)	1.53(2)

C(97)-O(44)	1.426(19)	C(115)-O(59)	1.48(2)
C(97)-C(98)	1.52(2)	C(115)-C(116)	1.54(2)
C(98)-O(46)	1.432(19)	C(116)-O(61)	1.409(19)
C(98)-C(99)	1.50(2)	C(116)-C(117)	1.55(2)
C(99)-O(42)	1.458(19)	C(117)-O(57)	1.443(18)
C(99)-C(100)	1.50(2)	C(117)-C(118)	1.48(2)
C(100)-O(45)	1.44(2)	C(118)-O(60)	1.43(2)
C(101)-O(76)	1.35(3)	C(119)-O(62)	1.362(18)
C(101)-C(102)	1.43(3)	C(119)-O(61)	1.380(18)
C(101)-O(47)	1.49(3)	C(119)-C(120)	1.59(2)
C(102)-O(48)	1.45(3)	C(120)-O(63)	1.42(2)
C(102)-C(103)	1.49(3)	C(120)-C(121)	1.48(2)
C(103)-O(49)	1.39(2)	C(121)-O(64)	1.44(2)
C(103)-C(104)	1.53(2)	C(121)-C(122)	1.46(2)
C(104)-O(51)	1.410(19)	C(122)-O(66)	1.45(2)
C(104)-C(105)	1.53(2)	C(122)-C(123)	1.58(2)
C(105)-O(47)	1.44(2)	C(123)-O(62)	1.377(17)
C(105)-C(106)	1.54(3)	C(123)-C(124)	1.48(2)
C(106)-O(50)	1.36(2)	C(124)-O(65)	1.37(2)
C(107)-O(51)	1.40(2)	C(125)-O(66)	1.35(2)
C(107)-O(52)	1.40(2)	C(125)-O(67)	1.47(2)
C(107)-C(108)	1.53(2)	C(125)-C(126)	1.54(3)
C(108)-O(53)	1.44(2)	C(126)-C(127)	1.34(3)
C(108)-C(109)	1.52(2)	C(126)-O(68)	1.48(3)
C(109)-O(54)	1.449(19)	C(127)-O(69)	1.45(3)
C(109)-C(110)	1.50(2)	C(127)-C(128)	1.71(4)
C(110)-O(56)	1.384(17)	C(128)-O(71)	1.30(3)
C(110)-C(111)	1.60(2)	C(128)-C(129)	1.55(3)
C(111)-O(52)	1.431(18)	C(129)-O(67)	1.40(2)
C(111)-C(112)	1.52(3)	C(129)-C(130)	1.55(3)
C(112)-O(55)	1.42(2)	C(130)-O(70)	1.43(2)
C(113)-O(56)	1.320(18)	C(131)-C(132)	1.37(4)
C(113)-O(57)	1.454(19)	C(131)-O(72)	1.44(3)
C(113)-C(114)	1.56(2)	C(131)-O(71)	1.48(3)
C(114)-O(58)	1.39(2)	C(132)-O(73)	1.45(3)
C(114)-C(115)	1.45(2)	C(132)-C(133)	1.49(3)

C(133)-O(74)	1.41(3)
C(133)-C(134)	1.51(3)
C(134)-C(135)	1.50(4)
C(134)-O(76)	1.51(3)
C(135)-O(72)	1.44(3)
C(135)-C(136)	1.82(5)
C(136)-O(75)	1.25(4)
C(53A)-C(54A)	1.21(4)
C(54A)-C(55A)	1.53(5)
C(55A)-C(56A)	1.1838
C(55A)-C(60A)	1.48(4)
C(56A)-C(57A)	1.57(5)
C(57A)-C(64A)	1.19(5)
C(57A)-C(58A)	1.21(3)
C(58A)-C(59A)	1.38(3)
C(59A)-C(60A)	1.37(3)
C(59A)-C(63A)	1.46(6)
C(63A)-O(14A)	1.30(5)
C(63A)-O(13A)	1.44(6)
C(64A)-O(16A)	1.54(6)
C(64A)-O(15A)	1.54(6)
C(53B)-C(54B)	1.11(5)
C(54B)-C(55B)	1.29(5)
C(55B)-C(56B)	1.46(5)
C(55B)-C(60B)	1.56(5)
C(56B)-C(57B)	1.25(5)
C(57B)-C(64B)	1.54(7)
C(57B)-C(58B)	1.68(6)
C(58B)-C(59B)	1.53(6)
C(59B)-C(60B)	1.34(5)
C(59B)-C(63B)	1.42(5)
C(63B)-O(13B)	1.16(4)
C(63B)-O(14B)	1.24(4)
C(64B)-O(15B)	1.17(6)
C(64B)-O(16B)	1.28(6)

C(2)-C(1)-C(6)	122.3(16)
C(1)-C(2)-C(3)	120.0(13)
C(1)-C(2)-C(32)	121.9(13)
C(3)-C(2)-C(32)	117.7(12)
C(2)-C(3)-C(4)	118.2(13)
C(3)-C(4)-C(5)	123.5(13)
C(3)-C(4)-C(31)	121.8(12)
C(5)-C(4)-C(31)	114.6(12)
C(6)-C(5)-C(4)	117.4(14)
C(5)-C(6)-C(7)	120.8(17)
C(5)-C(6)-C(1)	118.3(17)
C(7)-C(6)-C(1)	120.9(17)
C(8)-C(7)-C(6)	171(2)
C(7)-C(8)-C(9)	171(2)
C(14)-C(9)-C(8)	125(2)
C(14)-C(9)-C(10)	114.4(19)
C(8)-C(9)-C(10)	120.6(17)
C(11)-C(10)-C(9)	118(2)
C(10)-C(11)-C(12)	123(2)
C(13)-C(12)-C(11)	119.3(18)
C(13)-C(12)-C(15)	114.8(15)
C(11)-C(12)-C(15)	125.4(16)
C(12)-C(13)-C(14)	114(2)
C(9)-C(14)-C(13)	129(2)
C(20)-C(15)-C(16)	115.1(17)
C(20)-C(15)-C(12)	127.2(15)
C(16)-C(15)-C(12)	117.6(15)
C(17)-C(16)-C(15)	118(2)
C(18)-C(17)-C(16)	127(3)
C(17)-C(18)-C(21)	125.1(18)
C(17)-C(18)-C(19)	112.5(17)
C(21)-C(18)-C(19)	121.9(14)
C(20)-C(19)-C(18)	119.3(17)
C(15)-C(20)-C(19)	127.7(19)
C(22)-C(21)-C(18)	178.7(18)
C(21)-C(22)-C(23)	178.9(18)

C(28)-C(23)-C(24)115.9(15)
C(28)-C(23)-C(22)123.0(15)
C(24)-C(23)-C(22)121.1(13)
C(23)-C(24)-C(25)122.2(13)
C(24)-C(25)-C(26)118.1(12)
C(24)-C(25)-C(29)124.5(11)
C(26)-C(25)-C(29)117.3(12)
C(25)-C(26)-C(27)119.8(13)
C(28)-C(27)-C(26)115.2(13)
C(28)-C(27)-C(30)126.4(14)
C(26)-C(27)-C(30)118.2(12)
C(23)-C(28)-C(27)128.5(16)
O(6)-C(29)-O(5) 125.9(14)
O(6)-C(29)-C(25) 117.7(12)
O(5)-C(29)-C(25) 116.3(12)
O(7)-C(30)-O(8) 119.9(14)
O(7)-C(30)-C(27) 125.3(14)
O(8)-C(30)-C(27) 114.5(13)
O(2)-C(31)-O(1) 121.8(13)
O(2)-C(31)-C(4) 126.1(13)
O(1)-C(31)-C(4) 112.2(12)
O(3)-C(32)-O(4) 124.6(18)
O(3)-C(32)-C(2) 122.0(15)
O(4)-C(32)-C(2) 113.3(17)
C(38)-C(33)-C(34)119.6(16)
C(35)-C(34)-C(33)118.0(15)
C(35)-C(34)-C(61)121.2(16)
C(33)-C(34)-C(61)120.7(16)
C(36)-C(35)-C(34)121.4(14)
C(35)-C(36)-C(37)118.9(13)
C(35)-C(36)-C(62)121.0(13)
C(37)-C(36)-C(62)119.3(12)
C(38)-C(37)-C(36)121.8(13)
C(37)-C(38)-C(33)120.2(15)
C(37)-C(38)-C(39)120.9(13)
C(33)-C(38)-C(39)118.9(14)
C(40)-C(39)-C(38)171.0(15)
C(39)-C(40)-C(41)176.7(13)
C(46)-C(41)-C(40)122.2(13)
C(46)-C(41)-C(42)115.4(13)
C(40)-C(41)-C(42)121.8(12)
C(43)-C(42)-C(41)119.5(13)
C(42)-C(43)-C(44)122.8(13)
C(45)-C(44)-C(43)116.3(13)
C(45)-C(44)-C(47)125.5(13)
C(43)-C(44)-C(47)118.2(12)
C(46)-C(45)-C(44)121.4(17)
C(45)-C(46)-C(41)124.5(16)
C(52)-C(47)-C(48)116.6(15)
C(52)-C(47)-C(44)121.6(13)
C(48)-C(47)-C(44)121.7(14)
C(47)-C(48)-C(49)123.5(17)
C(48)-C(49)-C(50)116.9(17)
C(51)-C(50)-C(49)120(2)
C(51)-C(50)-C(53A)110(2)
C(49)-C(50)-C(53A)130(2)
C(51)-C(50)-C(53B)138(2)
C(49)-C(50)-C(53B)102(2)
C(53A)-C(50)-C(53B)
C(50)-C(51)-C(52)121.0(19)
C(47)-C(52)-C(51)121.9(15)
O(12)-C(61)-O(11)122.8(16)
O(12)-C(61)-C(34)117.6(16)
O(11)-C(61)-C(34)119.5(16)
O(9)-C(62)-O(10) 123.0(16)
O(9)-C(62)-C(36) 116.3(14)
O(10)-C(62)-C(36)120.2(14)
O(46)-C(65)-O(17)114.1(12)
O(46)-C(65)-C(66)109.6(12)
O(17)-C(65)-C(66)109.7(12)
O(18)-C(66)-C(67)114.5(14)
O(18)-C(66)-C(65)110.4(14)

C(67)-C(66)-C(65)107.6(13)
O(19)-C(67)-C(66)108.8(13)
O(19)-C(67)-C(68)107.2(12)
C(66)-C(67)-C(68)111.7(13)
O(21)-C(68)-C(67)111.0(12)
O(21)-C(68)-C(69)109.7(13)
C(67)-C(68)-C(69)104.7(12)
O(17)-C(69)-C(70)105.7(13)
O(17)-C(69)-C(68)115.0(13)
C(70)-C(69)-C(68)105.3(13)
O(20)-C(70)-C(69)109.9(15)
O(22)-C(71)-O(21)114.7(15)
O(22)-C(71)-C(72)109.3(14)
O(21)-C(71)-C(72)106.6(13)
O(23)-C(72)-C(73)110.8(14)
O(23)-C(72)-C(71)109.9(14)
C(73)-C(72)-C(71)105.3(14)
O(24)-C(73)-C(72)109.0(15)
O(24)-C(73)-C(74)107.5(14)
C(72)-C(73)-C(74)113.2(14)
O(26)-C(74)-C(73)105.4(13)
O(26)-C(74)-C(75)108.7(15)
C(73)-C(74)-C(75)111.2(15)
O(22)-C(75)-C(76)106.9(16)
O(22)-C(75)-C(74)113.0(16)
C(76)-C(75)-C(74)115.0(17)
O(25)-C(76)-C(75)114.2(19)
O(26)-C(77)-C(78)110.2(14)
O(26)-C(77)-O(27)112.8(13)
C(78)-C(77)-O(27)110.4(14)
C(77)-C(78)-C(79)116.1(15)
C(77)-C(78)-O(28)110.8(14)
C(79)-C(78)-O(28)111.2(14)
O(29)-C(79)-C(78)120.6(15)
O(29)-C(79)-C(80)108.4(14)
C(78)-C(79)-C(80)106.1(14)
O(31)-C(80)-C(81)111.2(14)
O(31)-C(80)-C(79)105.8(14)
C(81)-C(80)-C(79)115.3(15)
C(80)-C(81)-O(27)109.9(13)
C(80)-C(81)-C(82)110.5(15)
O(27)-C(81)-C(82)107.8(14)
O(30)-C(82)-C(81)114.2(17)
O(31)-C(83)-O(32)110.0(16)
O(31)-C(83)-C(84)112.4(18)
O(32)-C(83)-C(84)105.4(18)
C(85)-C(84)-C(83)115.1(19)
C(85)-C(84)-O(33)104.8(17)
C(83)-C(84)-O(33)105.6(18)
O(34)-C(85)-C(84)114.0(16)
O(34)-C(85)-C(86)101.8(13)
C(84)-C(85)-C(86)103.5(15)
O(36)-C(86)-C(87)106.2(12)
O(36)-C(86)-C(85)107.4(13)
C(87)-C(86)-C(85)109.9(13)
O(32)-C(87)-C(88)105.5(13)
O(32)-C(87)-C(86)109.9(12)
C(88)-C(87)-C(86)114.8(14)
O(35)-C(88)-C(87)113.7(15)
C(90)-C(89)-O(36)111.4(17)
C(90)-C(89)-O(37)114.0(17)
O(36)-C(89)-O(37)107.1(14)
C(89)-C(90)-O(38)116.7(18)
C(89)-C(90)-C(91)115.3(17)
O(38)-C(90)-C(91)105.8(16)
O(39)-C(91)-C(90)114.9(14)
O(39)-C(91)-C(92)111.1(13)
C(90)-C(91)-C(92)109.9(13)
O(41)-C(92)-C(93)110.5(11)
O(41)-C(92)-C(91)105.5(11)
C(93)-C(92)-C(91)113.5(11)
O(37)-C(93)-C(92)115.5(11)

O(37)-C(93)-C(94)102.9(11)
C(92)-C(93)-C(94)113.2(12)
O(40)-C(94)-C(93)111.6(11)
O(41)-C(95)-O(42)112.4(11)
O(41)-C(95)-C(96)110.4(12)
O(42)-C(95)-C(96)107.6(11)
O(43)-C(96)-C(95)107.8(12)
O(43)-C(96)-C(97)114.9(12)
C(95)-C(96)-C(97)111.2(12)
O(44)-C(97)-C(98)115.7(13)
O(44)-C(97)-C(96)105.5(12)
C(98)-C(97)-C(96)114.0(13)
O(46)-C(98)-C(99)113.5(13)
O(46)-C(98)-C(97)107.3(13)
C(99)-C(98)-C(97)111.1(13)
O(42)-C(99)-C(98)110.4(12)
O(42)-C(99)-C(100)107.4(13)
C(98)-C(99)-C(100)113.7(13)
O(45)-C(100)-C(99)110.4(13)
O(76)-C(101)-C(102)111(2)
O(76)-C(101)-O(47)111.3(18)
C(102)-C(101)-O(47)107.7(19)
C(101)-C(102)-O(48)110(2)
C(101)-C(102)-C(103)
O(48)-C(102)-C(103)117(2)
O(49)-C(103)-C(102)116.7(16)
O(49)-C(103)-C(104)110.8(14)
C(102)-C(103)-C(104)
O(51)-C(104)-C(103)106.7(13)
O(51)-C(104)-C(105)109.6(13)
C(103)-C(104)-C(105)
O(47)-C(105)-C(104)111.3(13)
O(47)-C(105)-C(106)105.2(14)
C(104)-C(105)-C(106)
O(50)-C(106)-C(105)110.8(15)
O(51)-C(107)-O(52)113.4(14)
O(51)-C(107)-C(108)110.4(14)
O(52)-C(107)-C(108)109.2(14)
O(53)-C(108)-C(109)108.3(14)
O(53)-C(108)-C(107)110.5(14)
C(109)-C(108)-C(107)
O(54)-C(109)-C(110)106.8(12)
O(54)-C(109)-C(108)110.0(12)
C(110)-C(109)-C(108)
O(56)-C(110)-C(109)110.6(12)
O(56)-C(110)-C(111)111.0(11)
C(109)-C(110)-C(111)
O(52)-C(111)-C(112)105.4(14)
O(52)-C(111)-C(110)111.4(11)
C(112)-C(111)-C(110)
O(55)-C(112)-C(111)112.9(16)
O(56)-C(113)-O(57)112.9(12)
O(56)-C(113)-C(114)107.2(13)
O(57)-C(113)-C(114)109.0(13)
O(58)-C(114)-C(115)116.2(15)
O(58)-C(114)-C(113)110.9(14)
C(115)-C(114)-C(113)
C(114)-C(115)-O(59)118.3(15)
C(114)-C(115)-C(116)
O(59)-C(115)-C(116)108.0(14)
O(61)-C(116)-C(115)107.9(14)
O(61)-C(116)-C(117)107.8(13)
C(115)-C(116)-C(117)
O(57)-C(117)-C(118)107.6(12)
O(57)-C(117)-C(116)107.9(12)
C(118)-C(117)-C(116)
O(60)-C(118)-C(117)110.1(13)
O(62)-C(119)-O(61)116.9(13)
O(62)-C(119)-C(120)111.1(13)
O(61)-C(119)-C(120)108.1(13)
O(63)-C(120)-C(121)114.0(14)
O(63)-C(120)-C(119)112.4(13)

C(121)-C(120)-C(119)
O(64)-C(121)-C(122)108.3(13)
O(64)-C(121)-C(120)112.7(13)
C(122)-C(121)-C(120)
O(66)-C(122)-C(121)108.4(13)
O(66)-C(122)-C(123)110.0(13)
C(121)-C(122)-C(123)
O(62)-C(123)-C(124)109.7(12)
O(62)-C(123)-C(122)111.1(12)
C(124)-C(123)-C(122)
O(65)-C(124)-C(123)114.2(14)
O(66)-C(125)-O(67)108.6(14)
O(66)-C(125)-C(126)108.6(16)
O(67)-C(125)-C(126)105.4(15)
C(127)-C(126)-O(68)104(2)
C(127)-C(126)-C(125)
O(68)-C(126)-C(125)106.4(18)
C(126)-C(127)-O(69)117(2)
C(126)-C(127)-C(128)
O(69)-C(127)-C(128)106(2)
O(71)-C(128)-C(129)115(2)
O(71)-C(128)-C(127)110(2)
C(129)-C(128)-C(127)
O(67)-C(129)-C(130)105.4(16)
O(67)-C(129)-C(128)114.5(18)
C(130)-C(129)-C(128)
O(70)-C(130)-C(129)110.4(17)
C(132)-C(131)-O(72)110(2)
C(132)-C(131)-O(71)110(2)
O(72)-C(131)-O(71)115(2)
C(131)-C(132)-O(73)114(2)
C(131)-C(132)-C(133)
O(73)-C(132)-C(133)102(2)
O(74)-C(133)-C(132)117(2)
O(74)-C(133)-C(134)114.5(19)
C(132)-C(133)-C(134)
C(135)-C(134)-C(133)
C(135)-C(134)-O(76)113(2)
C(133)-C(134)-O(76)103.8(19)
O(72)-C(135)-C(134)103(2)
O(72)-C(135)-C(136)103(2)
C(134)-C(135)-C(136)
O(75)-C(136)-C(135)104(3)
C(54A)-C(53A)-C(50)
C(53A)-C(54A)-C(55A)
C(56A)-C(55A)-C(60A)
C(56A)-C(55A)-C(54A)
C(60A)-C(55A)-C(54A)
C(55A)-C(56A)-C(57A)
C(64A)-C(57A)-C(58A)
C(64A)-C(57A)-C(56A)
C(58A)-C(57A)-C(56A)
C(57A)-C(58A)-C(59A)
C(60A)-C(59A)-C(58A)
C(60A)-C(59A)-C(63A)
C(58A)-C(59A)-C(63A)
C(59A)-C(60A)-C(55A)
O(14A)-C(63A)-O(13A)
O(14A)-C(63A)-C(59A)
O(13A)-C(63A)-C(59A)
C(57A)-C(64A)-O(16A)
C(57A)-C(64A)-O(15A)
O(16A)-C(64A)-O(15A)
C(54B)-C(53B)-C(50)171(4)
C(53B)-C(54B)-C(55B)
C(54B)-C(55B)-C(56B)
C(54B)-C(55B)-C(60B)
C(56B)-C(55B)-C(60B)
C(57B)-C(56B)-C(55B)
C(56B)-C(57B)-C(64B)
C(56B)-C(57B)-C(58B)
C(64B)-C(57B)-C(58B)

C(59B)-C(58B)-C(57B)
C(60B)-C(59B)-C(63B)
C(60B)-C(59B)-C(58B)
C(63B)-C(59B)-C(58B)
C(59B)-C(60B)-C(55B)
O(13B)-C(63B)-O(14B)
O(13B)-C(63B)-C(59B)
O(14B)-C(63B)-C(59B)
O(15B)-C(64B)-O(16B)
O(15B)-C(64B)-C(57B)
O(16B)-C(64B)-C(57B)
C(69)-O(17)-C(65)112.4(12)
C(68)-O(21)-C(71)117.1(12)
C(71)-O(22)-C(75)117.2(15)
C(77)-O(26)-C(74)122.4(12)
C(77)-O(27)-C(81)110.8(12)
C(83)-O(31)-C(80)121.2(15)
C(83)-O(32)-C(87)113.8(14)
C(86)-O(36)-C(89)117.2(13)
C(89)-O(37)-C(93)111.9(12)
C(95)-O(41)-C(92)118.7(11)
C(95)-O(42)-C(99)114.2(11)
C(65)-O(46)-C(98)118.6(11)
C(105)-O(47)-C(101)112.4(15)
C(107)-O(51)-C(104)123.3(13)
C(107)-O(52)-C(111)115.1(13)
C(113)-O(56)-C(110)119.8(12)
C(117)-O(57)-C(113)114.0(12)
C(119)-O(61)-C(116)122.6(12)
C(119)-O(62)-C(123)113.6(11)
C(125)-O(66)-C(122)118.3(13)
C(129)-O(67)-C(125)114.4(14)
C(128)-O(71)-C(131)120(2)
C(135)-O(72)-C(131)106(2)
C(101)-O(76)-C(134)123.2(19)

Table A.3. Hydrogen coordinates (x 10^4) and isotropic displacement parameters ($Å^2$ x 10^3) for RD **3**.

	x	y	z	U(eq)
H(1)	6650	3310	10739	60
H(3)	6452	4131	12207	31
H(5)	6548	2332	12162	34
H(10A)	6916	602	10928	85
H(10B)	5766	728	10727	85
H(11)	6267	-144	10366	104
H(13)	7131	861	9117	97
H(14)	7067	1683	9740	92
H(16)	6601	-824	9810	90
H(17)	6534	-1568	9155	114
H(19)	6022	-427	7883	56
H(20)	5976	281	8544	67
H(24)	7012	-3013	7858	28
H(26)	6260	-3679	6292	35
H(28)	5727	-2013	6636	45
H(33)	1351	-569	6907	57
H(35)	934	-2347	6912	35
H(37)	1572	-1530	5509	28
H(42)	2248	67	4505	23
H(43)	2078	872	3934	40
H(45)	1323	1858	5197	51
H(46)	1315	1046	5732	55
H(48)	1071	1533	3409	50
H(49)	1028	2303	2764	65
H(51)	2160	3353	4038	61
H(52)	2070	2577	4678	36
H(65)	6204	633	5876	34
H(66)	5908	1566	6282	57
H(67)	3916	1450	5708	38
H(68)	4574	1490	6926	41
H(69)	3813	463	6246	47

H(70A)	3592	494	7260	59
H(70B)	4251	-59	7127	59
H(71)	3596	1793	7374	57
H(72)	2080	2426	7330	53
H(73)	1504	1841	6265	60
H(74)	444	1676	7224	57
H(75)	1752	784	6889	71
H(76A)	583	490	7474	87
H(76B)	1709	326	7714	87
H(77)	-967	1333	6903	44
H(78)	-2126	1287	6152	44
H(79)	-595	1250	5492	53
H(80)	-2159	412	5546	56
H(81)	-162	195	6042	44
H(82A)	-1117	-639	5784	73
H(82B)	-889	-597	6458	73
H(83)	-2488	50	4676	84
H(84)	-2074	-180	3778	86
H(85)	-128	231	4211	52
H(86)	-837	-916	3727	43
H(87)	-112	-688	4916	44
H(88A)	73	-1669	4725	61
H(88B)	-801	-1599	5103	61
H(89)	238	-1476	3525	65
H(90)	1441	-1421	3014	73
H(91)	2092	-347	3553	40
H(92)	3361	-1369	3645	29
H(93)	2326	-1089	4561	30
H(94A)	3736	-1766	4710	38
H(94B)	2737	-2030	4893	38
H(95)	4777	-1134	4001	32
H(96)	5974	-435	4214	35
H(97)	4462	377	4411	41
H(98)	5949	-24	5290	48
H(99)	3932	-411	5142	43
H(10C)	5580	-882	5884	53

H(10D)	4763	-457	6090	53
H(101)	-603	7446	10294	93
H(102)	3	7580	11212	90
H(103)	1549	6810	11086	49
H(104)	1925	7989	11422	50
H(105)	1959	7658	10270	47
H(10E)	2832	8543	10521	67
H(10F)	1882	8670	10056	67
H(107)	3500	8035	11768	58
H(108)	5053	7560	12053	51
H(109)	4299	6698	11207	42
H(110)	6011	7435	11229	39
H(111)	4162	7594	10450	36
H(11A)	5594	8012	10133	86
H(11B)	4785	8500	10224	86
H(113)	7035	7111	10817	45
H(114)	7701	6237	10524	49
H(115)	5802	5861	10113	59
H(116)	7286	6156	9415	53
H(117)	5471	6791	9551	32
H(11C)	5906	6931	8643	56
H(11D)	5997	7530	8998	56
H(119)	6995	5730	8626	43
H(120)	6383	4818	8206	53
H(121)	4815	4986	8848	43
H(122)	4557	5018	7665	54
H(123)	4567	6074	8330	37
H(124)	4124	6569	7496	46
H(125)	3092	4846	7347	61
H(126)	1431	4557	7506	99
H(127)	2051	4939	8585	106
H(128)	429	5551	7826	104
H(129)	2394	6045	8136	78
H(13A)	1058	6710	7778	70
H(13B)	1898	6696	7371	70
H(131)	-511	6114	8169	111

H(132)	-1304	6235	8872	112
H(133)	445	5972	9628	76
H(134)	-607	7058	9411	108
H(135)	1293	6649	9152	111
H(13C)	1493	7823	9387	178
H(13D)	1539	7720	8723	178
H(56A)	1180	3896	1680	88
H(58A)	1790	5462	1228	36
H(60A)	2458	5020	2873	36
H(13E)	3329	5905	1697	184
H(16A)	374	4052	343	257
H(56B)	1431	3336	1357	36
H(58B)	582	4898	603	36
H(60B)	1212	4819	2335	36
H(13F)	736	5991	2107	31
H(15B)	866	3980	-299	116
H(1A)	6584	3732	13411	68
H(4)	6789	4500	10467	167
H(6)	7478	-4103	7976	73
H(8)	5912	-3227	5273	66
H(9)	1957	-2614	5323	94
H(12)	521	-781	7867	83
H(18)	5273	1665	5200	88
H(19A)	3873	2293	6269	68
H(20A)	4794	668	7838	149
H(23)	2951	2454	6399	99
H(24A)	479	2491	6160	102
H(25)	551	1049	8123	141
H(28A)	-1334	2169	5804	109
H(29)	-1623	1349	4762	116
H(30)	-2600	-452	5820	137
H(33A)	-1571	834	3668	145
H(34)	138	92	3362	109
H(35A)	-1835	-1822	4407	103
H(38)	155	-570	2955	132
H(39)	3331	-651	3007	102

H(40)	3128	-2243	3871	53
H(43A)	5587	-195	3382	88
H(44)	6200	756	4685	82
H(45A)	4383	-1402	6186	81
H(48A)	-219	6450	10973	202
H(49A)	1130	7255	12028	119
H(50)	1286	9133	10629	109
H(53)	4022	7177	12528	106
H(54)	6157	6604	11651	79
H(55)	5724	8698	11041	72
H(58)	6321	5960	11139	107
H(59)	7460	5245	10116	111
H(60)	7458	6893	8708	87
H(63)	6268	4531	9235	78
H(64)	4419	4148	8639	85
H(65A)	5117	5810	6999	79
H(68A)	2700	3938	7846	149
H(69A)	580	4727	8744	190
H(70)	937	6202	6775	95
H(73A)	-329	5252	9194	168
H(74A)	-399	5967	10279	140
H(75A)	-141	7772	9027	180